Oil & Natural Gas Technology

DOE Award No.: DE-NT0006554

Final Report

October 2008 to September 2012

GIS- and Web-based Water Resource Geospatial Infrastructure for Oil Shale Development

Submitted by:
Colorado School of Mines
1500 Illinois St.
Golden, CO 80401

Principal Authors: **Wei (Wendy) Zhou, PI**
Matthew D. Minnick
Mengistu Geza
Kyle E. Murray
Earl D. Mattson

Prepared for:
United States Department of Energy
National Energy Technology Laboratory

December 29, 2012

Office of Fossil Energy

DISCLAIMER

This information was prepared as an account of work sponsored by an agency of the U.S. Government. Neither the U.S. Government nor any agency thereof, nor any of their employees, makes any warranty, expressed or implied, or assumes any legal liability or responsibility for the accuracy, completeness, or usefulness, of any information, apparatus, product, or process disclosed, or represents that its use would not infringe privately owned rights. References herein to any specific commercial product, process, or service by trade name, trade mark, manufacturer, or otherwise, does not necessarily constitute or imply its endorsement, recommendation, or favoring by the U.S. Government or any agency thereof. The views and opinions of authors expressed herein do not necessarily state or reflect those of the U.S. Government or any agency thereof.

TABLE OF CONTENTS

LIST OF FIGURES

LIST OF TABLES

ABSTRACT

The Colorado School of Mines (CSM) was awarded a grant by the National Energy Technology Laboratory (NETL), Department of Energy (DOE) to conduct a research project entitled *GIS- and Web-based Water Resource Geospatial Infrastructure for Oil Shale Development* in October of 2008. The ultimate goal of this research project is to develop a water resource geospatial infrastructure that serves as "baseline data" for creating solutions on water resource management and for supporting decisions making on oil shale resource development.

The project came to the end on September 30, 2012. This final project report will report the key findings from the project activity, major accomplishments, and expected impacts of the research. At meantime, the gamma version (also known as Version 4.0) of the geodatabase as well as other various deliverables stored on digital storage media will be send to the program manager at NETL, DOE via express mail.

The key findings from the project activity include the quantitative spatial and temporal distribution of the water resource throughout the Piceance Basin, water consumption with respect to oil shale production, and data gaps identified. Major accomplishments of this project include the creation of a relational geodatabase, automated data processing scripts (Matlab) for database link with surface water and geological model, ArcGIS Model for hydrogeologic data processing for groundwater model input, a 3D geological model, surface water/groundwater models, energy resource development systems model, as well as a web-based geo-spatial infrastructure for data exploration, visualization and dissemination. This research will have broad impacts of the development of the oil shale resources in the US. The geodatabase provides a "baseline" data for further study of the oil shale development and identification of further data collection needs. The 3D geological model provides better understanding through data interpolation and visualization techniques of the Piceance Basin structure spatial distribution of the oil shale resources. The surface water/groundwater models quantify the water shortage and better understanding the spatial distribution of the available water resources. The energy resource development systems model reveals the phase shift of water usage and the oil shale production, which will facilitate better planning for oil shale development. Detailed descriptions about the key findings from the project activity, major accomplishments, and expected impacts of the research will be given in the section of "ACCOMPLISHMENTS, RESULTS, AND DISCUSSION" of this report.

ACCOMPLISHMENTS, RESULTS, AND DISCUSSION

This section will start with a detailed summary on the key findings from the project activity, major accomplishments, and expected impacts of the research, and then will describe the specific accomplishments task by task.

The key findings from the project activity are as followings:

- Spatial and temporal water distribution is highly variable in the Piceance Basin
- Surface water is limited within Piceance Basin, with largest discharge (Q) being Parachute and Roan Creek at ~20, 000 acre-ft/yr and ~30, 000 acre-ft/yr, respectively.
- Basin wide groundwater recharge is ~39,422 acre-ft/yr, balanced by spring Q and base flow of ~18,862 and 20,791 acre-ft/yr, respectively.
- Part of this flow could be utilized by building storing flow during spring runoff and peak flow events
- Alternative water sources have to be considered
    - Groundwater Pumping and Storage
    - Storage of unallocated spring runoff from the Colorado, White, and Yampa Rivers
- The versatile system dynamic modeling reveal that water consumption is not linearly related to oil shale production.
- Site construction and oil shale production have an overall water production and site remediation is the major water consumption phase
- Data Gaps
    - Fischer Assay Data
    - Characterization of Hydrogeologic Parameters, including
        - Fracture Network
        - Porosity and Permeability
    - Stream Flow
    - Potientmetric Surface Data for Upper and Lower Greenriver Aquifers
    - Comprehensive Water Quality
        - Both Surface and Groundwater
        - Understanding of Aquifer Baseline conditions
        - Characterization of Groundwater Mixing
    - Stream Flow Gains and Loss with Groundwater
    - Groundwater Quality (High TDS) is questionable for industrial use

Major accomplishments of the project include:

- An relational geodatabases, including all of the data collected, such as surface water, groundwater, geological, geomorphologic, oil shale (Fisher assays), surface water, ground water, and climate data sets
- Automated data processing scripts (Matlab) for database link with Surface water and Geological Model
- ArcGIS Model for Hydrogeologic Data processing for Groundwater Model Input
- Final models including the 3D Geological Model, Surface Water/Groundwater Modeling, Energy Resource Development Systems Modeling.
- Web-based geo-spatial infrastructure for data exploration, visualization and dissemination.

Expected impacts of the research are as followings:

- The geodatabase provides a "baseline" data for further study of the oil shale development and identification of further data collection needs.
- 3D geological model provides better understanding through data interpolation and visualization techniques of the Piceance Basin structure spatial distribution of the oil shale resources.
- Quantify the water shortage and better understanding the spatial distribution of the available water resources.
- Reveal the phase shift of water usage and the oil shale production, which will facilitate better planning for oil shale development.

Task 1.0 – Project Management Plan

During the month of October 2008 and the one third month of the November 2008, the PI revised and resubmitted the Project Management Plan (PMP), incorporating comments from the NETL Project Officer. This plan outlines the research to be performed during the entire three-year project. In addition, the PI wrote and submitted a statement of project objectives (SOPO), a two-page Project Summary, and the Technology Status Assessment.

Task 2.0 GIS-based Water Resource Geospatial Infrastructure

This task involves building a GIS-based water resource geospatial infrastructure for storing, managing, analyzing and displaying the data, and building a web-based GIS and a web-based data warehouse for storing and disseminating data. The sub-tasks within Task 2 are closely

related and dependent on one another. We have considered the connections between these subtasks before we defined the database schema during this quarter. Detailed descriptions about the progress on these subtasks are as followings.

Subtask 2.1 Regional "baseline" data collection and compiling

This subtask involves compiling data from various sources for the study area. Table 1 summaries the identified datasets, data sources, and geodatabase features. A brief descriptions of the dataset is also given in the table.

Table 1. Summary of datasets identified, collected, and compiled in the project geodatabase

NAME	SOURCE	DESCRIPTION	GEODATABASE FEATURE
Watersheds (HUCS)	NHDplus	Watershed polygons at various scales from the National Hydrologic Dataset	Basin Feature Class
Elevation	NED	Digital Elevation Models 90m, 30m, and 10m from the National Elevation Dataset	GeoRasters
Catchments	NHDplus	Lowest level of surface water divisions defined by the Stream Networks from the National Hydrologic Dataset	Catchment Feature Class
Stream Networks	NHDplus	Stream line data networked in a reach and nodal system from the National Hydrologic Dataset	Hydroline Feature Class
Flow Accumulation	NHDplus	Flow network and direction data linked to the Stream Network from the National Hydrologic Dataset	Related Table
Flow Gages	CDSS, NWIS	USGS Flow Gage Point Locations	Monitoring Point Feature Class
Flow Data	NWIS	Time Series Stream Flow Data linked to Flow Gage ID	Time Series Table
Daymet Extraction Points	Centroid of WARMF model catchments	Points calculated at centroids of WARMF model catchments for Daymet data extraction	Custom Point Feature Class
Precipitation Data	Daymet	Time Series Precipitation Data from Daymet linked to monitoring stations,	Time Series Table

(Time Series)		processed yearly, and monthly precipitation data trends for watersheds	
Meteorological Data (Time Series)	Daymet	Time Series Temperature Data and processed Temperature Datasets from Daymet	Time Series Table
Climate Monitoring Stations	**NOAA, CDSS**	**Point locations for Climate Monitoring Stations in and around the Piceance Basin**	**Monitoring Point Feature Class**
Climate Monitoring Stations	NOAA	Downloaded time series for up to 55 climate/weather parameters	Time Series Table
Surface Water Quality	NWIS, EPA STORET	Water Quality Data linked to monitoring locations	Monitoring Point Feature Class
Aerial Imagery	USGS, NAIP, ESRI Services	Color Aerial Imagery at varying resolutions	Raster Catalog
Geologic Maps	CGS, USGS	Images of geologic maps at various scales, georeferenced, from the CGS and USGS	GeoRasters and GeoArea feature class
Subsurface Geology	USGS, CSM Database	Borehole data from exploration wells including geophysical data, formation tops, oil shale richness data Input for 3D Geologic Model	GeoVolume Multipatch Feature Class
Wells	NWIS	Water Wells with production and source data	Well Point Feature Class
Water Level Data	NWIS	Time Series Data of Water Level Measurements for Wells	Time Series Table
Ground Water Quality	NWIS	Water Quality Data Associated with Wells	Time Series Tables
Hydrogeologic Data	CGS, USGS	Hydrologic Parameter data derived from cores and pumptests	Tables
Land Cover	NLCD	Vegetation and Barren Land Data from the National Land Cover Dataset	Raster Feature Set
Land Use/Ownership	BLM	Land Use and Ownership Data	Custom Polygon Feature Class
Base Map Layers	**USGS, ESRI Services**	**General map data including roads, towns, population, site names, USGS topographic maps**	**ESRI Services not Included in Geodata-**

			base
Springs	CDSS	Point Data for Locations and Time Series Tables for Flow	HydroPoint Feature Class
Spring Flow	CDSS	Time Series Data of Water Flow from Spings	Time Series Tables
Diversions	CDSS	Irrigation Ditchs, Stock Ponds, Reservi-ors, Stream Pumping Locations and Wells	WaterDis-charge and WaterWith-draw Point Feature Clas-ses
Diversion Flow	CDSS	Time Series Data of Water Flow and Usage	Time Series Tables
Pumping Tests	TEOSR	Testes conducted by various institu-tions throughout the years compiled from non-digital documents	Point Feature Class
Surficial Geological Structure	Digitized from USGS Geologic Map	surface expression of faults in Piceance Basin	Polyline Fea-ture Class
Surficial Alluvial Deposits	Digitized from USGS Geologic Map	surficial alluvial deposits that make up the stream valleys in the Piceance Ba-sin	Polygon Fea-ture Class
Geother-mal	Colorado Geologic Survey	Bottom Hole Temperature Data from Oil and Gas Wells	Point Feature Class

It is worth mention that we have created several digital products after existing digital maps and tabular data ran out. These digital products include the pumping testing maps from tests conducted by various institutions throughout the years compiled from non-digital documents (Figure 1), the surface expression of faults in Piceance Basin was digitized from USGS geologic maps (Figure 2), the surficial alluvial deposits that make up the stream valleys in the Piceance Basin digitized and added to the database (Figure 3). It is important to define the extent and volume of the surficial alluvial aquifers in the Piceance Basin system. Alluvial valleys are in direct connection with the shallow groundwater table and surface water. Quantifying the storage capacity of the alluvial aquifers is an important step in characterizing available water sources and potential shallow groundwater injection storage opportunities.

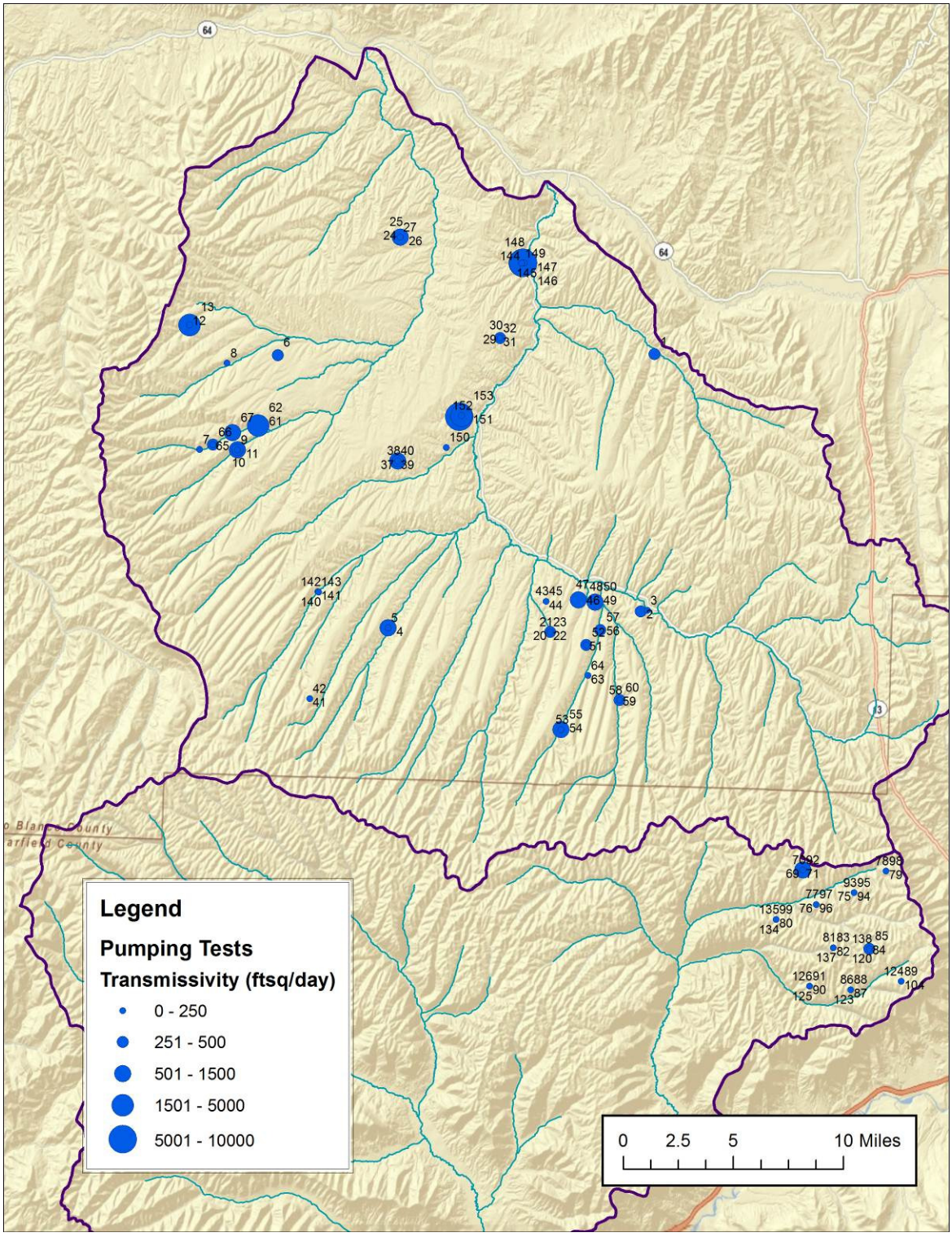

Figure 1. Pumping tests map of Piceance generated from non-digital documents which shows testes conducted by various institutions throughout the years.

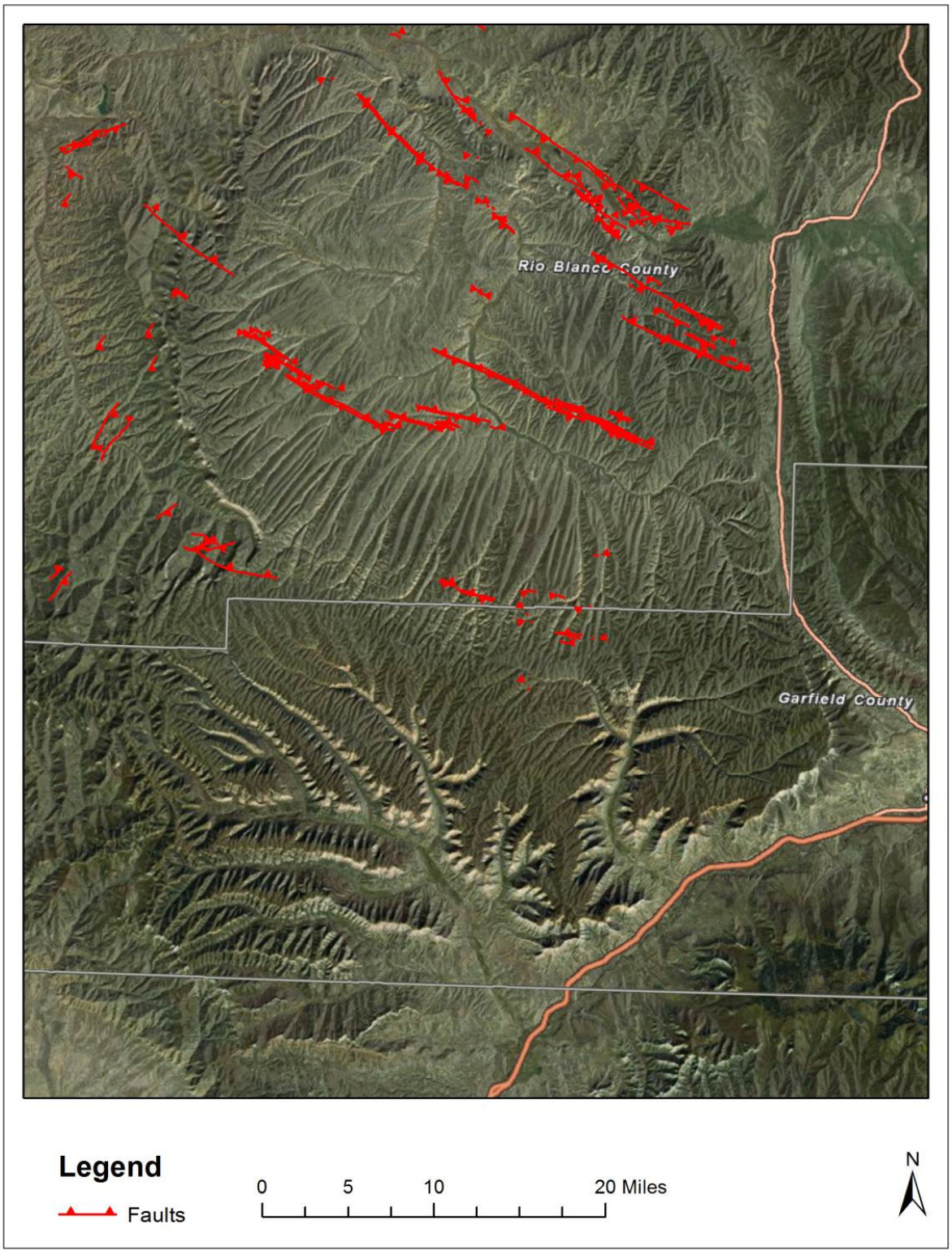

Figure 2. Faults digitized from USGS 100k Geologic Maps of the North and South Piceance Basin.

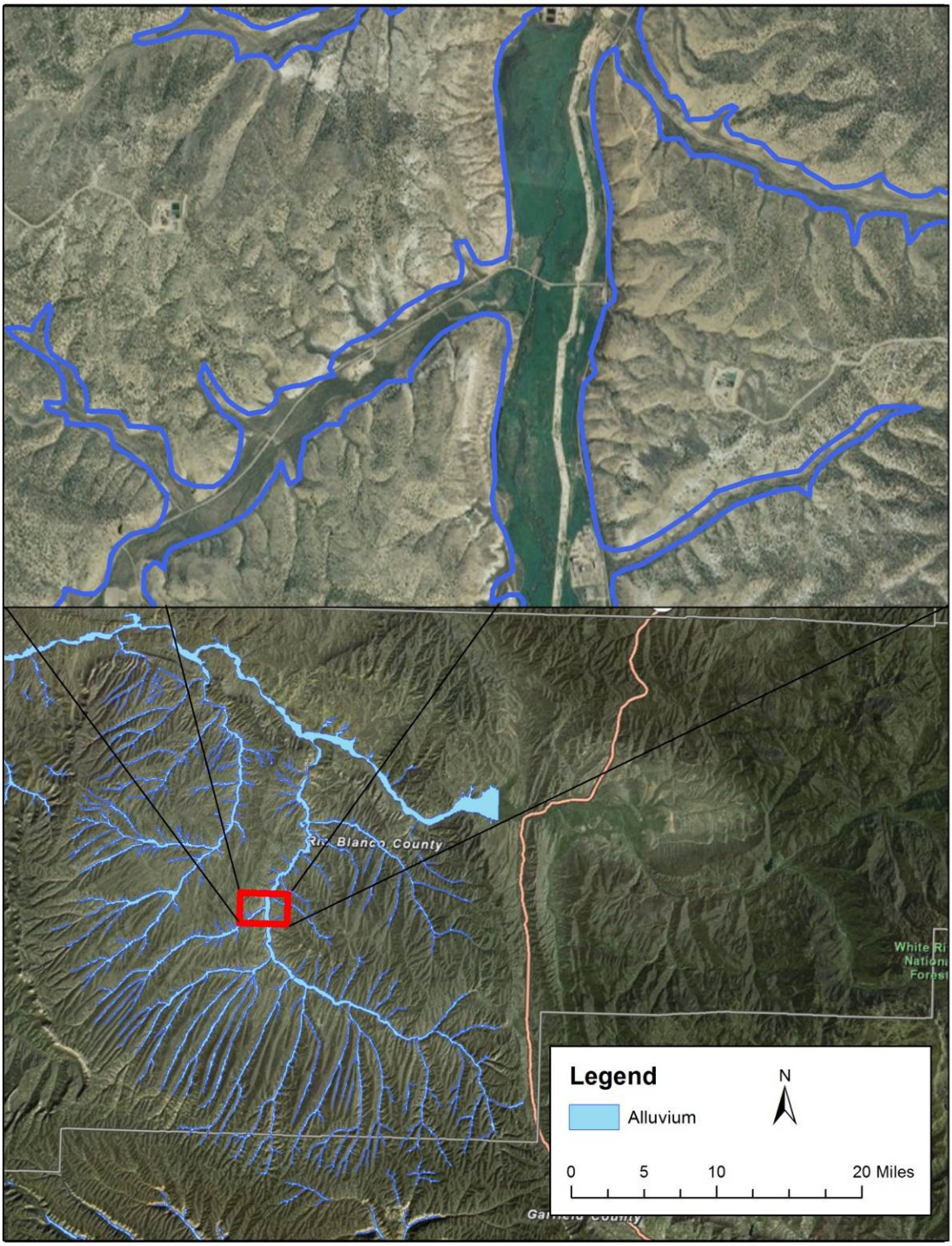

Figure 3. Extent of Alluvial deposits digitized from the USGS 100k Geologic Maps of North and South Piceance Basin.

The final version of the project database is named as gamma version (also known as Version 4.0 by the CSM research team). Figure 4 shows visual UML (Unified Modeling Language) data model diagram of the gamma version geodatabase. This has become a GIS industry standard in data model documentation and was first developed on the ArcGIS Hydro Model.

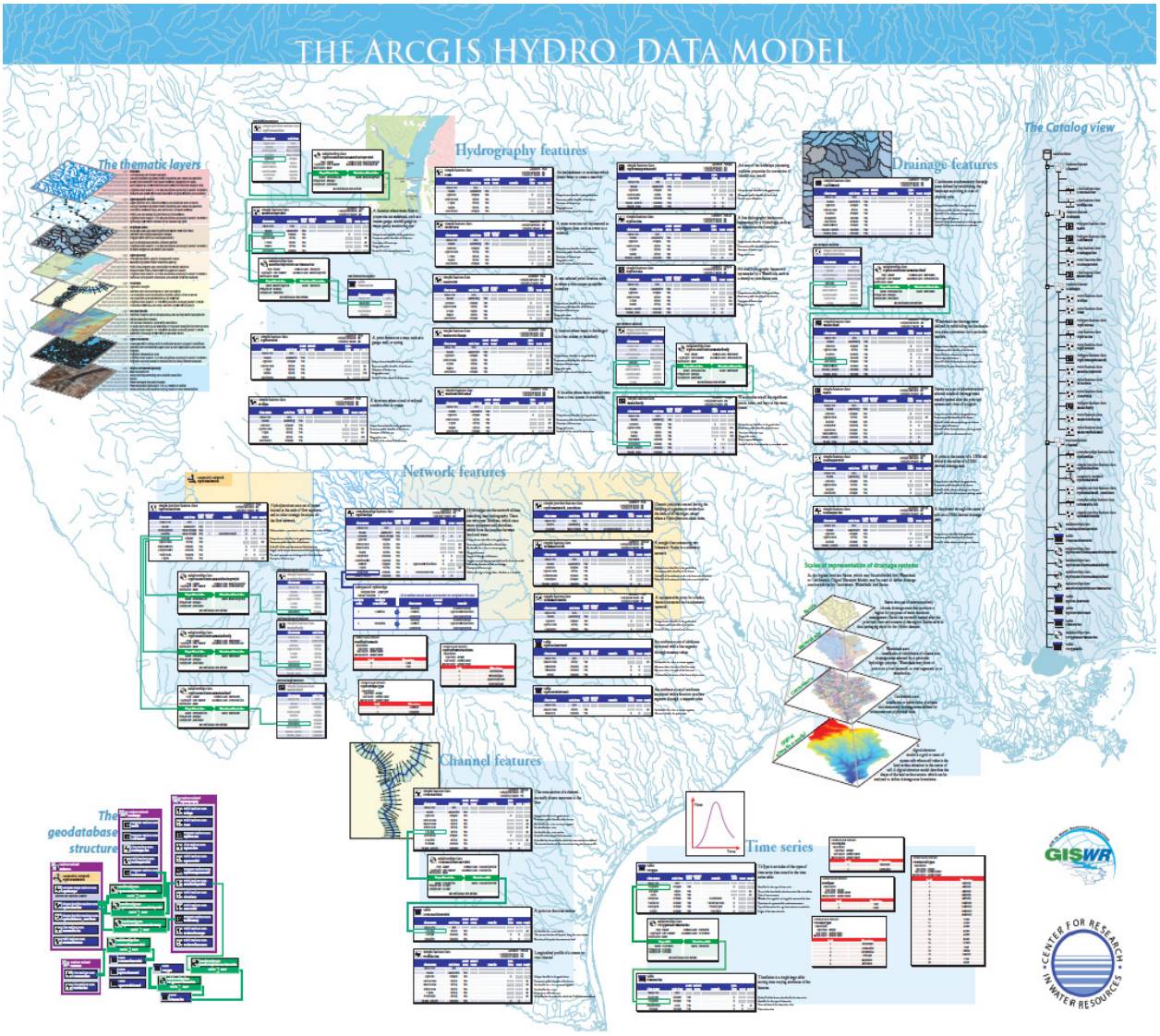

Figure 4. ArcGIS data model UML diagram documentation for the ArcHydro data model. A similar format is being constructed for the final documentation of the Piceance Oil Shale project database.

Subtask 2.2 Regional "baseline" data integration, storing, and managing

The current industry standard relational database for water resource analysis on the ArcGIS platform, Arc Hydro and Arc Hydro Ground Water, was chosen as the database schema for the prototype database framework at this point. Arc Hydro is a desktop geodatabase that provides a schema to store analyze water resource related data. Currently Arc Hydro has two separate geodatabase schemas, one to support surface water datasets and one to support groundwater datasets. The Arc Hydro framework supports a custom tool bar in ArcGIS for analytical analysis of the data. At this time we have left the databases separate and will be breaking them down into their basic components and rebuilding them into one geodatabase. The Arc Hydro schema provides an adequate starting point but is not sufficient to support all the goals of the project. The schema will be customized to include support for the surface water output WARMF and output from the systems dynamic model once these requirements have become clear. Once the final geodatabase is perfected and populated with all the available data we have gathered it will be migrated to SQL Server 2008 to be the support for the Arc Server web site.

Arc Hydro Data Model (AHDM) Framework

The definition of the database schema was accomplished by selecting a "data model" on which to base the project geodatabase. A model is a simplified representation of a real world phenomenon or system. Models are used to help us better understand the phenomenon or system by retaining its features and relationships. A "data model" is the representation of a real world phenomenon or system within a database having a conceptually logical framework. When designing a data model the main features of the system must be defined using geographic features, tabular data and relationships between those features as cardinality or topological relationships. A well designed model or data model allows for efficient analysis of the system behavior. The Arc Hydro Data Model (AHDM) was selected as the database schema for this project because it supports the fundamental data that must be used in this project; while being extensible, flexible, and adaptable to our modeling and web-based applications.

Water resources data are often managed differently for a surface water system versus a groundwater system; we elected to build separate databases in this stage of the project: an Arc Hydro Surface Water (AHSW) geodatabase, and an Arc Hydro Ground Water (AHGW) geodatabase. We are maintaining two separate databases at this stage because it allows us to better manage the subtasks and avoid duplication of effort. The basic framework of the AHGW Geodatabase is represented in Figure 5, which shows the relationship between the database features/objects and the real world.

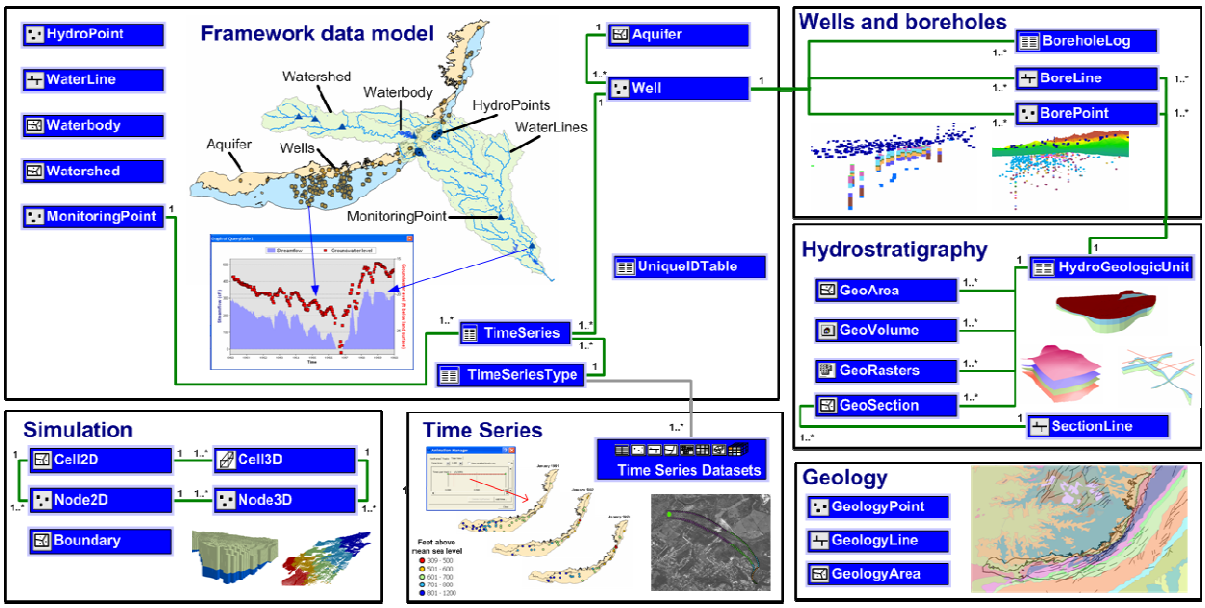

Figure 5. Arc Hydro Data Model (AHDM) Framework

Wells, boreholes, aquifers, and hydrogeologic units are some of the main features commonly used in groundwater studies; thus, are represented in the AHGW geodatabase. The AHDM (Figure 5) was built in ArcGIS™ and is dependent on the objects available in ArcGIS; therefore, objects such as points, lines, and polygons are used to represent the main features of a groundwater system (wells, boreholes, aquifers). These objects are related to tabular data that represent a 3rd dimension (depth or elevation) and/or a 4th dimension (time).

Three-dimensional (3D) Geologic Modeling

3D geologic modeling, visualization and volume calculation are essential for in-place nature resource evaluation. A fully attributed 3D geologic model of the Piceance Basin is developed for this project to support groundwater modeling, and spatial referencing of the dynamic systems model. The 3D geologic model was built based mainly on the USGS Fischer Assay, Geologic Tops data, and 10 meter DEM.

In order to make a reliable 3D geologic model, a lengthy process of model QA/QC was conduct to correct issues in the model. The process involved signaling out each interpolated surface and verifying data distribution and resulting structure representation. The final top surface for the Mahogany Zone of the Green River formation is shown in Figure 6. The digitized structure information from USGS geologic maps is overlain on the surface interpolation to verify consistency in the layers. This was done for all twenty-two

surfaces currently in the model. Approximately 50 to a 100 data points were added to each surface based on keeping consistency in the structure and average layer thickness to fill out missing sections of the original data. From these layers then a full basin scale model was reconstructed at various grid resolutions (Figure 7). Once this was completed then cross sections could be extracted from the model and exported to a 3-D geospatial dataset in the project database. These layers and cross sections than can be served out via ArcGIS service and accessed through ArcExplorer (Figure 8).

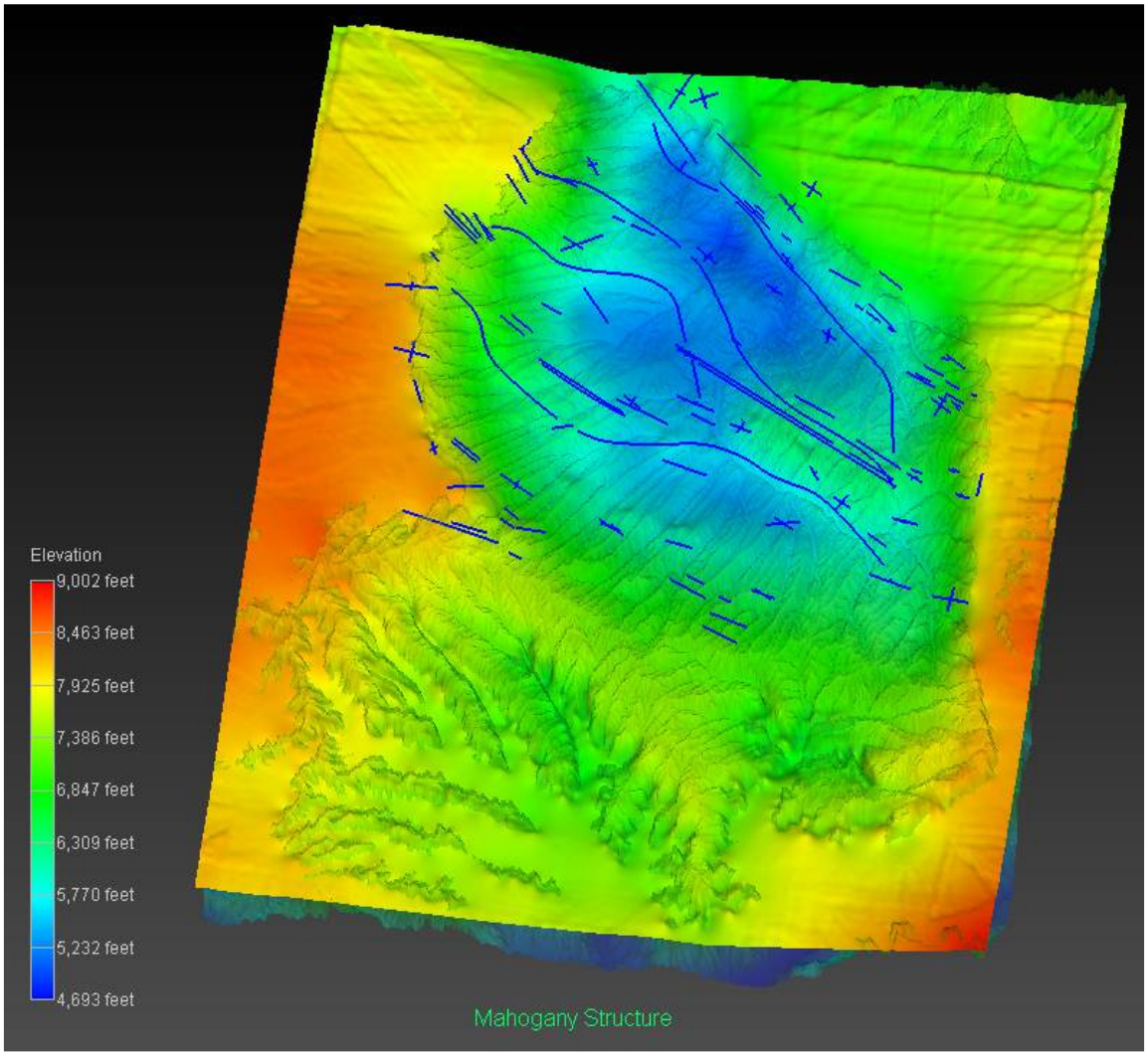

Figure 6. Image of the top of Mahogany surface in the Green River Formation colored by elevation which reveals the layer structure which is then verified via the USGS structural interpretations.

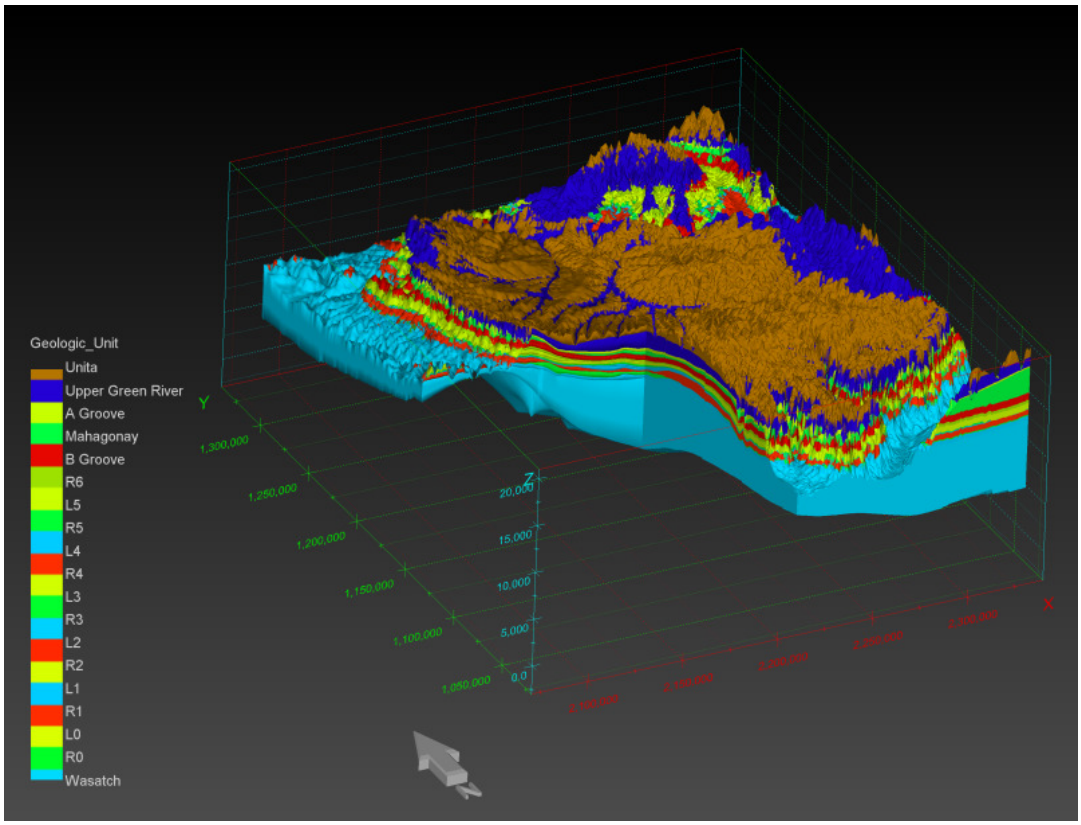

Figure 7. Output of a basin wide model post QA/QC with a vertical exaggeration of 10 times.

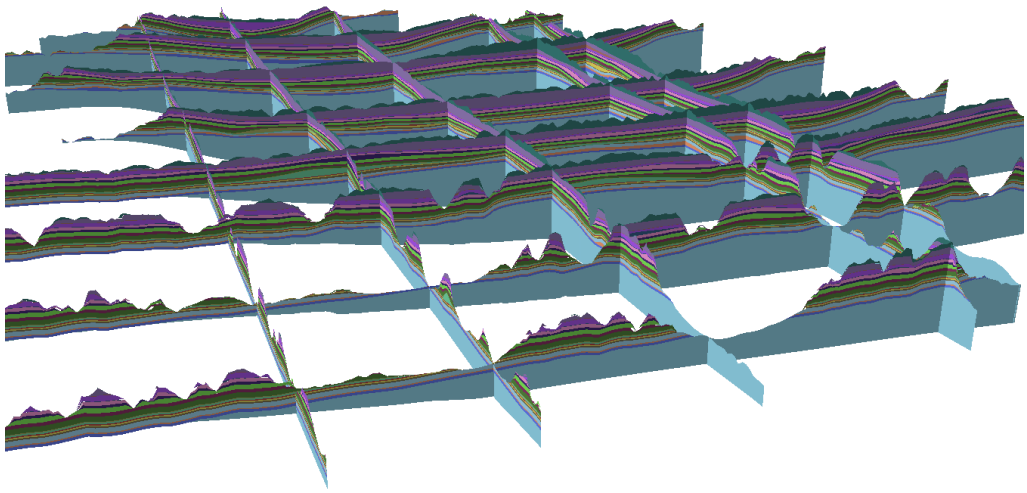

Figure 8. A fence diagram in ArcGIS stored in a 3-D dataset in the project database exported from the 3D geologic framework.

As part of the 3D geologic framework output and input file generation for the retort systems model an initial retort-distribution grid was created to generate individual retort cells for detailed data interpolation (Figure 9). Each grid cell than can be input into the 3-D geologic framework to create a retort block (Figure 10). Other datasets then can be interpolated into the 3D retort framework including fisher assay resource assessments, water content, fracture distribution and hydrogeologic parameters (Figure 11). The intention of the generating the individual retort cells is then to produce data input files for the Systems Dynamic Model. This will then facilitate specific spatial locations for water use curves needed to process each retort or grid within the model.

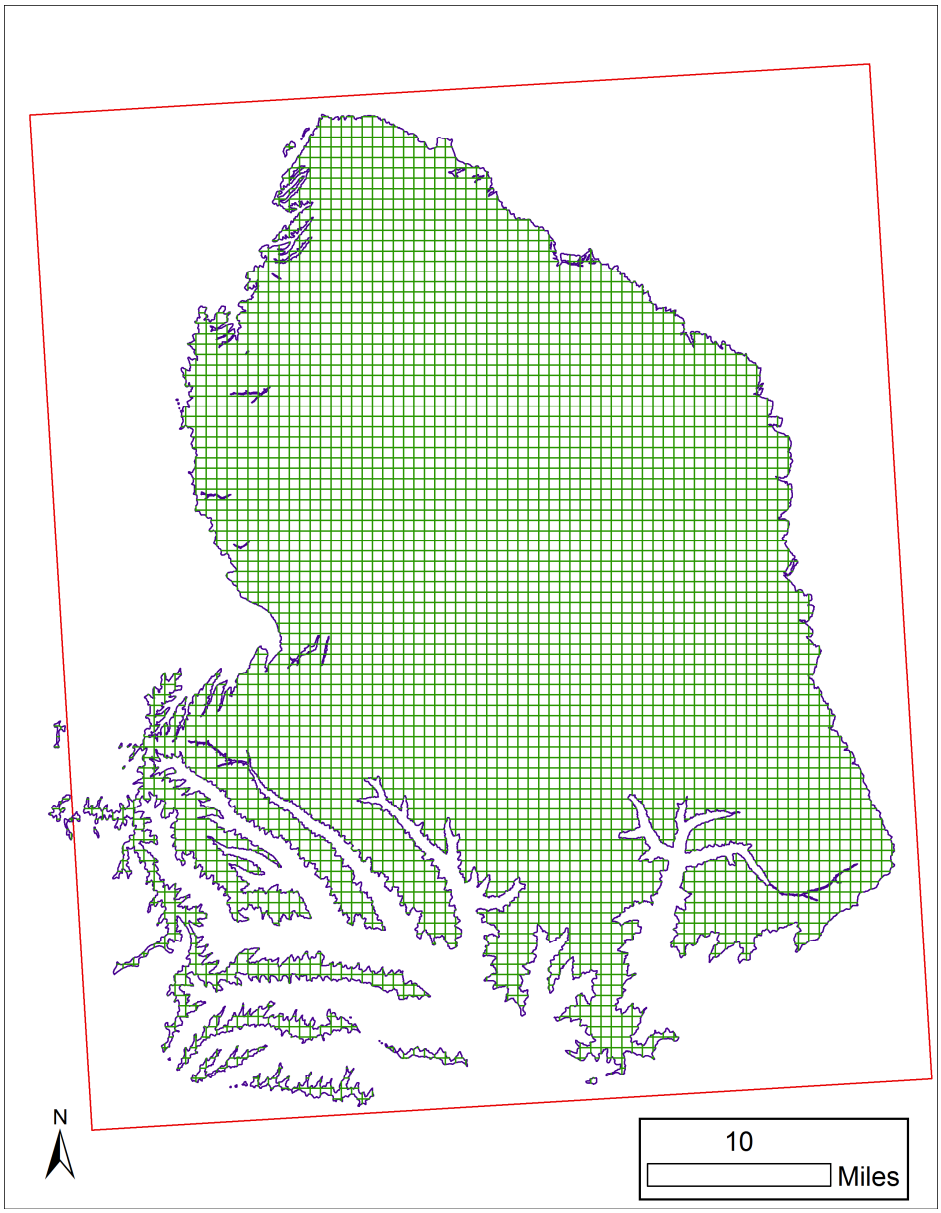

Figure 9. Map of initial grid used to generate spatially tied retort cells within the 3-D geologic framework.

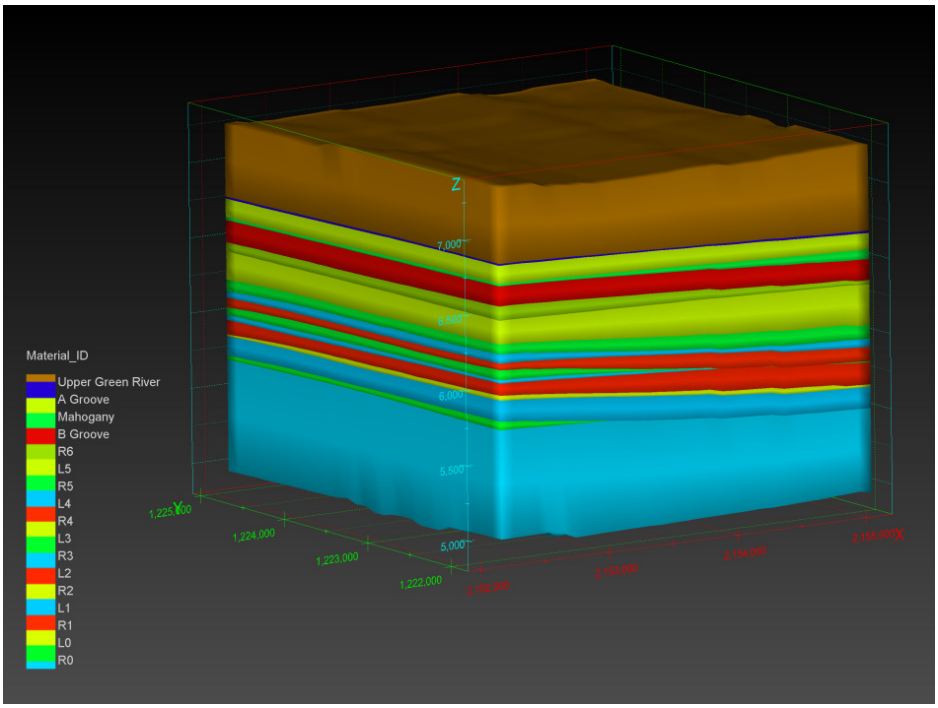

Figure 10. Single retort cell within the Green River formation. Cells size is 3000 x 3000 x 2300 ft XYZ.

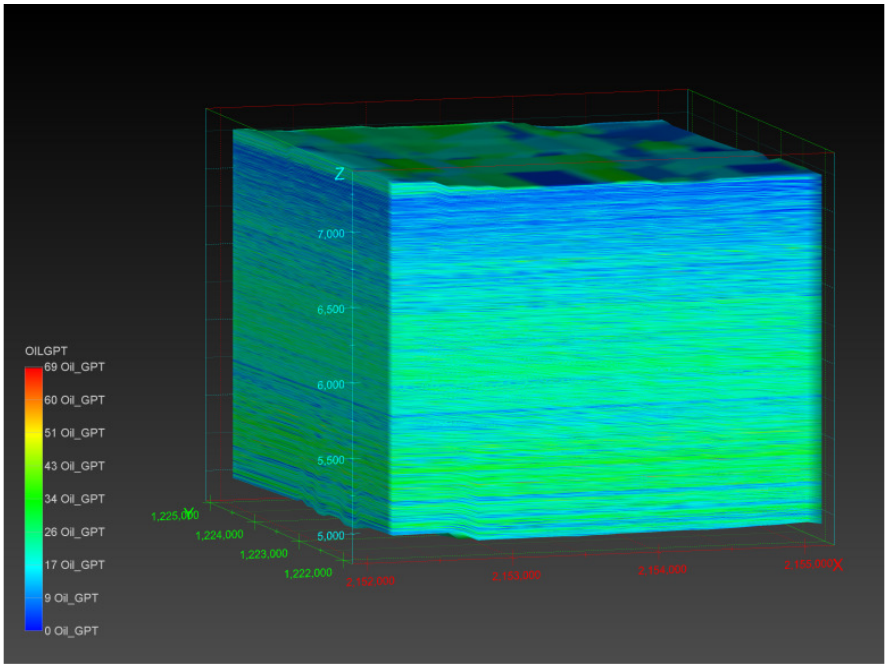

Figure 11. Image of Fischer Assay data, oil shale resource gallons/ton, interpolated into extracted retort framework.

Subtask 2.3 Regional "baseline" data manipulation and customized GIS analytical tool development

Data processing is frequently needed before data were integrated into geodatabases. Customized tools in the format of MATLAB scripts and ArcToolBox model were developed around this project. We have been developed (not necessarily in this quarter) five MATLAB scripts for this project during the past quarters.

- MatLab script that reads raw climate data files and populates Arc Hydro format tables.
- MatLab script that reads data exported from an Arc Hydro format database query and generates climate input files of met stations and DayMet data for the surface water model WARMF.
- MatLab script that reads data exported from an Arc Hydro format database query and generates flow input files of stream gauges and diversions for the surface water model WARMF.
- MatLab Scripts for Processing USGS Tops Data into an MVS input file
- MatLab script for automatic generation of WARMF diversion .FLO files.
- MatLab script that post-processes the results from WARMF model

In addition to MatLab scripts, Several GIS analytical tools (i.e., ModelBuilder models) were developed to process hydrogeologic data directly from the AHGW Geodatabase. The goals of the collective analytical tools were to build a three-dimensional (3D) hydrogeologic framework model that could be used as the foundation for a groundwater flow model.

ArcGIS ModelBuilder models were stored in a GroundWaterToolbox and tested in the first two years of the project performance period. Analytical tools included:

- ComputeRasterSurfaces Tool – designed to compute raster surfaces for the top of geologic zones based on borehole x, y, z input or from contour input
- ComputeMultipatch Tool – designed to build vector-based multipatch feature classes that represent geologic volumes
- VolumeCalculation Tool – designed to calculate the volume of geologic zones by computing the difference between a user-specified top zone and bottom zone.

A series of rasters, tins, and multipatches were constructed using ModelBuilder tools and data in the groundwater geodatabase. Rasters of saturated thickness were com-

puted by taking the difference between the elevations of the tops of successive layers. Modeled saturated thickness of the Mahogany zone ranged from 13 to 249 feet, with a mean thickness of 137 feet. Modeled thicknesses for other layers were highly variable and in some cases very unrealistic. It was desirable to produce reasonable saturated thickness values directly from the raw data in the groundwater geodatabase; however, prior attempts to use Fisher Assay data points yielded even more unrealistic outputs. The difficulty in producing a reasonable hydrogeologic framework was likely due to the basin shape and sparseness of data, particularly around the basin perimeter.

After considerable effort to automate construction of a GIS-based 3D hydrogeologic framework with ArcGIS ModelBuilder, the output datasets were inconsistent with the conceptual model. For example, layers that were lower in the stratigraphic column (i.e., Lower Aquifer) were computed to be higher elevation than overlying layers (i.e., Mahogany). These erroneous results were observed at the perimeter of the basin where the "dip" of the stratigraphic units was greatest due to the basin shape. Therefore, the analytical tools were of little value to the project and deleted from the geodatabase. Top and bottom elevations of the Upper Aquifer (UA), Mahogany Zone, and Lower Aquifer (LA) were manually manipulated as part of Task 5.0 and stored in the Lay1_node, Lay2_node, and Lay3_node feature classes of the MODFLOW_input feature dataset.

Subtask 2.4 Web-based GIS development

A Dell R710 GIS server has been set up to house the databases on SQL Server and host an ArcGIS Server website. The server appliance (known as Caprica6 by the CSM team) is installed in a secure environmentally controlled data center on the CSM campus.

The project team selected the Adobe Flex API to develop custom map interface for the rich internet application. The Adobe Flex API provides high level ArcGIS functionality with a modern Web 2.0 graphical user interface, GUI. An Adobe Flex 2.2 coding platform was installed on the project server which includes the Adobe Flash Builder 4 interactive development environment, IDE. The development environment was configured for the Piceance basin ArcServer project to include a ESRI ArcGIS Server for Flex coding library. Currently the web mapping interface is being developed to run within the Adobe Air runtime environment and will be migrated to a full internet application to be deployed via an IIS service using the development server. Version one of the Flex application is expected to be up and running by the end of the first quarter in 2011 to replace the current out-of-box ESRI mapping application that provides the current web mapping interface.

Flex 3D Viewer Development

A method is being researched for displaying 3D GIS files via the Arc Server and the web mapping interface. Currently ESRI does not have an "out of box" application for 3D isometric viewing in the Flex API. One option is to create an Arc Explorer data service to use in the free Arc Explorer viewer which is similar to Google Earth. This is an acceptable and easy option to implement. Though it requires the user to have Arc Explorer installed and is not optimum to view 3D multipatch files that represent subsurface objects. Another potential option was found in an opensource code library called Papervision3D to render 3D multipatch files in Flash isometric viewer window. This is still in a development phase but a general work flow has been established. Workflow for 3D Viewer Development is as followings:

1. Export ArcGIS Multipatch File to a Collada (.dae) file using ArcToolbox. A Collada file is an opensource XML format for creating 3D files.
2. Open Collada file in Maya 2011 an Autodesk 3D development program.
3. Export file from Maya using a OpenCollada plugin. This step formats the XML based .dae file with the proper options and headers for consumption in the PaperVision3D Flex plugin.
4. Import new Collada file into a Flash Builder project file and link to viewer code (Figure 12).
5. Compile and run Flash 3D viewer to display 3D GIS object (Figure 13).

Development Issues to Overcome:

1. Addition of Colors and Textures to 3D files in Flash viewer
2. Performance of rendering and caching through remote web viewer.

```
package {
	import flash.events.Event;

	import org.papervision3d.events.FileLoadEvent;
	import org.papervision3d.objects.parsers.DAE;
	import org.papervision3d.view.BasicView;

	[SWF (width="800", height="600", backgroundColor="0x223344", frameRate="30")]

	public class DAE2 extends BasicView
	{
		public var dae:DAE;

		public function DAE2()
		{
			super(800, 600, false);

			dae = new DAE();
			dae.load("assets/OpenCOl_Maya_Test.dae");
			//dae.load("assets/torusknotbaked.dae");

			scene.addChild(dae);
			dae.scale = 1;
			camera.fov = 40;
			camera.z = -200;

			addEventListener(Event.ENTER_FRAME, enterFrame);
		}

		public function enterFrame(e:Event) : void
		{
			dae.yaw((400-mouseX)*0.03);
			dae.pitch((300-mouseY)*0.03);
			singleRender();

		}
	}
}
```

Figure 12. Code for implementation of 3D isometric viewer in a Flex API using the Papervison3D open source library.

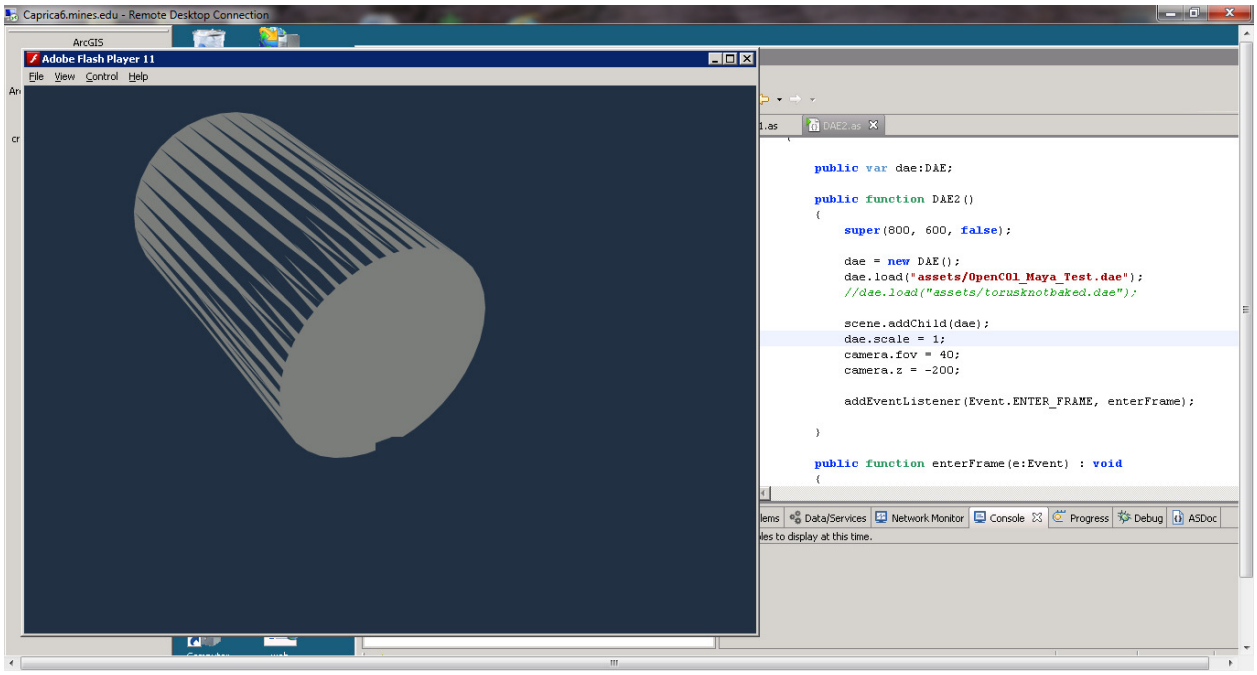

Figure 13. Screenshot of development level isometric 3D Flash Player rendering of ArcGIS multipatch object.

Data Downloading

The server server (known as Caprica6 by the CSM team) is installed in a secure environmentally controlled data center on the CSM campus. It is not a good choice for Caprica6 to host data download due to CSM firewall and data access restrictions. Never the less, the data downloads format would be for zip files for the entire geodatabase or multiple portions of the geodatabase, and documentation.

Task 3.0 Web-based Geospatial Infrastructure and data dissemination

Task 3.0 and subtask 2.4 are closely related. With the development of the project, the project team has decided that subtask 2.4 is a better way to disseminate data. The web-mapping site *subtask 2.4) has built to a level, such that it serves as a portal of the web-based geospatial infrastructure for this project and has the capacity for data dissemination.

Task 4.0 Energy Resource Development Systems Models: A Framework for Decision Support

As part of this project, researchers at Idaho National Laboratory (INL) constructed a system dynamic model to evaluate the water balance for *in-situ* oil shale conversion. The model is based on a systems dynamics approach and uses the Powersim Studio 9™ software package. Three phases of an in-situ retort were consider; a construction phase primarily accounts for water needed for drilling and water produced during dewatering, an operation phase includes the production of water from the retorting process, and a remediation phase water to remove heat and solutes from the subsurface as well as return the ground surface to its natural state. Throughout these three phases, the water is consumed and produced. Consumption is account for through the drill process, dust control, returning the ground water to its initial level and make up water losses during the remedial flushing of the retort zone. Production of water is through the dewatering of the retort zone, and during chemical pyrolysis reaction of the kerogen conversion. The major water consumption was during the remediation of the in-situ retorting zone.

A detailed description of the System Dynamic Model is given below. The complete Water System Dynamic Model Report by INL (INL/EXT-12-27365 Revision 1) can be found in Appendix A of this report.

Systems Dynamics Model

The water usage model is based on three phases of in the overall development of the resource: construction, operation, and remediation. In each of these development stages, water usage is very different. During the construction phase water is primarily used for drilling and for dewatering the reservoir prior to heating. During the operation phase, water will be produced from the reservoir as a result of the heating and subsequent conversion of organic matter and dehydration of minerals. During the remediation phase, water will largely be used to flush the reservoir to remove heat and potential contaminants. In addition, water will likely be used to re-establish native plant growth at the surface. These interacting processes are simulated using a systems dynamics model that solves first-order differential equations in time to simulate the evolution of a system.

The model is constructed using the Powersim Studio™ (version 9.01), however, the energy and mass balance modules in the Operations phase were first simulated in the Stella computer code then transferred to PowerSim. Both system dynamic software packages consist of four key objects: levels (stocks), flows, auxiliaries (converters), and links (connectors) where the object names in parentheses used in Stella. Complex systems can be described by assembling these objects with proper descriptions of system characteristics.

- Levels (Stocks) –a reservoir that holds mass or heat.

- Flows –describe mass transfer between levels (stocks), or between the system and the surrounding environment.
- Auxiliary (Converters) –provide the parameters and equations used to calculate the flows or to summarize information.
- Links (Connectors) –show the flow of information through the system. What converters control what flows and how flows depend on the values of levels (stocks).

Using these four objects, a model of an *in-situ* retort was built.

Construction Phase

The three key uses/production of water during the construction phase are for drilling, reservoir dewatering and dust control. The modules used to describe water consumption/production during these activities are provided in the following sections.

Well Drilling

There are four types of wells that must be drilled to implement the oil shale development: 1) freeze wells, 2) heater wells 3) production/dewatering wells, and 4) and monitoring wells. To determine water usage we first calculate the number of required wells, then the time to complete the drilling, and finally the amount of water required for the activity.

Number of wells calculations

The number of wells is calculated from the input desired retort dimensions, and well spacing. Freeze wells are a fairly simple calculation of the calculated perimeter divided by the sum of the desired freezer well spacing and the freeze well diameter. Figure 14 illustrates the linking of the necessary variables to the calculation. This figure also uses the buffer zone distance to calculate the heater area, width and length. These values are used to calculate the number of heater wells (Figure 15) which is the products of the truncated value of 4*(heated area length)*(heated area width)/(heater well diameter + $(2)^{0.5}$*heater well spacing). The number of monitoring wells is set to a fixed value (currently 3).

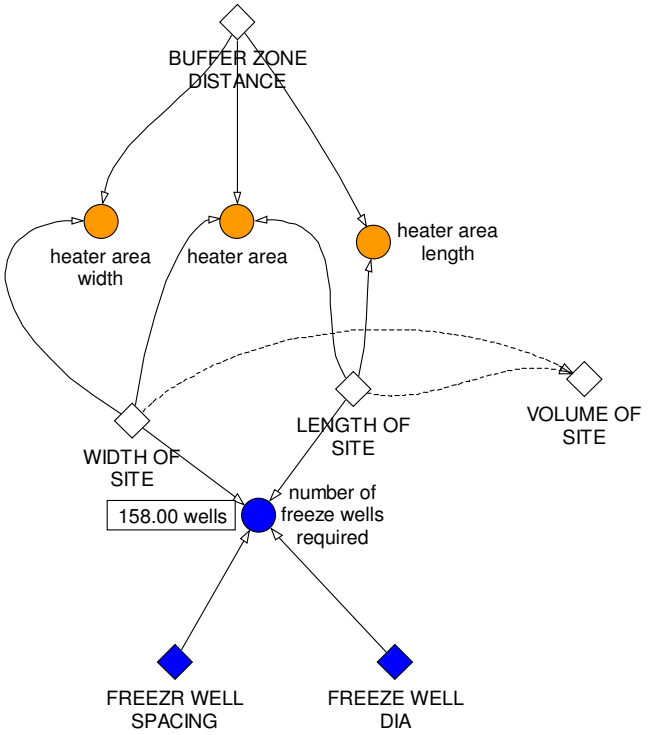

Figure 14. Calculation of the number of freeze wells, heated area width, length and area based on the inputted width and length of the site.

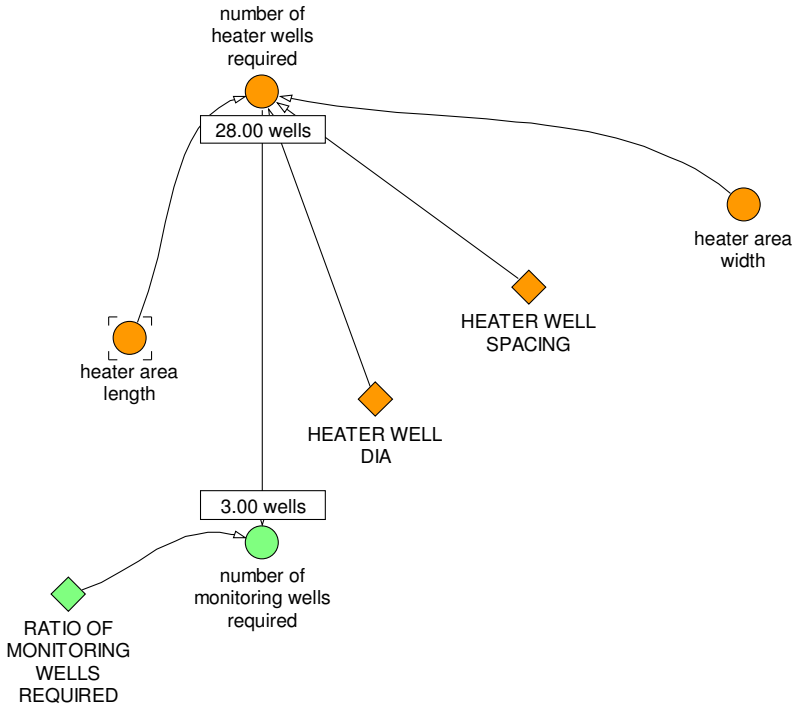

Figure 15. Calculation of the number of heater wells that are needed based on heated area calculations.

Time to complete well drilling calculations

Individual well drilling time is determined from the total depth of the retort below land surface divided by the estimated well drilling speed (Figure 16). In this case, the well drilling speed of 8 feet per hour calculated from the Shell's plan of operation statement that it required 2 months to complete 157 wells with two rigs. At this time, all wells are considered equal to the depth of the site, but the program was designed to easily change that assumption. It is also assumed that all wells have the same drilling speed regardless of use or the specific drilling rig used.

The sequence and timing of the drilling is calculated in a sequential fashion with the assumed order of that the freeze walls are first followed by the production/dewatering wells, heater wells, and finally the ground water monitoring wells. Variables used to calculate the total drilling time (Figure 17) are the number of drilling rigs and the time it takes to drill each well. All rigs are assumed to be working on the same set of wells at any time.

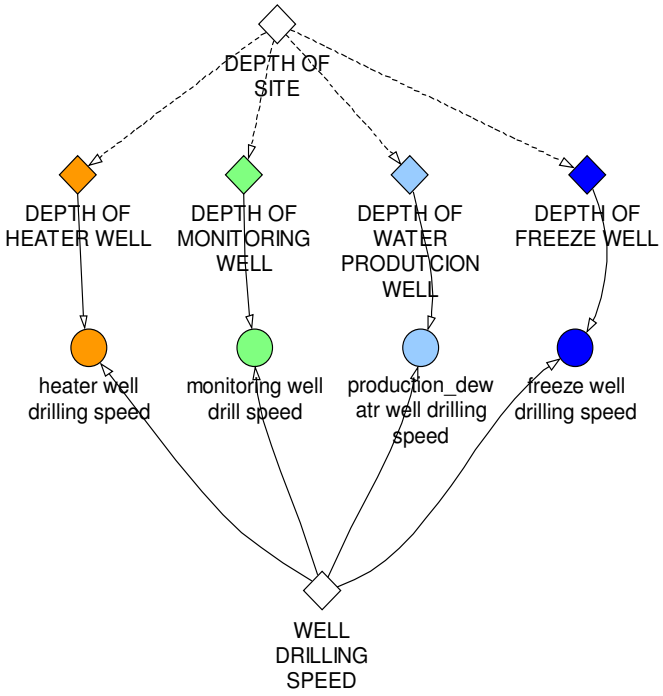

Figure 16. Calculation of the time it takes to complete each of the required wells.

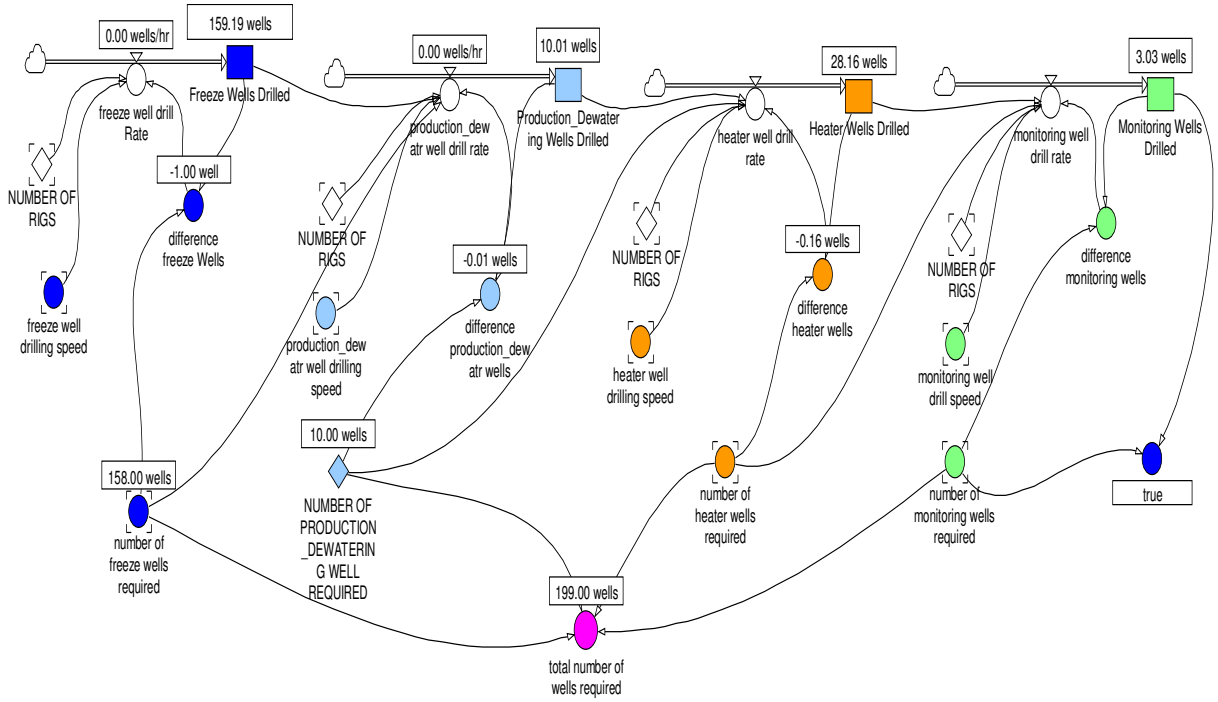

Figure 17. Calculation of the time it takes to complete all of the required wells.

Water usage calculation

Now that the number of wells needed and the time spent on each well is calculated, the amount of water required to construct these wells and the rate of water use can be determined. Drilling water use rate is calculated from the "drill lube and removal water requirement" (which can be thought as the volume of drilling fluids needed to fill the hole as the bit advances) multiplied by the drilling speed, plus the mud and seepage loss all multiplied by the recycle efficiency (Figure 18). In our case, the "drill lube and removal water requirement" is assumed to be 10 gallons per foot of drill advancement, mud loss and seepage loss. In our case, the mud loss makes up the greatest portion of the water use (about 5 times the amount of the seepage and drill bit advance combined).

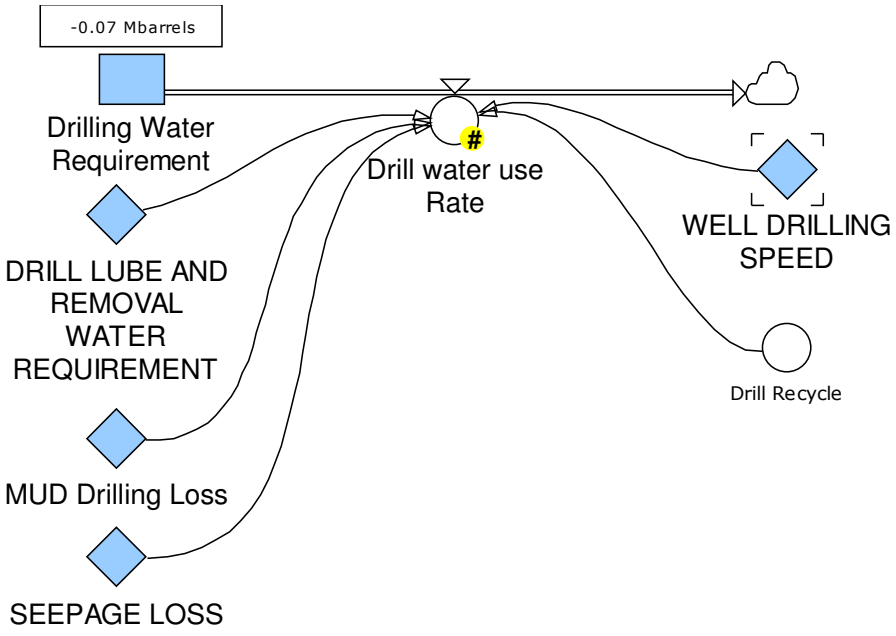

Figure 18. Calculation of drilling water rate.

Reservoir Dewatering

Prior to heating of the oil shale, water contained in the pore space of the oil shale retort volume will be removed by pumping. The volume of water to be removed is calculated from the volume of oil shale within the freeze wall and the effective porosity of the oil shale. A logic variable "dewater start" is used to initiate the dewatering of the retort volume once the freeze wells are in place. The rate of water extraction is a function of the user defined pumping rate for each well multiplied by the number of water production wells. At this time, the pumping rate is set as a constant but could be modified at a later date to be a more realistic function. The amount of water to be pumped from the retort is determined from the effective porosity multiplied by the retort volume.

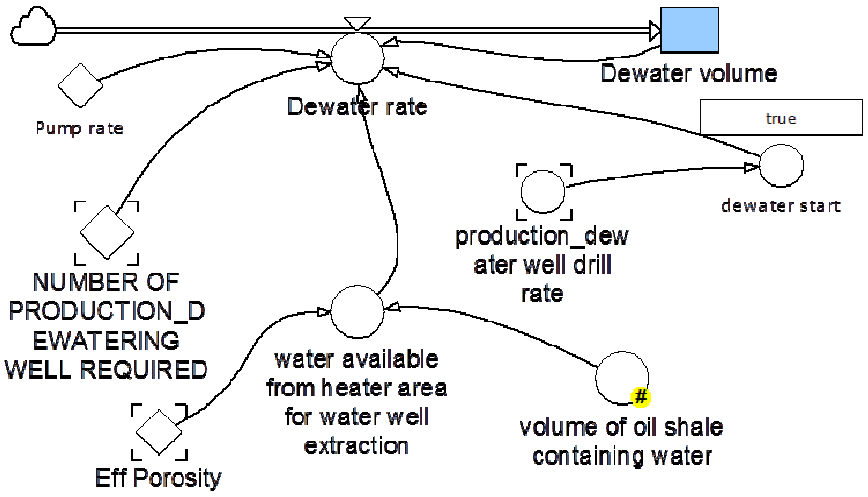

Figure 19. Calculation of water extraction rate.

Dust Mitigation

Dust mitigation is assumed to be a constant rate of water use based on delivery of one 10,000 gallon truck delivered to the site each day (equivalent to 3 gpm). To determine the total amount of water during drilling, the dust mitigation rate is added to the drill water use rate for the time required to drill the wells. Total water usage during construction was 0.16 Mbarrels for this example. Main water uses were for dust mitigation and drill. Dust mitigation resulted in 0.09 Mbarrels of water required. Drilling water requirements were slight less at 0.07 Mbarrels.

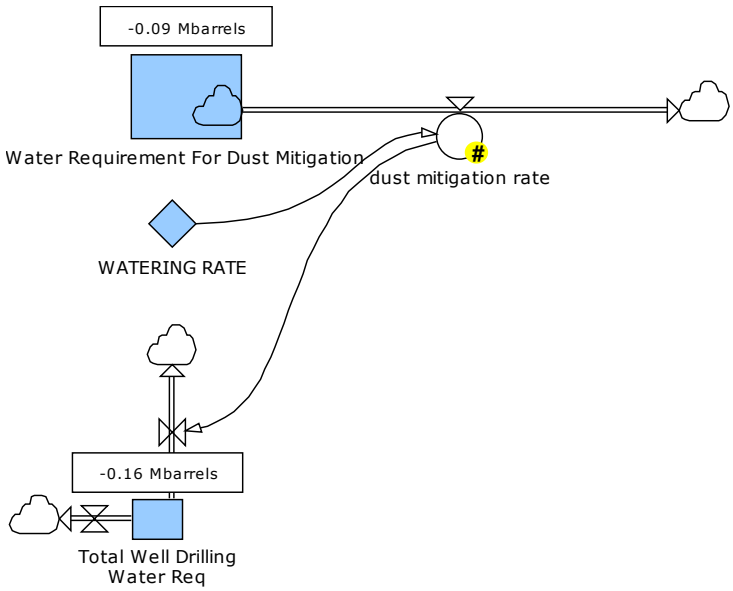

Figure 20. Calculation of dust mitigation rate.

Operation Phase

The second phase of oil shale development is the operation of the retort. A simple model is used to calculate the temperature increase in the retort. *In-situ* retort heaters are often designed in terms of their power output in kilowatts (kW). Therefore we will input heat into the retort and calculate the temperature of the retort. The temperature will be used to update the heat capacity, phase change and reaction kinetics. The operation model will be composed of 5 components; a temperature/pressure model to update properties, a heat model, a rock model, a water model and an oil/kerogen model. The energy and mass balance modules in the were first simulated in the Stella computer code then transferred to PowerSim.

Temperature / Pressure model

The retort is assumed to start off in equilibrium with the natural geothermal gradient and the natural hydrostatic pressure head. Using the geothermal gradient of 34 ºC km^{-1} (Blackett 2004) and an overburden thickness of 330 m, and a retort zone thickness of 330 m gives a median retort initial temperature of about 25 ºC. Hydrostatic head calculated for the same depth is 3000 kPa.

The relation between temperature and heat is important for the retorting operation. There is a causal loop relation between temperature and heat through the specific heat of the components of the retort. The specific heat is a function of temperature, and the relation between temperature and heat depends on the specific heat. The relation between heat and temperature for a system is given by:

$$Q_s = \sum_i m_i \left(s_i T + v_i \right) \tag{1}$$

where:

Q_s = total heat in the system (J)
m_i = mass of component i (kg)
s_i = specific heat of component i (J kg^{-1} K^{-1})
T = temperature of system (K)
v_i = heat associated with any phase changes (J kg^{-1})

Equation 1 can be solved for T, and used to calculate temperature from the total heat and the masses of components in the retort. Thus, heat is the independent variable, and temperature is the dependent variable.

The properties of water and steam as a function of temperature and pressure have been extensively studied and very comprehensive, and complicated, equations defining the properties of water as a function of these two state variables have been developed (Haar, Gallagher, and Kell 1984). For our purposes, simple relations were determined by fitting equations to data using a non-linear, least squares fitting program. The equations are given in the text, and plots are shown that illustrate the fit of the equations to the data.

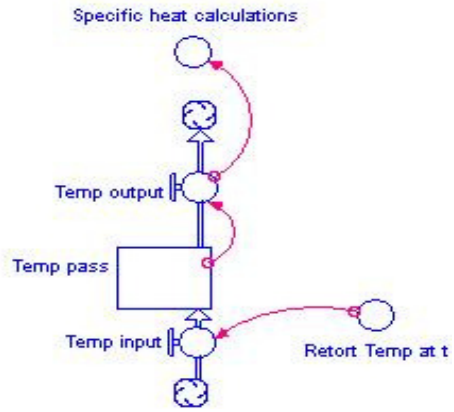

Figure 21. Stella routine to pass temperature between time steps.

The component's specific heat in the model are functions of temperature. Therefore, a feedback loop is included in the model (see Figure 21) that saves the current retort temperature, and allows it to be used in the next time step to calculate the specific heats for the next time step. Temperature variable specific heat is included in the model for water, steam, rock, and kerogen. Temperature-dependent specific heat of vaporization of water is also included. Pyrolysis is endothermic, and some heat will be consumed in the reaction. This consumption of heat for pyrolysis is not included in the model.

Specific heat of water and steam

The specific heat of water is relatively constant from 0 to about 300 ºC (

Figure **22**). Above that temperature, it rises sharply reaching a peak at the critical point. In this model, the equation for specific heat is extrapolated to as high in temperature as needed. This is not an important issue for water as water has all boiled off to steam long before the critical point is reached. The equation used for the specific heat of water is:

$$s_w = \frac{4163.773 - 0.02363 \cdot T^2}{1 - 7.1383 \times 10^{-6} \cdot T^2} \qquad (2)$$

where temperature is in ºC.

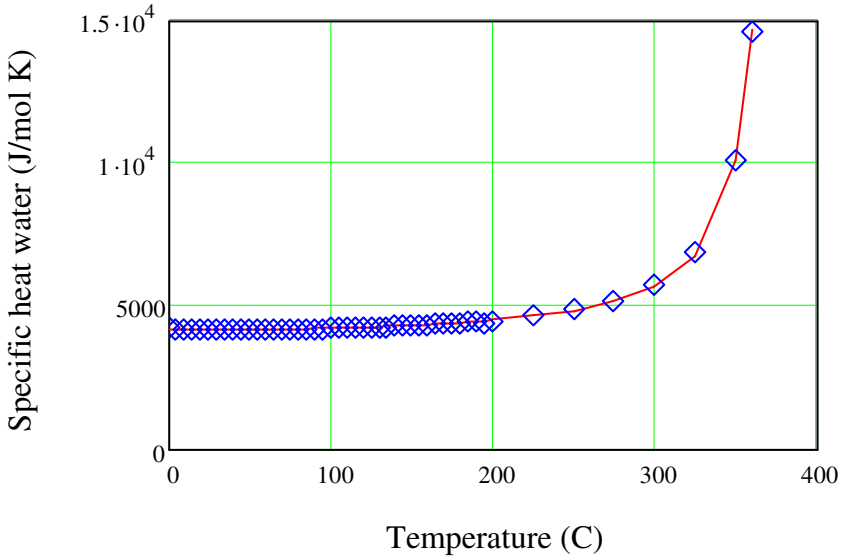

Figure 22. Specific heat of water as a function of temperature below the critical point.

The specific heat of steam increases gradually as a function of temperature. Data from the NIST chemistry web book were fit to a polynomial:

$$s_{st} = 1831.27 + 0.476158 \cdot T + 3.3172 \times 10^{-4} \cdot T^2 - 1.6206 \times 10^{-7} \cdot T^3 \quad (3)$$

This equation is continuous through the critical point of water, and so is used for all temperatures.

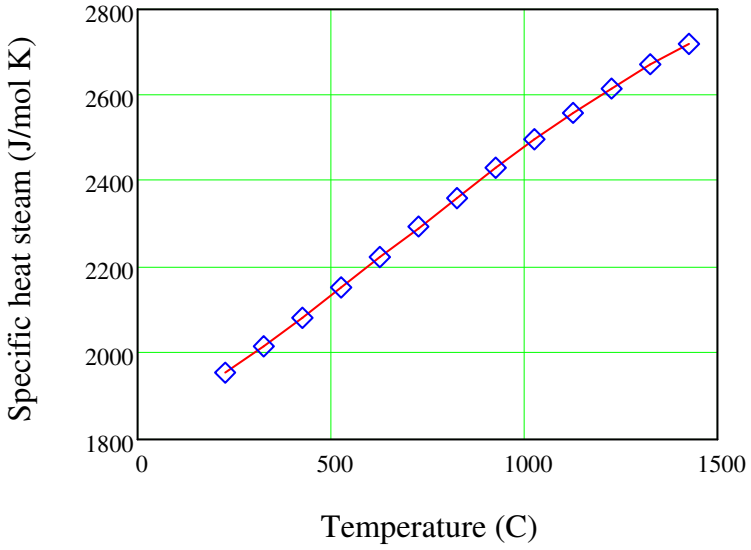

Figure 23. Specific heat of steam as a function of temperature.

The heat of vaporization of water is also a function of temperature (Figure 24). The heat of vaporization is not continuous through the critical point, as the heat of vaporization looses meaning above the critical point. As almost all phase changes between water and steam take place well below the critical point, this should not be a problem. A linear equation (dashed brown line) was fit to the heat of vaporization data below a temperature of 200 ºC to prevent negative values of heat of vaporization. The polynomial used is given by:

$$v_w = 2.5\times10^6 - 2649.8\cdot T \quad (4)$$

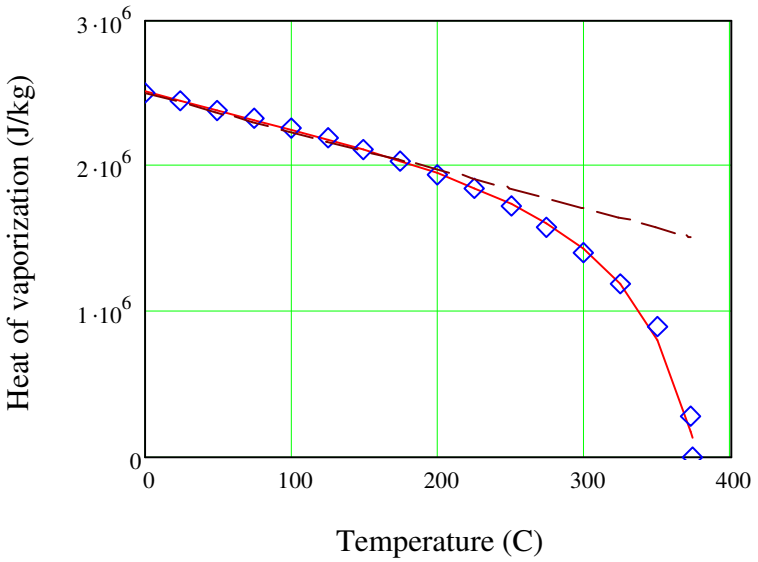

Figure 24. Heat of vaporization of water as a function of temperature.

Specific heat of rocks and kerogen

Data on the specific heat for a wide range of rocks and minerals was analyzed by Waples and Waples (2004). These authors found that the specific heat data as a function of temperature (ºC) were fit well by normalizing the data to the specific heat at 200 ºC. The polynomial used to fit the reduced data is plotted in Figure 25 and is given by:

$$s_r = 0.716 + 1.720\times10^{-3}\cdot T - 2.13\times10^{-6}\cdot T^2 + 8.95\times10^{-10}\cdot T^3 \quad (5)$$

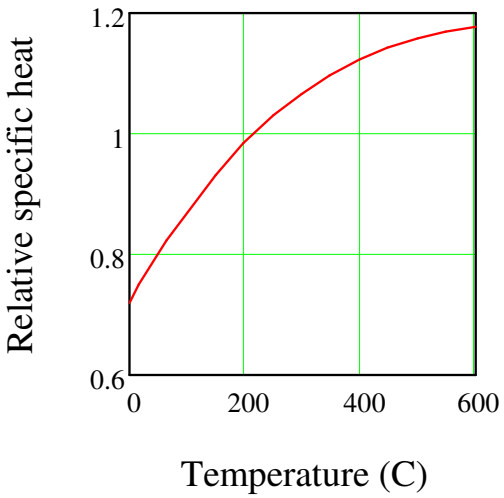

Figure 25. Reduced specific heat referenced to 200 ºC as a function of temperature.

This equation fits both the mineral matter in the Green River formation, and the kerogen content. The specific heat at 200 ºC for the kerogen is 1965 J kg^{-1} K^{-1} and for the shale is 1113 J kg^{-1} K^{-1} (Waples and Waples 2004).

Heat model

The primary objective of this exercise is to quantify the energy balance for an oil shale retort. We therefore need a model for the flow of energy into the retort, between the different components within the retort, losses of energy to the surrounding environment, and finally, the amount of energy extracted from the retort. This balance will drive the economics of the retorting process. Heat or energy is the proper variable to use in the retorting model, not temperature. Temperature is an intensive state variable that will depend on the heat in the system, but is not a conserved component. The relation between temperature and heat is given by equation l.

The primary object of the heat model is a stock identified as retort heat (
Figure **26**). This stock contains all the heat that is present in the reservoir. This heat is distributed among a number of different phases within the reservoir, but the sum total of heat is recorded in this one stock. The units for the stock retort heat are joules (J).

The initial condition for the amount of heat in this stock depends on the ambient temperature in the reservoir, the mass of other components in the reservoir, and the heat capacity of those components. For initial conditions, an ambient temperature was determined using the geothermal gradient of 34 ºC km^{-1} (Blackett 2004). From the Shell EIS, the overburden is about 330 m thick, and the retort zone is about 330 m thick. The median depth of the retort is then about 500 m. Sur-

face temperature is set at 8 ºC. This gives a retort initial temperature of about 25 ºC. Using Equation 1, an initial temperature of 25 ºC, the masses of other components in the retort, and the specific heat of those components at 25 ºC, the initial retort heat is calculated by the model.

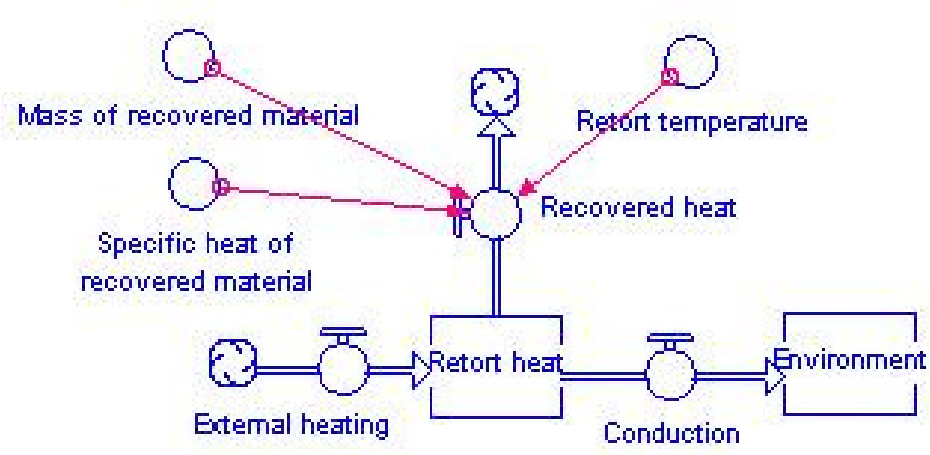

Figure 26. Heat model.

Two other stocks are included in the heat model, a stock for heat lost to the environment (i.e., the formation outside the retort), and a stock for heat recovered at the surface in produced products (steam, oil, and gas). These stocks sum the heat removed from the retort, and are initially 0 J.

There are three flows associated with retort heat: external heating, conduction to the environment, and heat extracted to the surface. As energy flows, the units are J day^{-1}. External heating represents the energy added to the retort to raise the temperature to induce pyrolysis of the kerogen. This is assumed to be a constant flux boundary condition. Two parameters are used to describe this heating; a heating rate in J day^{-1}, and a duration in days of total heating. The duration is used in a STEP function to turn off heating after the heating duration has elapsed. From the EGL EIS and the Shell EIS, heating durations on the order of several years are indicated. EGL provides a heating rate in their EIS of 2.1×10^{11} Btu yr^{-1} (6.1×10^{11} J day^{-1}). Heats of retorting are also given by EGL and by Rajeshwar et al. (1979) that give the amount of heat required to retort 1 kg of oil shale. These numbers range from 4.4×10^{5} J kg^{-1} to 1.7×10^{6} J kg^{-1} depending on the grade of the oil shale involved. Given some estimates of the mass of kerogen in the retort (~2×10^{9} kg, discussed below), and the heat of retorting, the total amount of heat needed to complete the retort can be estimated to be between 4×10^{14} and 1.6×10^{15} J. For heating rates on the order of 6×10^{11} J day^{-1}, the heating duration ranges from 1.8 to about 7 years. These calculations give us a range of heating rates and durations to serve as a starting point for defining the energy input to the retort, and are generally consistent with estimates provided by the energy companies.

Heat added to the retort will be lost by thermal conduction to the surrounding country rock. Thermal conduction is described by Fourier's law of heat conduction:

$$Q = -A \cdot k \cdot \frac{\Delta T}{\Delta x} \tag{6}$$

where

Q = heat transfer (J day^{-1})
A = area across which heat is conducted (m^2)
k = thermal conductivity (J m^{-1} day^{-1} K^{-1})
ΔT = temperature difference (K)
Δx = distance between retort and environment (m)

The thermal conductivity of Green River oil shale ranges from $6x10^4$ to $1.6x10^5$ J m^{-1} day^{-1} $ºK^{-1}$ (Rajeshwar et al. 1979). From geometry of the retorts given by Shell and EGL, the surface area of the retort is calculated to be 60,000 m^2. From the Shell EIS, which gives a distance of 75 m from the retort edge to the freeze wall, a distance to the environment is set at 75 m. The temperature difference is calculated from the difference between the retort temperature, and the temperature of the environment, 25 ºC. This is therefore a constant temperature boundary condition. Once the retort is up to temperature, the conductive heat loss will be on the order of $1x10^{10}$ J day^{-1}. We will assume that heat conduction is in steady state at all times. This is a large simplification as there will be a significant temperature transient during heating. For this model, we assume a linear temperature drop between the retort and the environment is maintained at all times and that the distance to the constant temperature boundary conditions does not change.

Once retort operations start, steam, oil, and gas will be produced from the retort. As these components are removed from the reservoir, they will carry a certain amount of heat with them. The amount of heat extracted from the reservoir will depend on the mass extracted, the temperature of the extracted component, the specific heat of the component, and any heat consumed by phase changes. Equation 1 is used to calculate the heat extracted from the retort by removing steam, oil, and gas. For steam, an extra term is added that accounts for the heat of vaporization of the steam. No heat of reaction or vaporization is included for oil or gas. For calculation of the heat extraction, the mass of extracted components is obtained from other calculations in the model. How these masses are calculated is discussed later. The equation used to calculate the flow of heat to the surface is:

$$Q = M_{st}\left(s_{st}T + v_{st}\right) + M_{oil}s_{oil}T + M_{gas}s_{gas}T \tag{7}$$

where:

Q = heat flow to the surface (J day^{-1})
M_{st} = mass of steam extracted (kg day^{-1})
M_{oil} = mass of oil extracted (kg day^{-1})
M_{gas} = mass of gas extracted (kg day^{-1})

s_{st} = specific heat of steam (J kg^{-1} K^{-1})
s_{oil} = specific heat of oil (J kg^{-1} K^{-1})
s_{gas} = specific heat of gas (J kg^{-1} K^{-1})
v_{st} = heat of vaporization of steam (J kg^{-1})
T = temperature of retort (K)

The heat extracted from the retort can be used on the surface in plant operations. However, no credit in the model is taken for this recovery of energy. Operations that do recover some of the heat from the retort would increase the overall efficiency of the operation.

Rock model

The rock model consists of two objects. There is a single stock that represents the mineral grains of the Green River shale formation. The second object is used to calculate the kerogen mass associated with the retort rock mass. We assume no geochemical reactions with regard to the mineral grains at the temperatures achieved by in situ retorting, so there are no changes in the rock model. The purpose of the rock model is to include the mass of inorganic solids into the calculation of the amount of heat needed to bring the reservoir to the desired temperature for pyrolysis. The mass of rock is calculated from the volume of the retort and the bulk density of Green River shale. The retort volume is calculated to be $6.37x10^5$ m^3. At a bulk density of 2500 kg m^{-3}, there is a total rock mass of $1.59x10^9$ kg. There are no flows to or from this stock.

A second component of the rock model is to calculate the mass of kerogen in the retort. This mass is then passed as an initial condition to the oil model. The kerogen model takes as input the grade of the oil shale in gal ton^{-1}, because this is the number most often used to describe how rich the formation is. The grade is determined from a Fischer assay of the oil shale. For this model, we assume the Fischer assay extracts all of the kerogen from a sample. The laboratory yield in gal ton^{-1} is converted to m^3 kg^{-1}, then multiplied by the oil density. This gives kg of oil generated. Not all kerogen is converted to oil, some remains as char and some is lost to gases. From the stoichiometry of the pyrolysis reaction (Campbell et al. 1980), we estimate that 69.5% of the kerogen is converted. Therefore, the kg of oil is divided by 0.695 to convert the oil to total kerogen. For an oil shale with a grade of 25 gal ton^{-1}, the grade is $1.04x10^{-4}$ m^3 kg^{-1}. Assuming an oil specific gravity of 35 °API (850 kg m^{-3}), the kerogen content of the rock is 0.127 kg kerogen per kg of oil shale. This is a typical number from the published literature. For the total rock mass in the retort, the total kerogen is calculated to be $2.0x10^8$ kg. The expected oil yield from pyrolysis is calculated to be $1.4x10^8$ kg or $1x10^6$ barrels. The kerogen model takes as input the grade in gal ton^{-1}, and calculates the kg of kerogen associated with the kg of oil shale in the retort. This is passed to the oil model as an initial condition.

Water model

The water model in the oil shale retort model is very important for the energy balance calculations. Water has very high specific heat, and the heat of vaporization of water to steam is also very high. Therefore, the heating and vaporization of water in the retort will play a very important role in heating of the retort. The water model consists of three stocks, one for water, a second for steam, and third for steam produced to the surface (Figure 27). These water and steam stocks are connected by a two directional flow representing boiling and condensation. Mass transfer through this flow will depend on the temperature and pressure of the reservoir. Connected to the steam stock is a flow from the retort to the surface that represents steam extraction. We assume no pumping of water from the retort to draw-down water in the system prior to heating. Because this activity would precede heating, it could be incorporated by changing the initial conditions in the water stock.

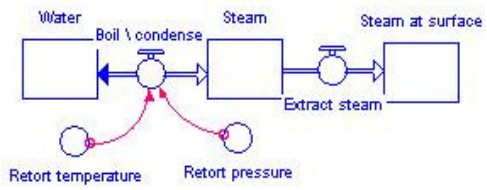

Figure 27. Water model used in Stella.

The steam stock is initially set to 0 kg. The water stock is initialized assuming the oil shale is water saturated. The initial mass of water in the stock is calculated form the volume of the retort ($6.37x1^{-5}$ m^3), the porosity of the retort (0.057), and the density of water (1000 kg m^{-3}). The initial water mass calculated in this way is $3.61x10^7$ kg. The flow that represents boiling and condensation of water is based on the pressure and temperature at which water boils or steam condenses in the retort. These calculations depend on the temperature and pressure of the retort. A very simplified model of the thermal properties of water and steam is included in the model. We assume that the system is constrained to the water - steam equilibrium curve. Retort pressure is equal to the saturated steam - water curve plus hydrostatic pressure. When, during heating, the vapor pressure of steam exceeds the hydrostatic pressure, water begins to boil. When cooling, when the pressure drops below hydrostatic pressure, water begins to condense.

Hydrostatic pressure is calculated from the mass of water above the retort, and is given by

$$\rho gh = 1000 \text{ kg m}^{-3} * 9.8 \text{ m sec}^{-2} * 300 \text{ m} = 3000 \text{ kPa} \quad (8)$$

where

ρ = density of water (kg m^3)

g = acceleration of gravity (m sec^{-2})

h = depth of retort (m)

The equation for steam pressure (P_v) in the retort in kPa as a function of temperature (ºC) is given by:

$$P_v = \exp\left(\frac{-0.534487 + 0.72 \cdot T}{1 + 0.00443 \cdot T}\right) \tag{9}$$

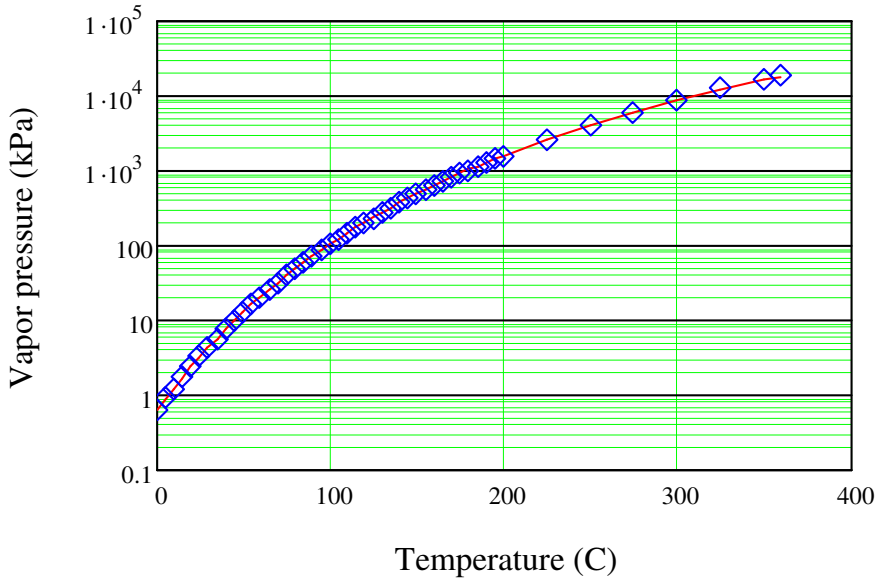

Figure 28. Vapor pressure of steam as a function of temperature used in retort model.

We can also solve this equation to calculate the boiling temperature (T_b ºC) of the reservoir from the hydrostatic confining pressure (P_c kPa):

$$T_b = \frac{7.00766 + 14.00823 \cdot \ln(P_c)}{1 - 0.06127 \cdot \ln(P_c)} \tag{10}$$

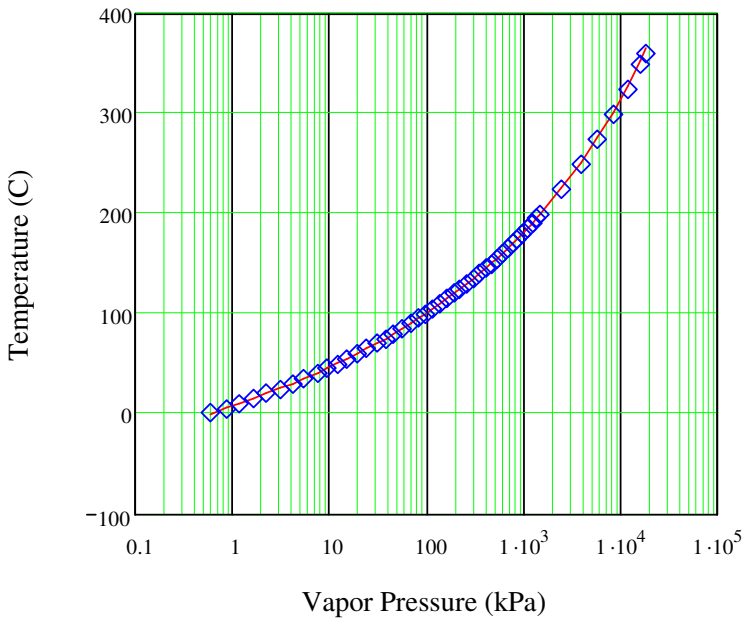

Figure 29. Function and curve to calculate boiling temperature from the hydrostatic confining pressure on the reservoir.

In the model, heat is added to the water raising the temperature. When the temperature of the retort exceeds the boiling temperature based on the hydrostatic pressure, then water begins to turn into steam. The logic of the calculation must allow for flow in both directions, that is both boiling and condensation. The equation used for the flow is:
If (confine_temp > retort_temp) then

$$M_{s\to w} = \frac{(T_r - T_c)\cdot M_s \cdot s_s}{v_s} \tag{11a}$$

else

$$M_{w\to s} = \frac{(T_r - T_c)\cdot M_w \cdot s_w}{v_s} \tag{11b}$$

When the retort temperature either exceeds the boiling temperature or drops below the boiling temperature, there is a temperature difference that has to be corrected. Multiplying this temperature difference by the specific heat of the phase and the mass of phase defines the number of joules needed to bring the temperature back into equilibrium. Dividing by the number of joules kg^{-1} consumed or liberated by the phase transformation reaction, gives the mass of phase transfer needed to bring the temperature back into equilibrium. Note that T_r–T_c changes sign giving positive and negative flows through this flow object.

The final component of the water model is a flow from the steam stock to the surface that represents extraction of steam from the retort. Flow to the surface is assumed to be a function of the amount of steam with a constant fraction of the remaining steam removed per unit time. This gives the mass of steam extracted to the surface (M_{st}) used in equation 7.

Kerogen / Oil model

Pyrolysis occurs in the absence of oxygen, so that the organic matter is broken down into less complex (shorter chain) organic molecules. Light, hydrogen-rich products are driven off, leaving behind a carbon-rich char. Formation of oil occurs at temperatures between about 400 and 500 ºC. Kerogen, with an initial C/H mole ratio of about 0.67 undergoes three pyrolysis reactions (Campbell et al. 1980; Huss and Burnham 1982):

1) Primary pyrolysis occurs between 350 and 500 ºC, oil is driven off generating a residual char with a C/H ratio in the range of 1 to 1.6;
2) Secondary char pyrolysis occurs between 500 and 650 ºC, hydrogen gas and methane gas are driven off, the residual char has a C/H ratio between 1.6 and 4.3.
3) above 650 ºC, hydrogen gas, ammonia, and hydrogen sulfide are driven off, leaving the char with little hydrogen.

Writing out the stoichiometry of the primary pyrolysis reaction, we get the following generalized (and much simplified) reaction for pyrolysis (Huss and Burnham 1982):

$$C_1H_{1.5}O_{0.05} \rightarrow 0.014\ CO_2(g) + 0.015\ H_2(g) + 0.012\ C_3H_8\ (g) + 0.018\ H_2O + 0.72\ C_1H_{1.7}\ (oil) + 0.228\ C_1H_{0.63}\ (char) \quad (12)$$

Temperatures during *in-situ* retorting will be constrained to less than 500 ºC, unless combustion is induced in the retort by introducing air. In writing this simplified reaction, we assume all O in carboxyl groups forms carbon dioxide, and that hydrogen is combined in hydrocarbon products with a C/H ratio of about 0.5 representing paraffins, olefins, and naphthenes. This indicates that about 20% of the initial carbon will end up in char. Converting the reactants and products in Equation 12 back to weights, we get that for each kg of kerogen pyrolyzed, the yield will be 0.043 kg of CO_2(g), 0.695 kg of liquid hydrocarbons, 0.037 kg of hydrocarbon gases, and 0.202 kg of char. The mass of hydrocarbons, or the lengths of the hydrocarbon chains, will range from methane to much more complex molecules. This range of molecules will result in a wide range of boiling points for the reaction products. As result, there will be a mix of volatile and liquid hydrocarbons, and the mix will vary as the retort temperature varies relative to the boiling points of the hydrocarbons.

The reaction kinetics of kerogen pyrolysis have been extensively investigated (Campbell and Burnham 1980; Braun and Burnham 1986; Bar et al. 1986; Skala et al. 1990). Experimental conditions have mainly covered the very high heating rates and atmospheric pressure conditions of surface retorts. Kerogen is a complex organic molecule, and is broken down into a wide range of product molecules during pyrolysis. The composition of the products will depend on temperature, pressure, and the heating rate. Therefore, a single, or even a series, of kinetic reactions can not readily describe the kinetics of kerogen pyrolysis. Most thermogravimetric analyses of oil shale response to heating, however, indicate that kerogen breakdown occurs in a single peak around 400 ºC (
Figure **30**). An additional reaction occurs at a temperature of about 700 ºC, but this is higher than temperatures expected for in situ retorting. Because the thermal gravimetric response shows a single peak, a number of authors have used simple one component models of kerogen pyrolysis.

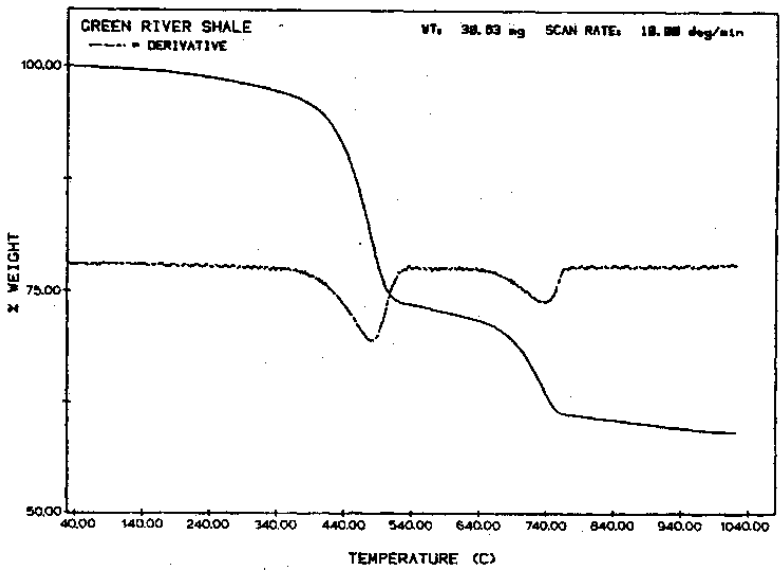

Figure 30. Thermal gravimetric and differential thermal gravimetric curves for a Green River oil shale specimen (Earnest 1982).

For systems that are too complex to be characterized in a fundamental way, it is common to describe the reaction in terms of a lumped pseudo species (Burnham and Braun 1999). A first order lumped parameter kinetic model was fit to kerogen decomposition by Campbell et al. (1978) and is adopted for this model. It is a single reaction model that describes the overall reaction of kerogen to oil. Combining this kinetic model with the stoichiometric model in equation 12, provides a means to model the retort. For a single first order pyrolysis reaction taking place under a constant heating rate ($dT/dt = C_r$), the rate of product evolution is given by (Burnham and Braun 1999):

$$\frac{dM}{dT} = \frac{-A_f}{C_r} \cdot \exp\left[-\frac{E_a}{RT} - \left(1 - \frac{2RT}{E_a}\right) \cdot \left(\frac{A_f RT^2}{C_r E_a}\right) \cdot \exp\left(\frac{-E_a}{RT}\right)\right] \quad (13)$$

where

E_a = Activation energy (J mol^{-1})
A_f = Preexponential frequency factor (day $^{-1}$)
M = Mass of kerogen (kg)
R = Gas constant (J mol^{-1} $^oK^{-1}$)
T = Temperature (^oK)
C_r = Constant heating rate (^oK day^{-1})
t = time (day)

Temperature and time are related by the heating rate so that the change is mass with respect to temperature can also be related to the change in mass with respect to time.

$$\frac{dM}{dt} = \frac{dM}{dT} \cdot \frac{dT}{dt} \quad (14)$$

Several studies have been conducted to measure the activation energy and frequency factor for oil shale pyrolysis. These have been conducted at both constant temperature increase and at constant temperature. Results of a few of these studies are summarized in Table 2.

Table 2. Compilation of kinetic rate parameters for oil shales.

Source Rock	Frequency Factor (day^{-1})	Activation energy (J mol^{-1})
Spanish[a]	$1.8x10^{13}$	150
Anvil Points[a]	$7.3x10^{20}$	247
Clear Creek[a]	$2.4x10^{21}$	254
Israel[b]	$8.0x10^{10}$	118
Anvil Points[c]	$2.6x10^{18}$	220

a. Torrente and Galan (2001)
b. Bar et al. (1986)
c. Campbell et al. (1978)

The temperature of maximum pyrolysis yield for kerogen falls within a narrow range of about 420 to 440 ºC (Huss and Burnham 1982; Clayton et al. 1992), but only for high heating rates; on the order of 2880 ºK day^{-1} (2 ºC min^{-1}). At lower heating rates, the conversion of kerogen occurs at lower temperatures (Figure 31). At the lower heating rates expected for an *in-situ* retort, the conversion should occur at lower temperatures.

Figure **31** shows that kerogen conversion can be expected to happen relatively quickly once temperatures reach the vicinity of 400 ºC.

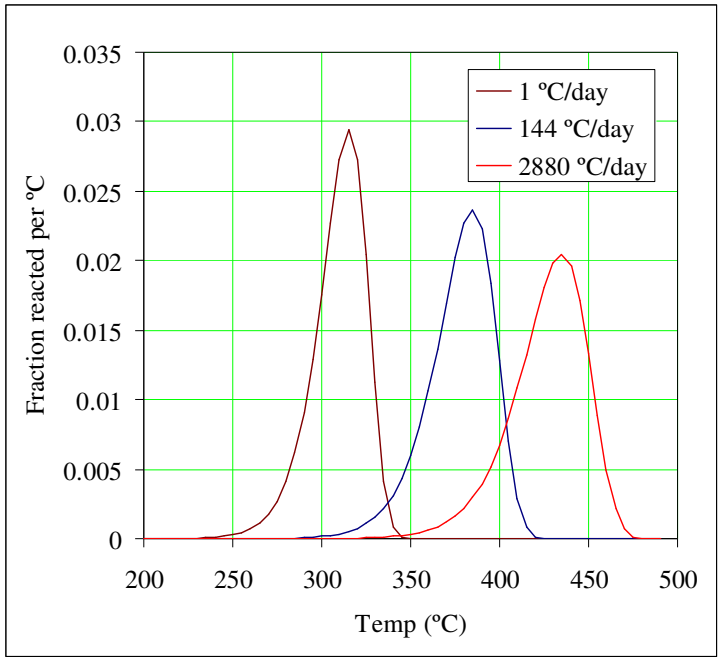

.

Figure 31. Mass reaction rate of kerogen as a function of retort temperature at different heating rates. Highest rates are representative of surface retorts. Lowest rate is more representative of in situ heating rates.

Surface retorting takes place at atmospheric pressures, so little work has been done on the effects of pressure on kerogen conversion. Burnham and Singleton (1983) investigated pyrolysis of Green River oil shale at pressures to 2.74 MPa (Figure 32). The experiments were kinetic experiments carried out at constant heating rate. They found a small decrease in oil yield with increasing pressure for the same heating rate. There are insufficient data to parameterize a pressure effect on pyrolysis of oil shale, so pressure was not included in the Stella model.

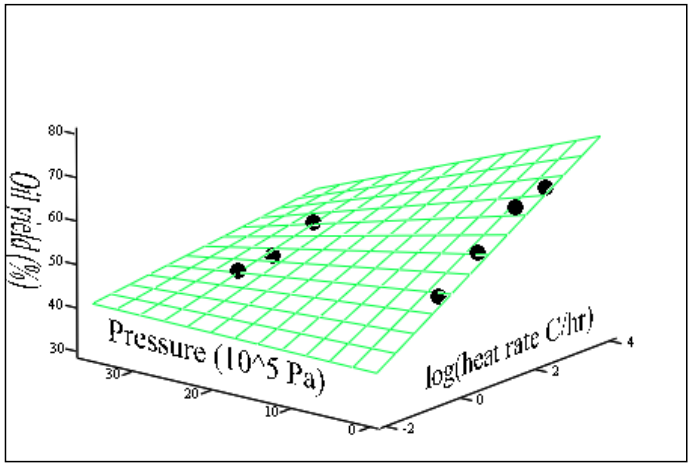

Figure 32. Effect of heating rate and pressure on oil yield (Burnham and Singleton 1983).

The kinetic model used to simulate kerogen pyrolysis is given by:

$$\Delta M = M_{t-1} A_f \cdot \exp\left(\frac{-E_a}{R \cdot T}\right) \cdot \Delta t \qquad (15)$$

The oil model calculates the mass of kerogen pyrolyzed in a time step using equation 15, then uses the mass fractions of products calculated from equation 12 to distribute mass to the product stocks (

Figure **33**).

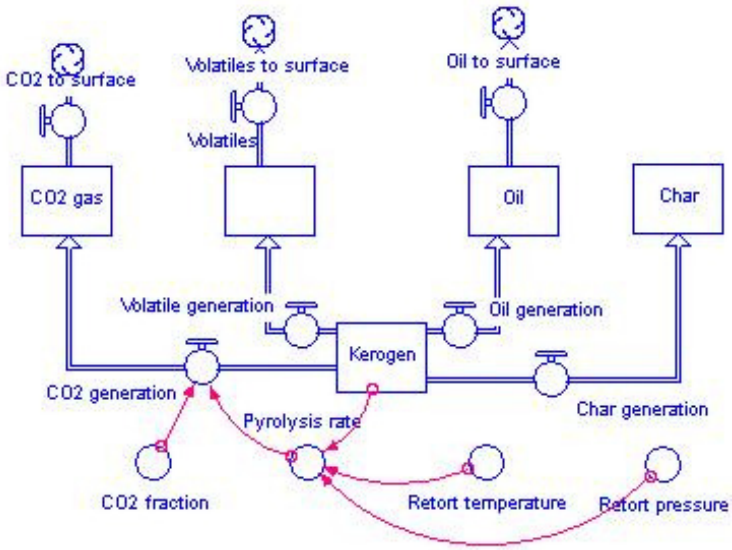

Figure 33. Model used to calculate the pyrolysis of kerogen to products in the retort. Calculation of flows is illustrated for CO_2. The other flows are calculated in the same fashion.

The initial kerogen content is calculated from the oil shale grade in the rock model. The other stocks are set to 0 as an initial condition.

Converters and Accumulators

There are a number of accumulators that keep track of the total masses of components extracted at the land surface. The amount of energy recovered in joules is calculated from the mass of oil and gas extracted at the surface. The Carbon Trust gives an energy content of oil of 12,751 kW hr ton^{-1}. This converts to a conversion factor of $4.6x10^7$ J kg^{-1} for liquid hydrocarbons. For hydrocarbon gas, the energy content is 11 kW hr m^{-3} according to the Carbon Trust. Because we generate kg of gas, the volumetric energy content must be converted to a mass based energy content. We assume that the gas is methane with a mass of 10 g mol^{-1} and use the ideal gas law to convert a volume of gas to kg of gas. The energy content of the gas hydrocarbons is calculated to be $9.7x10^7$ J kg^{-1}.

The model also accumulates carbon dioxide at the surface so that the generation of greenhouse gases from in situ retorting can be evaluated.

The model was run using a 1-day time step for a period of 4,000 days. The Runge-Kutta 4 integration method was used. A time step of 5 days gave results that differed by 0.2% from the 1-day time step. A time step of 0.5 days gave the same results as the 1-day time step. One day was selected for modeling runs.

Base Case Results

The model was simulated using the parameters discussed above. The grade of the oil shale was set at 25 gal ton^{-1}. As heat is added to the retort, the pressure and temperature increase until the vapor pressure of steam exceeds the confining hydrostatic pressure. This occurs at a temperature of 232 ºC at 860 days (

Figure **34**). The temperature profile flattens while boiling occurs as heat added to the retort is consumed by boiling. The pressure increases during boiling, and so the boiling temperature increases slightly and is not constant as it would be for atmospheric conditions.

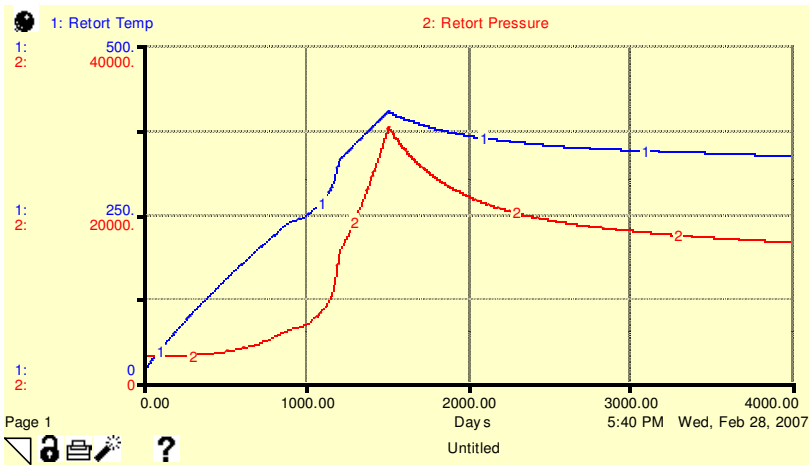

Figure 34. Increase in temperature and pressure with heating of the retort.

The rate of kerogen pyrolysis reaches a critical point at about 1100 days (

Figure **35**) and kerogen is rapidly converted to products. This rate of conversion is based on very small scale laboratory experiments, and may not be realistic for application to retort scale simulation. Measurements of the frequency factor and activation energy for the kerogen pyrolysis reaction show a wide range of values (Table 2), so there may be some uncertainty in this transformation rate. The laboratory rates predict complete conversion of the kerogen in about 200 days. Gas volatiles in the model are extracted rapidly and have been recovered at the surface by 1550 days.

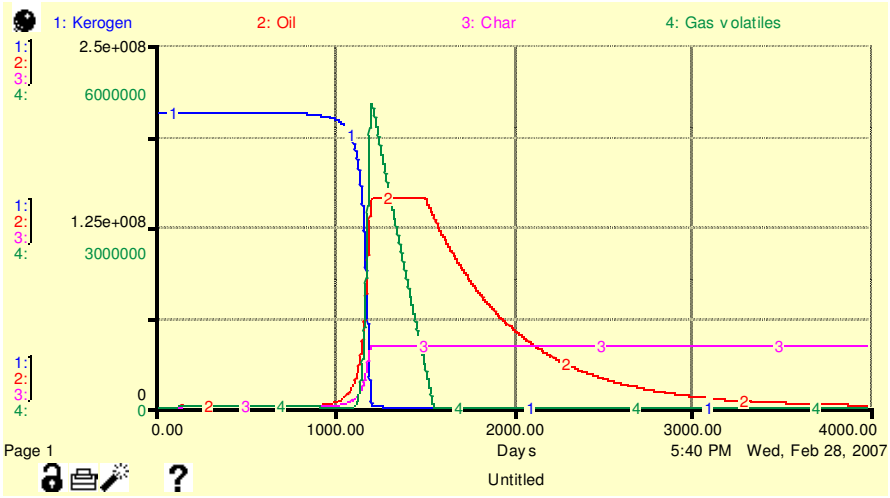

Figure 35. Distribution of kerogen and kerogen pyrolysis products as a function of time.

Most of the heat added to the retort goes to heating up the rock matrix (Figure 36). Water and kerogen also heat up. At day 860, boiling of the water releases all the energy contained in

water and transfers the energy to steam. There is more energy in the steam than in the water because the steam contains the heat of vaporization. About day 1100, the heat in kerogen is released as kerogen is pyrolyzed to gas and liquid hydrocarbons. As soon as the retort temperature rises above ambient, conduction to the surrounding environment serves as a heat loss. When heating stops on day 1500, heat in the retort begins to decline by conduction to the environment.

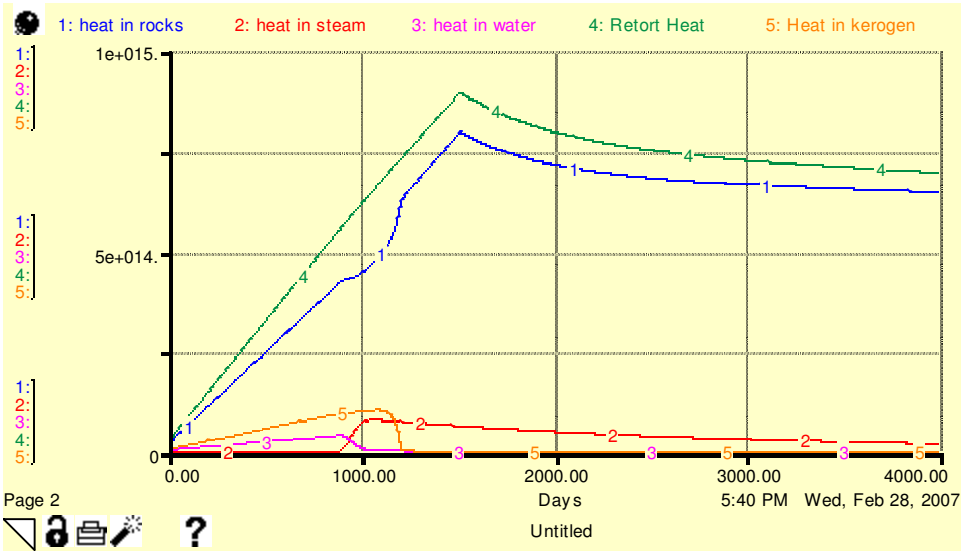

Figure 36. Distribution of energy (heat) in the retort during the first 1500 days.

The simulation indicates that the *in-situ* retorting produces much more energy than consumed to drive the pyrolysis reaction (Figure 37). A total of 9.4×10^{14} joules of energy are needed to bring the retort up to 400 ºC. The energy contained in the oil and gas withdrawn from the retort amounts to 7.3×10^{15} joules, or about 8 times the energy expended. Oil recovered from the retort (Figure 38) are 1.0×10^{6} barrels. Based on the initial estimate of 25 gal ton^{-1} as the grade of oil shale, the predicted recovery is 1.05×10^{6} barrels. To recover 1 million barrels of oil, 8700 tonnes of carbon dioxide are generated. This oil recovery is probably optimistic. There are only about 7400 barrels of oil left in the retort. It is unlikely that the oil would drain from the pores so completely. The factor of 8 energy recovery factor is probably optimistic by a factor of 2. This would suggest that something like 500,000 barrels of oil could be recovered from this retort.

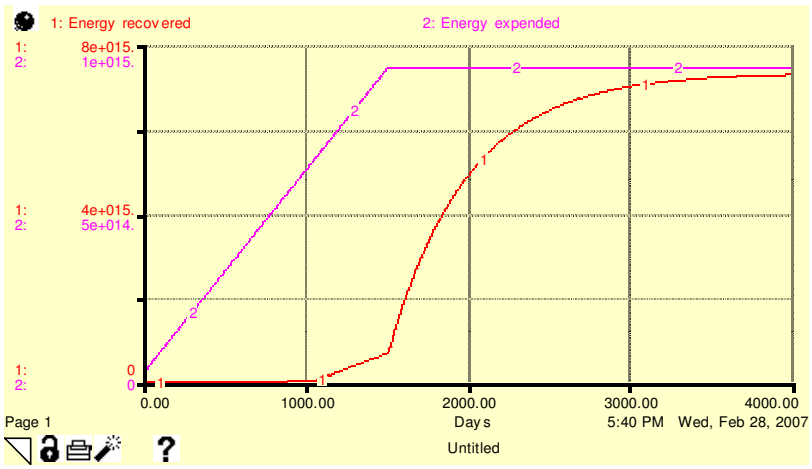

Figure 37. Energy expended and energy recovered from the retort (joules).

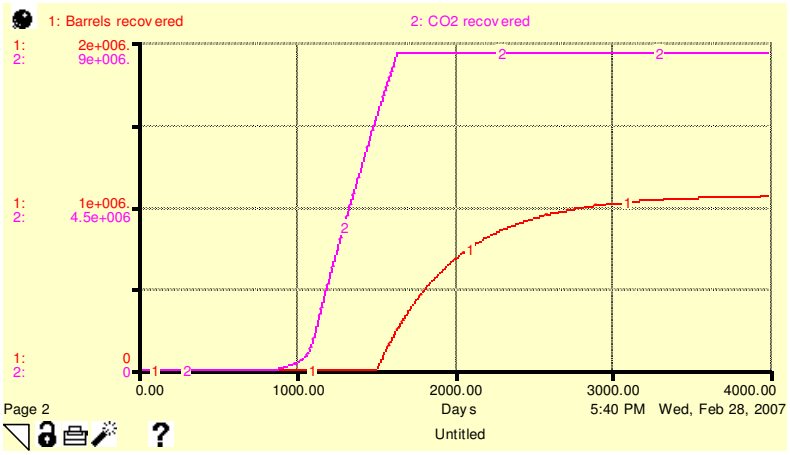

Figure 38. Barrels of oil and kg of CO2 recovered from the retort.

Sensitivity studies

Evaluating the parameters in the model that have the most uncertainty leads to identification of the following parameters:

- The rate of kerogen conversion
- Initial water content
- Heat conduction out of the retort

A wide range of kinetic parameters are reported in the literature. If the rate of conversion is much slower than predicted, then the heating time may not be sufficient to convert all of the kerogen to oil. The longer the heating time, the more energy needed to start the reaction. The frequency factor and activation energy cannot be varied independently. Therefore, values for the

two Anvil Points samples shown in Table 2 were simulated. The base case was the Anvil Point values from Campbell et al. (1978). It turns out that the number of barrels recovered is not very sensitive to the reaction kinetics over a wide range of values. As can be seen from Figure 35, the pyrolysis reaction is very rapid. Slowing the reaction to some extent delays the conversion a little bit, but does not prevent conversion. Only when extreme values are used for the kinetic parameters does the reaction rate slow to the point that conversion is not complete. Therefore, kinetic factors are not likely to be an important consideration for in situ retorting.

The initial water content can increase the heat capacity of the retort, diverting heat from the raising the temperature, and impacting the conversion of kerogen. The water content of the retort was doubled. This may have the effect of including water bound to minerals, which will be driven off the minerals when boiling occurs, and so does need to be included in the water model. When this simulation is run, the peak retort temperature drops, and the amount of heat bound up in steam increases. However, the temperature drops only to 367 ºC from about 400 ºC. The pyrolysis reaction is still fast enough to convert all the kerogen to oil, and the oil yield is relatively unaffected.

The final simulation evaluates heat conduction out of the retort. Thermal conductivity for oil shale reported by Rejeshwar et al. (1979) range from $6x10^4$ to $1.5x10^5$ J m^{-1} day^{-1} $ºK^{-1}$. The base case uses the lower number; the upper number would allow more heat to be lost to the surrounding rocks. When a thermal conductivity of $1.6x10^5$ J m^{-1} day^{-1} $ºK^{-1}$ is used, the retort takes longer to heat up. The retort still hits a maximum temperature of 393 ºC, which is sufficient to drive pyrolysis, but it doesn't reach this temperature until day 1492. Pyrolysis occurs about day 1180 versus day 1100 under the base case. This is not significant. Oil generation does occur somewhat later, but there is generally complete conversion of the kerogen.

Operation summary

The above analysis is necessary to determine the approximate length of time needed to operate the retort and remove the gas and oil products. Over this time, a small amount of water is produced via the kerogen conversion during heating (Equation 12). Most of the produced water is from the conversion of water entrapped in the isolated pores (and residual water in effective pores) as steam. A small amount of water consumption would be necessary during daily operations. Water used for cooling of surface equipment is not included in these calculations. The operation time is also used to establish the beginning of the site remediation stage.

Remediation Phase

Once the operation stage is completed, the site must be remediated. As part of this remediation effort, the retort zone may be flushed with water to remove excess heat and mobile con-

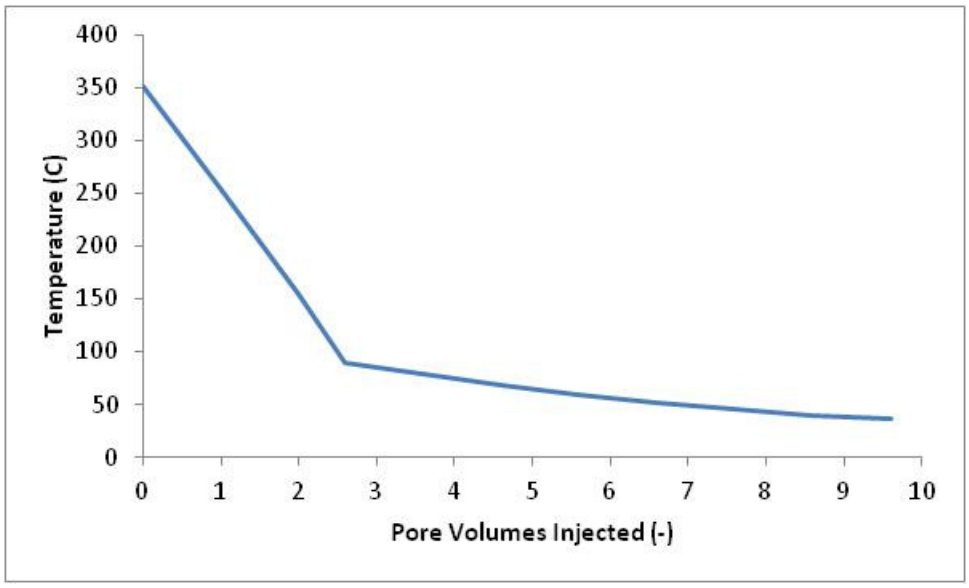

Figure 39. Retort cooling as a function of injected pore volumes.

taminants. A calculation was performed to examine the number of pore volumes of water injected into an expired retort to evaluate the cooling rate due to the heat extraction of the injected water. Input water was assumed to be 25°C and the system was assumed to be a well mixed reactor. The final porosity was assumed to be 10% and therefore a pore volume is equilvent to 10% of the total volume. During the first few injected pore volumes heat is removed from the reservoir via heating of the water to its boiling point, vaporization of the water, and heating the steam to the retort temperature. Within 3 pore volumes, the temperature drops from 350°C to 100°C. Below this temperature, the rate of cooling significantly decreases because the only heat removal mechanism is the sensible heating of the water injected water. At this time, each pore volume of injected water will decrease the retort temperature approximately 5° to 10°C (depending on the initial retort temperature) and ambient temperature is achieved in less than 10 pore volumes. Although these calculations do not take into account actual transport or pressure changes within the retort, it does provide enough information to suggest that the flushing to reduce contaminant concentrations will determine the number of pore volumes that need to be flushed through the system.

Modeling results for Shell's Oil Shale Test Project (Shell, 2006) suggest that a 20 pore volume flush will be necessary for reduce contaminants down to an acceptable level. In their simulations they thought this would be achievable in 2 years of flushing. We used a similar approach for the remediation phase in the system dynamic model. Since flushing of contaminants takes more pore volumes than the cooling of the retort, we will assume that 20 pore volumes is the volume of water that needs to be handled. We will also assume that the water will be treated at the surface and reused during subsequent flushes.

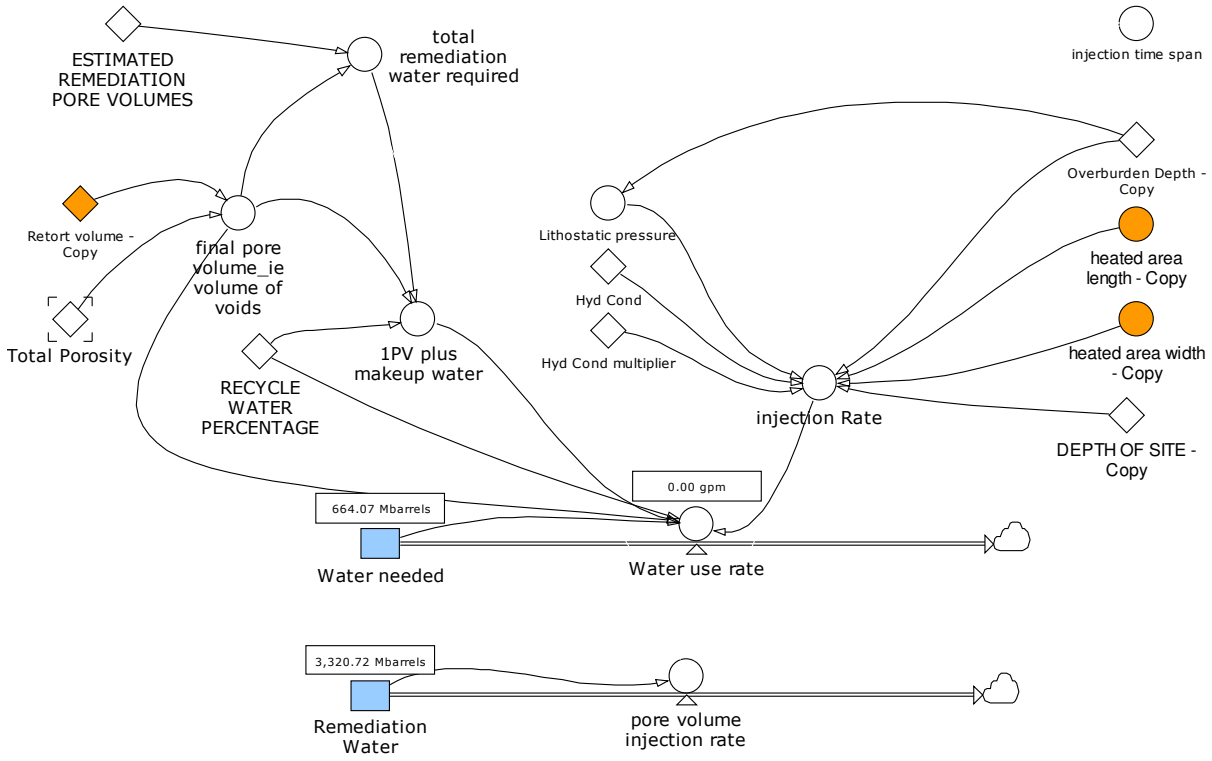

Figure 40. Remediation of the retort through subsurface flushing.

Figure 40 illustrates the system dynamic module for the remediation system. The total remediation water required is a function of the total porosity, retort volume and the required number of pore volumes needed to be flushed through the system. The total porosity is a user defined value typically higher than the initial effective porosity, due to the removal of kerogen during the retort process. The actual water needed is less than the total remediation water required due to recycling of the water. The first pore volume is needed to refill the retort volume with water. After that initial filling, water will be recycled from the injection wells to the production wells and any water losses will be accounted for in the recycle water percentage. At this time the recycle water percent is set as a constant, and would account for water loss through the freeze wall, and makeup water needed for the water treatment on the surface.

The time necessary to complete the remediation is determined by the injection rate and the total amount of water required. We used a one dimensional form of Darcy's Law to describe the injection rate. The area was determined from retort length parameters. The hydraulic conductivity was from the initial site information that can be multiplied by a factor to account for any increases in the hydraulic conductivity due to the retorting process. The pressure gradient is currently based on the lithostatic pressure (via the overburden depth) and $1/10^{th}$ the width of the site. These values are used to calculate the time to pump 20 pore volumes of water and to develop the water requirement values as a function of time.

Task 5.0 Surface Water and Groundwater Modeling

Surface Water Modeling

Introduction

Oil shale development has diverse water quality and water quantity impacts. Development of Western oil shale resources will require significant quantities of water for mine and plant operations, reclamation, and associated economic growth. Department of Energy (DOE) report indicates that current estimates based on updated oil shale industry water budgets for new retorting methods will be 1 to 3 barrels of water per barrel of oil. For an oil shale industry producing 2.5 MMBbl/d, this equates to between 105 and 315 million gallons of water per day (MGD). These numbers include water requirements for power generation for in-situ heating processes, retorting, refining, reclamation, dust control and on-site worker demands.

According to this DOE fact sheet report, municipal and other water requirements related to population growth and industry development will require an additional 58 million gallons per day. In areas where exists oil shale (in the West), water will be drawn from local and regional sources. The major water source would be rivers, which have to support the water demands from municipal, industrial, and agricultural activities in addition to baseline environmental flows. Stream flow levels will be affected as a result of water demand from the oil shale industry. Thus, there will be tremendous impacts to aquatic habitat. Watershed analyses are needed to develop resource management strategies to manage the impacts of oil shale operations while maintaining stream flows and other water needs.

In addition to water quantity issues, there are water quality issues. There is a possibility of oil spills because of large amounts of shale oil produced, processed, and transported. If they cannot be contained or removed, detrimental impacts would occur to aquatic biota. Oil and grease in public water supplies cause an objectionable taste and odor, and might ultimately endanger public health. Sedimentation problems will be increased because large amounts of land will be disturbed, which will increase the area's susceptibility to erosion. Erosion from disturbed areas is an order of magnitude higher than pristine undisturbed areas. Impacts of open-cast mining can be environmentally detrimental. For example, mining-related stream sediment levels have been found to be much higher than those associated with other land-use changes, such as deforestation, agricultural intensification, road-building, and urbanization. Aquatic habitat is affected by turbidity levels. Thus, enhanced sediment following the initiation of mining is a source of concern. Stream temperature could also be altered due to a warm wastewater discharge from power plants, by consuming cool water, or by lowering the ground water table. An oil shale industry will use land for access to sites, for facilities, for mining, for retorting, for oil upgrading, and for waste disposal. Large area is disrupted by mining activities and waste disposal operations. The disturbed sites should be reclaimed through revegetation. Chemical fertilizers are

used for reclaiming land, which could be potential sources of nitrogen, and phosphorous in ground water discharge, runoff from raw and spent shale, and municipal wastes. Toxic trace elements and organic chemicals from stack emissions from processing operations, chemicals used in upgrading and gas processing, leachates from raw and retorted shale, and associated industrial and municipal wastes are also a concern because of their potential impact on aquatic life, and on human health through drinking water supplies and irrigation. However, water quality issues are beyond the scope of this study.

Model Selection and Development: Piceance basin, Colorado

Several GIS based watershed models such as Hydrologic Simulation Program-Fortran (HSPF), Soil and Water Assessment Tool (SWAT), Storm Water Management Mode (SWMM), and Watershed Analysis Risk Management Framework (WARMF) have been reviewed before implementing the watershed analysis. Most of these models have the capacity to simulate both water quality and water quantity. The model selected is preferred to be able simulate all relevant compartments of the hydrologic system. This includes precipitation, snowmelt, evapotranspiration, infiltration and runoff, stream flow, reservoir operation, ground-water flow, and chemical transport if water quality is considered. Typically, no single model is capable of simulating all relevant processes. WARMF has been selected for this study. The model is capable of simulating surface water hydrology including the impact of water use on stream flow and pollutant transport and reactions. A river basin is divided into a network of land catchments, stream segments, and lakes for hydrologic and water-quality simulations. Stream flow is calculated based on water balance.

The WARMF model

WARMF uses daily time steps and requires daily precipitation, minimum and maximum temperature, cloud cover, dew point temperature, air pressure and wind speed. WARMF calculates daily runoff, shallow groundwater flow, and water quality of a basin that is divided into catchments, stream segments, lakes and reservoirs. A water-balance approach is used to calculate the hydrologic budget for each catchment resulting in runoff and groundwater flow to river segments (Chen et al., 2001). An impervious surface will produce immediate runoff. On pervious surfaces the water may infiltrate, flow as surface runoff or remain as storage on surface.

Several land use types can be defined in each catchment in WARMF. Each catchment can be divided into five soil layers. Each layer is assigned a thickness, initial soil moisture content, horizontal and vertical hydraulic conductivities, field capacity, and saturated moisture content. Lateral flow from a layer is based on Darcy's Law, where the head gradient is approximated as the slope of the land surface. The water balance is used to compute moisture content of each layer based on infiltration into the layer, percolation out of the layer, lateral inflow and outflow,

and evapotranspiration (ET). Darcy's Law is used for groundwater flow between catchments or from catchments to streams (i.e. base flow).

The model considers both total free surface water evaporation and soil transpiration in the computation of potential evapotranspiration. The model simulates snow accumulation and snowmelt by air and/or rain under open conditions and those under canopy cover. It has capability to simulate reservoir operations and requires reservoir bathymetric data in the form of stage-area relationship for simulation. The reservoir flow balance is predicated on conservation of mass.

A mass-balance approach is used for calculating chemical transport. The mass balance approach accounts for sources and losses including atmospheric deposition, and reactions. Stream water quality data collection is in progress. We will run the WARMF model for contaminants relevant to oil shale production. WARMF also accepts point sources discharging directly to stream and diversions from stream.

Model Development

The total drainage area included in this study is about 1600 square miles. The northern portion, the Piceance-Yellow (14050006) is about 900 sq. mi. and drains into the white river. The southern portion, Parachute-Roan (14010006) is about 700 sq. mi. and discharges into Colorado River. Based on the USGS Land Use Land Cover data (LULC) data, the land use classification in the watershed includes residential, commercial, forest, shrub land, pasture, and limited agricultural areas. More than 50 % of the watershed classified as forested or shrub land.

WARMF model requires GIS data layers, namely digital elevation model (DEM), and land use/ land cover. It also requires time series data, which includes weather data and stream flow data for hydrologic calibration. Point sources, stream diversion and pumping data and also air quality data can also be added to the model.

The DEM data for the basin was obtained from the USGS database, which offers a seamless DEM coverage of the entire United States (Figure 41). The land cover layer was derived from the National Land Cover Dataset (NLCD) (Figure 42). The U.S. EPA BASINS system or other sources can be used to download basic input coverages on DEM, land use and streams.

The watershed delineation for WARMF for Piceance basin was done using BASINS (Better Assessment Science Integrating point & Non-point Sources). The watershed is divided into several catchments. The catchments are grouped into four major sub watersheds based flow outlets (Figure 43). The watershed has four independent outlets corresponding to each of these 4 sub watersheds. Each major sub watershed is divided into several catchments. Thus, the entire watershed was divided into 90 catchments. Model calibration was done using gage data for each of these outlets (discussed later). Two of the sub watersheds make the Southern Piceance basin.

The remaining two are in the Northern Piceance basin. BASINS provides several tools for watershed delineation including an automatic delineation tool. WARMF doesn't have provisions to do the delineations; hence, BASINS automatic delineation tool was used to do the watershed delineation. After the catchment, land use and stream layers were processed in BASINS, they were imported into WARMF. The DEM, land use and stream coverages were processed to make them compatible with WARMF data input requirements.

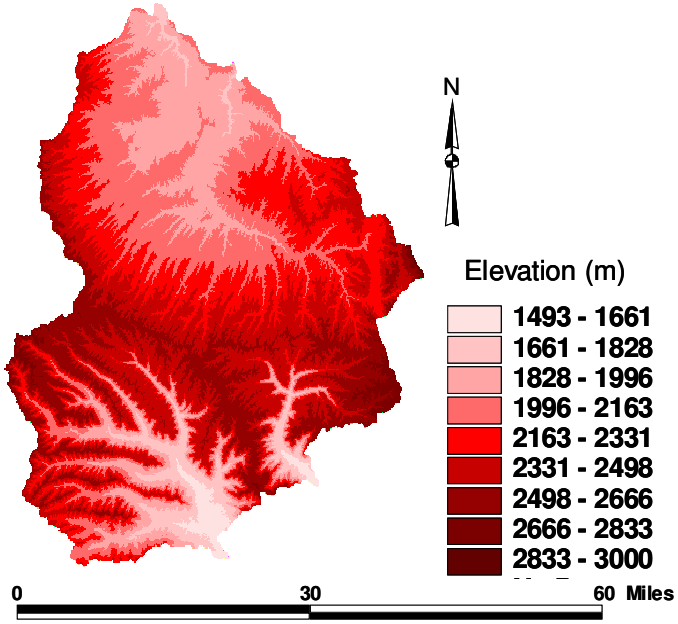

Figure 41. Digital Elevation Model of Study area

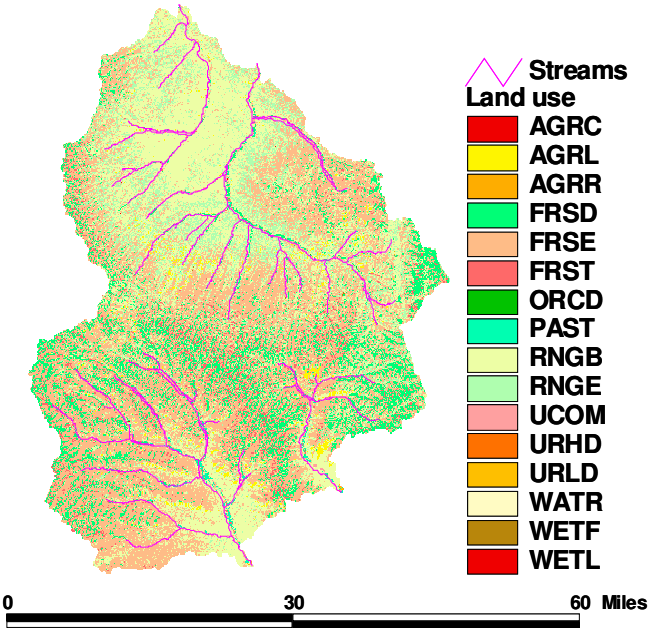

Note:
AGRL=Agricultural Land-Generic,
AGRR=Agricultural Land-Row Crops,
BERM=Bermudagrass,
FRSD = Forest-Deciduous,
FRSE= Forest-Evergreen, FRST=Forest-Mixed,
PAST=Pasture,
RNGE= Range-Grasses,
UCOM= Commercial, URLD=Residential-Low-Density, WATR=Water

Figure 42. Land Cover Classification for the study area

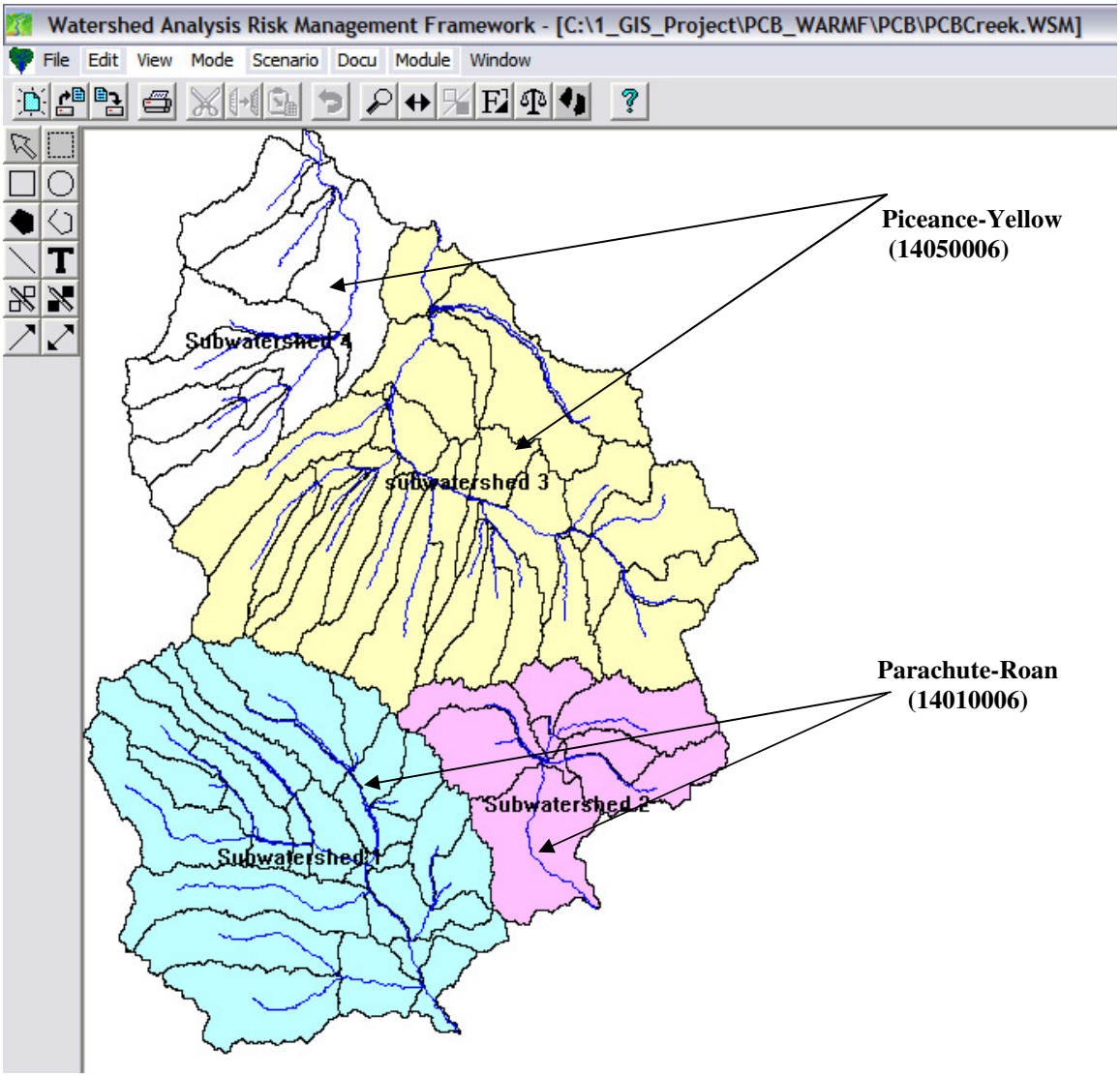

Figure 43. Watershed delineation and subdivisions for study area

Climate data

We had initially planned to use the Daymet climate data. The Daymet climate data is available from 1983-2003. *Daymet* is a model that generates daily values of temperature, precipitation, humidity, and radiation over large regions. *Daymet* provides a fine resolution, spatially continuous daily meteorological data. The Daymet has a better spatial resolution. The data is also currently available free of charge. Using the daymet, we extracted meteorological data for the centroid of each catchment. Thus, *90 station* data has been generated one for each catchment. The expectation was the Daymet data will improve our predictions because of its spatial resolu-

tion. However, we observed that Daymet overestimated precipitation especially during low rainfall conditions. Our initial simulation using WARMF model showed that the model calibration would not produce realistic parameter values if daymet were used. Thus, climate station data has been used. The station data is from National Climatic Data center ,NCDC, (NCDC, 2007). NCDC is freely available data, which contain daily records of precipitation, minimum and maximum temperature, wind speed, dew point temperature, cloud cover and air pressure. We obtained climate data from Grand Valley, Grand Junction stations, Rifle and Meeker stations.

Stream flow data

Daily time series stream gage data has been obtained from USGS gage stations in the watershed. The data was organized in to a format suitable to import it to WARMF for calibration. Few of the stream gage stations are shown in Figure 44. The watershed consists of two hydrologic units as described earlier. The northern portion, the Piceance-Yellow (14050006) discharges into the white river. The southern portion, Parachute-Roan (14010006) discharges into Colorado River. Most of the USGS gage data stations in the southern Piceance are relatively old dating back to year 1983. The watershed consists of two hydrologic units. The northern portion consists of the Piceance and Yellow creeks discharging into the white river. The southern portion consists of Parachute and Roan creeks discharges into Colorado River. The four major sub catchments are Piceance and Yellow creeks in the north and Parachute and Roan in the south. Each of the subbasins were calibrated independently. The gage station on each of the sub watersheds has data from different periods. The northern sub watersheds; the Piceance and Yellow have recent stream gage data up to year 2008. The gage stations in the southern sub watersheds; Parachute and Roan, are relatively old. Thus, we set the simulation period for Northern basins from year 1996 to 2008, a period of 13 years. The first 3 years are used as spin-up period for parameter initialization. The remaining 10 years are used as calibration period. The southern basins have to be calibrated for a different time period than the northern subbasins. The simulation period for Roan Creek was set from 1971 to 1981 and the simulation period for the Parachute Creek was set from 1973 to 1986. The first 3 years were used as spin up period in each case.

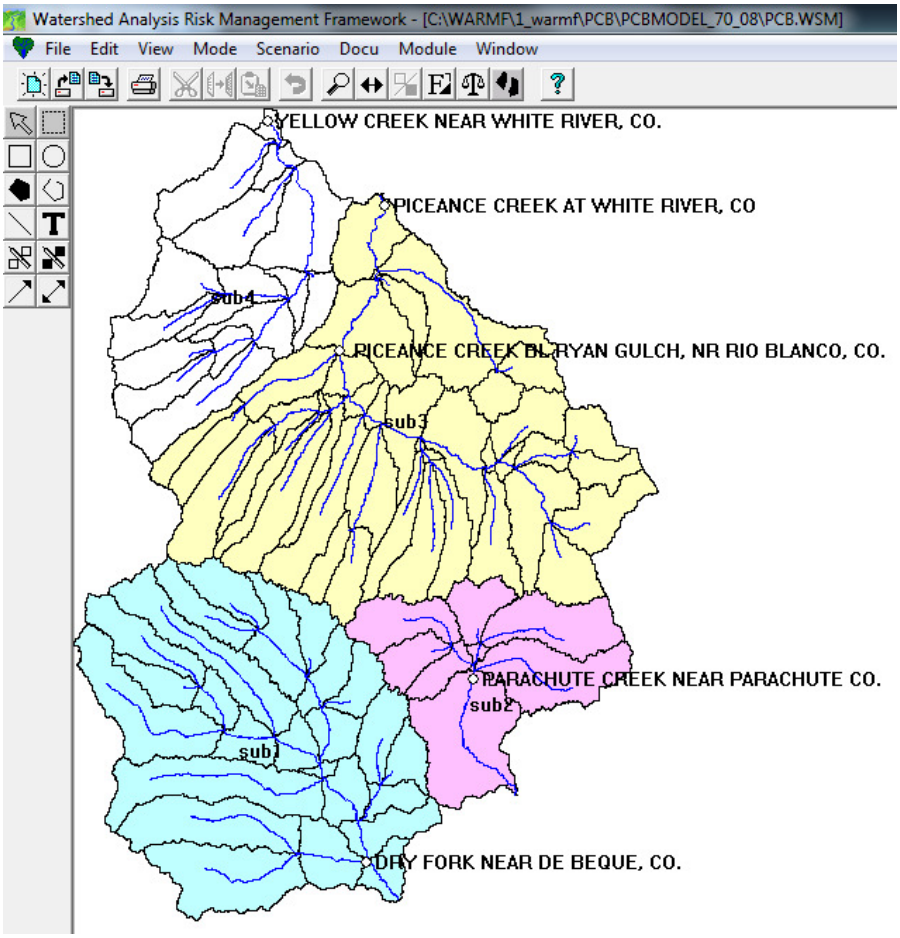

Figure 44. Piceance basin –Subbasins and stream flow gage stations

Hydrologic parameter sensitivity for WARMF model

We implemented an auto calibration tool (UCODE) for model-sensitivity analysis and parameter estimation using WARMF. It is not practical to use all parameters in calibration especially for a distributed model with a large number of parameters. Thus, it is necessary to identify sensitive model parameters that could be reasonably estimated, and hence reduce the number of parameters to be determined via calibration. A strategy for reducing the number of parameters is to use sensitivity analysis on the model output to identify parameters that do not have a major influence on model response (i.e., stream flow). In this study, UCODE (Poeter et al., 2005) was used for sensitivity analysis. Details about sensitivity and auto calibration using UCODE can be obtained from Poeter et al. (2005) and a brief summary of the method of sensitivity analysis is presented below.

Composite scale sensitivities (CSS) are used in UCODE to indicate the importance of an observation to the estimation of a parameter. CSS is the average value of the sensitivities associated with a parameter calculated at each observation point, and reflects the overall sensitivity of simulated values to a parameter (Hill and Tiedeman, 2007). Parameters with larger CSS are

more readily, and more precisely, estimated. To compare the relative sensitivity of parameters another relative measure (CSS ratio) is used. The CSS ratio is useful for identifying parameters that can be estimated because it reflects the sensitivity of a parameter relative to the parameter with the highest sensitivity. It is the ratio of the CSS of a parameter to the maximum CSS and varies between 0 and 1. The parameter with maximum CSS will have a CSS ratio of 1.0. Parameters with CSS less than 0.01 are insensitive, difficult to estimate and are associated with larger uncertainty (Hill and Tiedeman, 2007).

A sensitivity analysis was done for each of the four subwatersheds independently. Parameters included in the sensitivity analysis and sensitivity results for each of the subwatersheds are listed in Figures 45 to 48 below. Climate related parameters such as precipitation weighting factor, average temperature lapse rate, evaporation magnitude, evaporation skewness, snow melting rates for forest areas and open areas and soil related parameters such as porosity, filed capacity and hydraulic conductivity were all important parameters in all the of the four subwatersheds. WARMF uses a water balance approach to estimate runoff, and these parameters are particularly relevant to water balance. The climate parameters directly control the available water, while the remaining soil parameters dominate the run-off term. Thus it is reasonable that stream flow is sensitive to these parameters. Stream flow output was generally sensitive to identical set of parameters in all of the four subwatersheds although there are some differences in parameter relative sensitivities. For instance the snowmelt rates and temperature lapse rate were more important in Parachute –Roan than in Piceance- Yellow. This is reasonable because of the relative differences in altitude and topography.

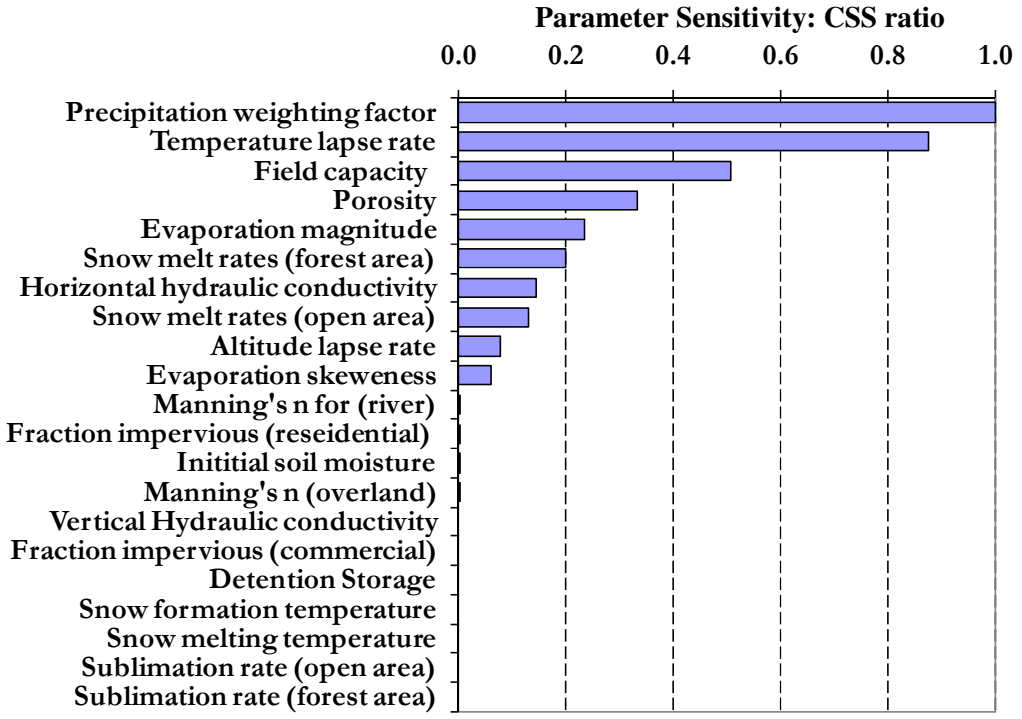

Figure 45. Parameter Sensitivity results for Roan Sub watershed.

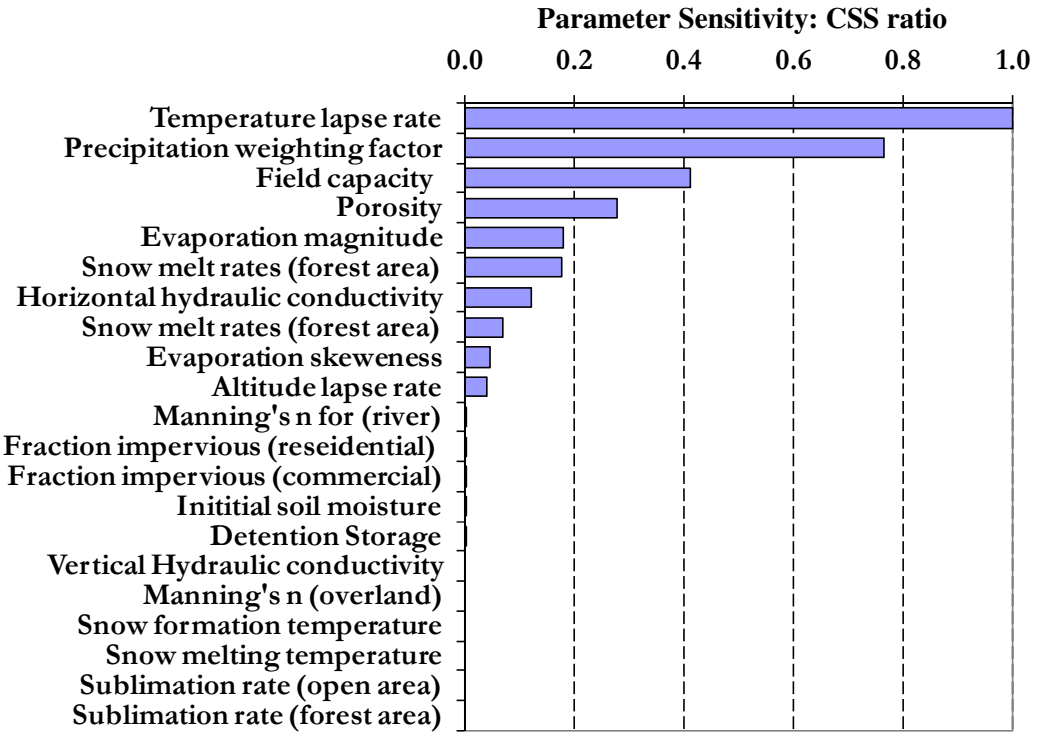

Figure 46. Parameter Sensitivity results for Parachute Sub watershed.

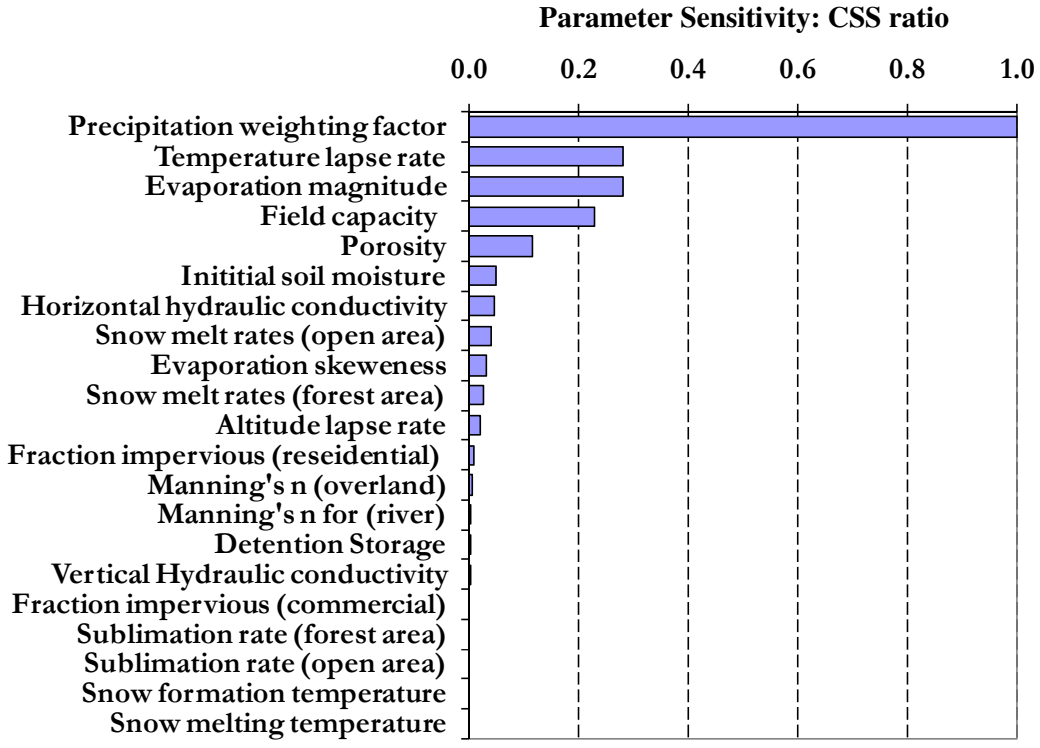

Figure 47. Parameter Sensitivity results for Piceance Sub watershed.

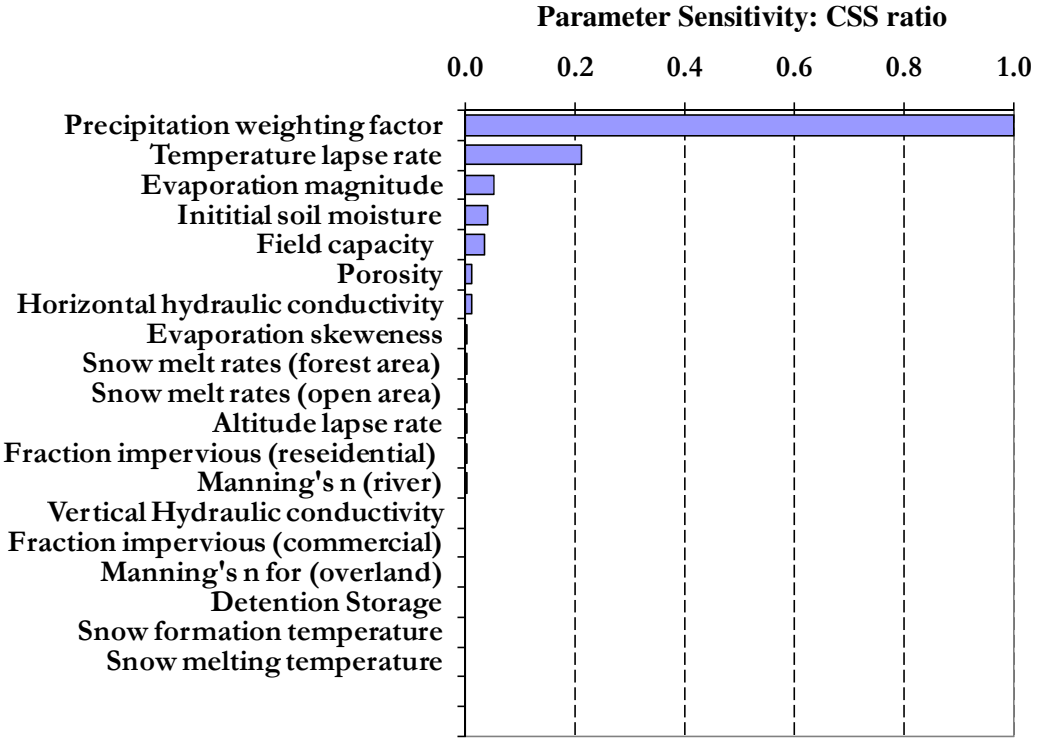

Figure 48. Parameter Sensitivity results for Yellow Sub watershed.

Model calibration

The sensitivity analysis described above was done to identify sensitive model parameters that could be reasonably estimated, and hence reduce the number of parameters to be determined via calibration. It was determined through the sensitivity analysis that climate related parameters such as precipitation weighting factor, average temperature lapse rate, evaporation magnitude, evaporation skewness, snow melting rates for forest areas and open areas and soil related parameters such as porosity, filed capacity and hydraulic conductivity were all important parameters in all the of the four subwatersheds.

After sensitivity analysis, we implemented the auto calibration tool, UCODE (Poeter et al., 2005) for calibration. WARMF simulation results were compared against measured stream flow data. UCODE minimizes the sum of weighted-squared-residuals with respect to the parameter values using a modified Gauss-Newton method. UCODE facilitates evaluation of data shortcomings by identifying low sensitivities and high parameter correlations (indicators of non-unique solutions). This improves understanding of the system and can lead to an improved conceptual model, which in turn results in a better mathematical representation of the model. During calibration, UCODE executes WARMF repeatedly; comparing the simulated and observed values and adjusting selected input parameter values to obtain the best fit (achieve the

minimum sum of weighted squared residuals). When parameter values changed less than 1% between iterations, the calibration was considered converged and the set of parameter values that yielded the best fit was designated as the optimal values.

Most of the parameters were fixed and only a few were adjusted during automatic calibration process. Parameters that were adjusted during calibration include climate related parameters (precipitation weighting factor and average temperature lapse rate) and soil property related parameter (hydraulic conductivity). It is observed that improving the match between observed and simulated flows during low-flow conditions degraded the match during high-flow conditions. The fit between simulated and observed values were relatively better during low flow conditions. This is a common situation in watershed-scale modeling where changes in input parameters that are required to improve the match of simulated and observed high flows result in a degraded match to observed low flows, and vice versa because all aspects of the relevant processes are not included in the modeling codes (Geza et al, 2010). The modeler may choose to improve the model performance for either high or low flows at the expense of a poorer model performance for the alternate flow condition depending on the intended use of the model (e.g. flood versus base flow prediction). Parameter values for each sub watershed are shown in Table 3 and calibration results are shown in Figures 49 to 52.

Table 3. Hydrologic parameters included in the sensitivity analysis ‡

Parameter	Parameter values				Units
	Parachute	Roan	Yellow	Piceance	
Fraction impervious; Res. area	0.8	0.8	0.8	0.8	--
Fraction impervious; Com. area	0.3	0.3	0.3	0.3	--
Evaporation magnitude	0.6	0.6	1.0	1.0	--
Evaporation skewness	1.4	1.6	1.0	1.0	--
Snow formation temperature	0.0	0.0	0.0	0.0	deg c
Snowmelt temperature	0.0	0.0	0.0	0.0	deg c
Snowmelt rates (open area)	0.1	0.1	0.1	0.1	cm/^{o}c/day
Snowmelt rates (forest area)	0.1	0.1	0.1	0.1	cm/^{o}c/day
Sublimation rates (open area)	0.0	0.0	0.0	0.0	cm/day
Sublimation rates (forest area)	0.0	0.0	0.0	0.0	cm/day
Detention storage	1.00	1.00	1.00	1.00	%
Manning's n for catchment s	0.01	0.02	0.02	0.02	--
Precipitation weighting factor	1.20	1.18	1.00	0.75	--
Temperature lapse rate	10.0	10.0	3.82	5.50	deg c
Altitude lapse rate	0.003	0.009	0.009	0.009	deg c/m
Initial moisture	0.20	0.20	0.20	0.20	m^3/m^3
Field capacity	0.15	0.15	0.15	0.15	m^3/m^3
Saturation moisture	0.30	0.30	0.30	0.30	m^3/m^3
Horizontal conductivity	1.07	23.47	0.354	0.072	m/day
Vertical conductivity (derived)	0.53	0.5	0.15	0.03	m/day
Manning's n for river	0.03	0.03	0.03	0.02	--

.

Each sub watershed was calibrated independently. In the northern portion of the basin, the Piceance and Yellow (14050006) discharge into the white river. In the southern portion of the basin, Parachute and Roan (14010006) discharge into Colorado River. The southern sub watersheds produce relatively more flow than the Northern sub watersheds. Northern Subwatersheds don't produce flow significant enough for diversion and use. Thus, more focus was given to the southern subbasin during calibration. The northern subwatersheds; the Piceance and Yellow have recent stream gage data up to year 2008. The gage stations in the southern subwatersheds; Parachute and Roan, are relatively old. Thus, we set the simulation period for Northern basins from year 1996 to 2008, a period of 13 years. The first 3 years are used as spin-up period for parameter initialization. The remaining 10 years are used as calibration period. The southern basins have to be calibrated for a different time period than the northern subbasins. The simulation period for Roan Creek was set from 1971 to 1981 and the simulation period for the Parachute Creek was set from 1973 to 1986. The first 3 years were used as spin up period in each case. Calibration results are shown in figures 9 to 12 below. The calibrated model can be used for scenario analysis to evaluate effect of diversion for oil shale production on stream flow.

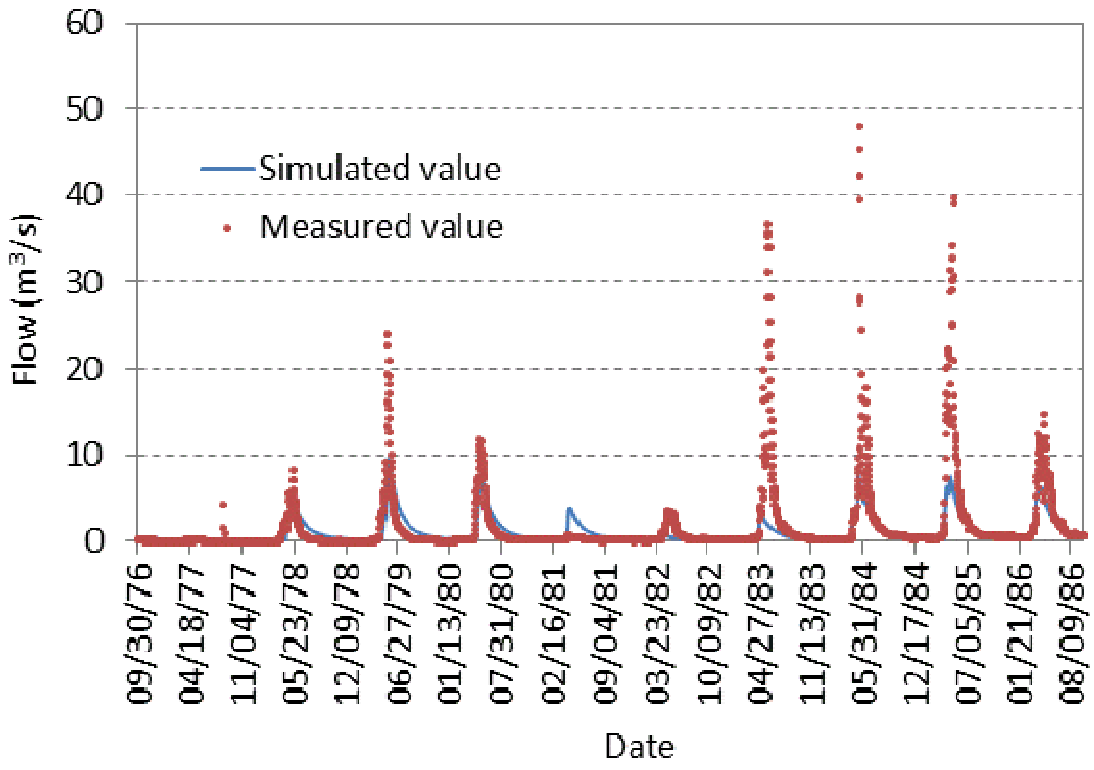

Figure 49. Calibration results for Parachute Creek near Parachute, CO (see Figure 44).

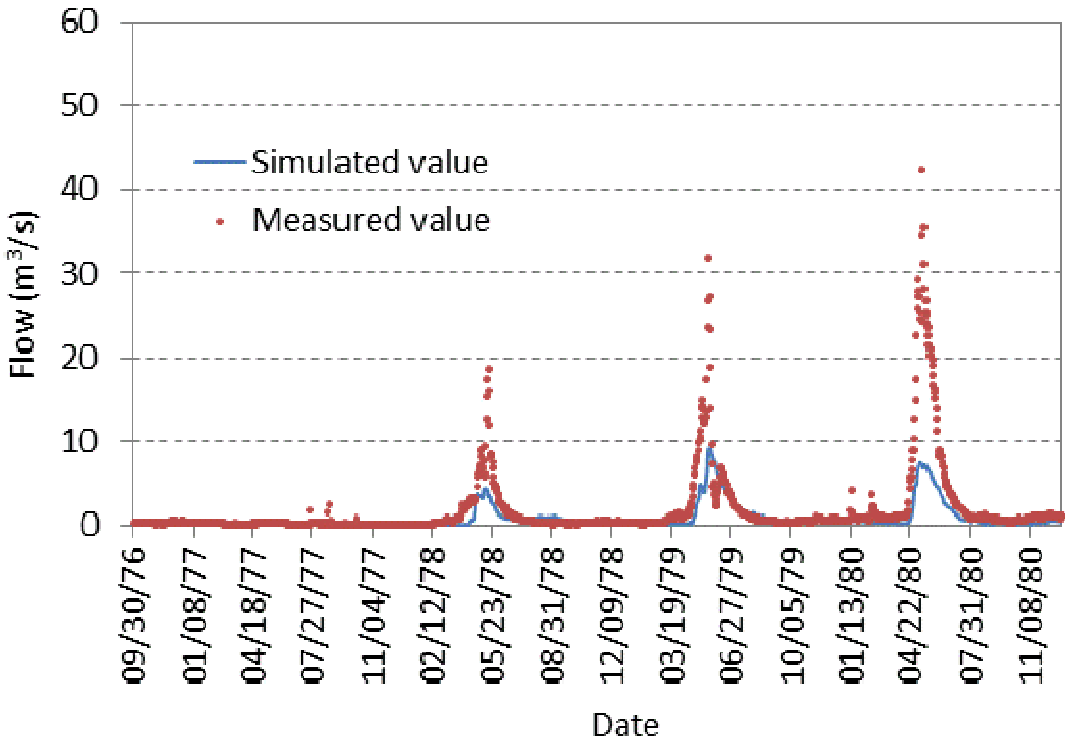

Figure 50. Calibration results for Roan Creek near De BeQue, CO (see Figure 44).

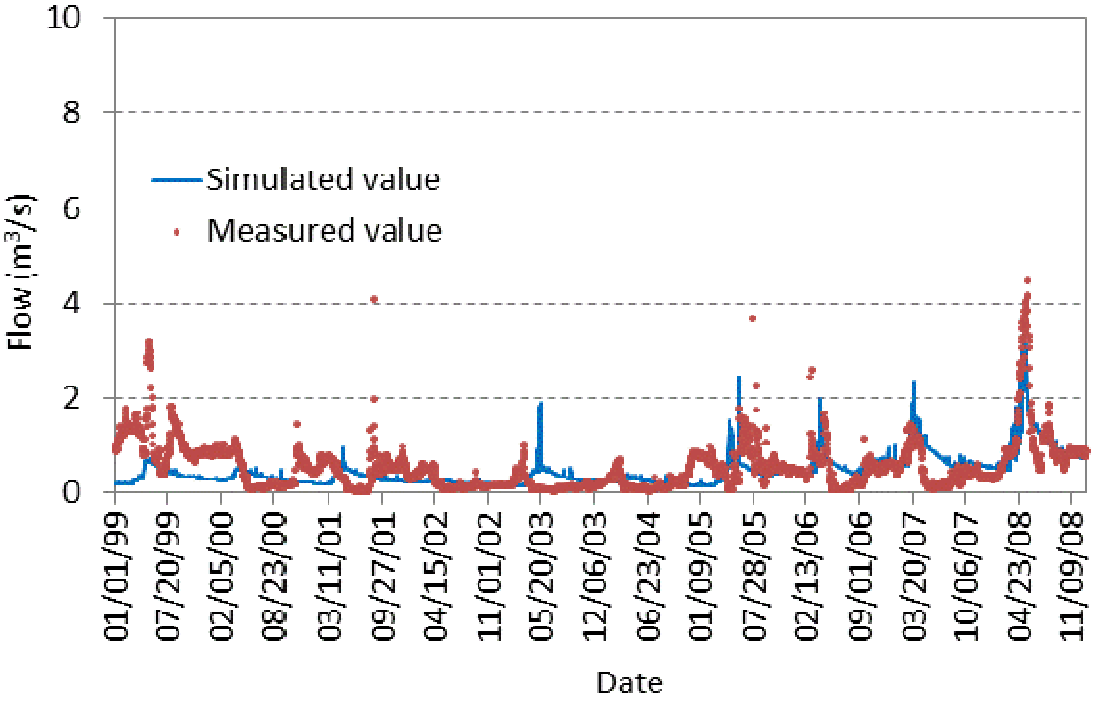

Figure 51. Calibration results for Yellow Creek near White River, CO (see Figure 44).

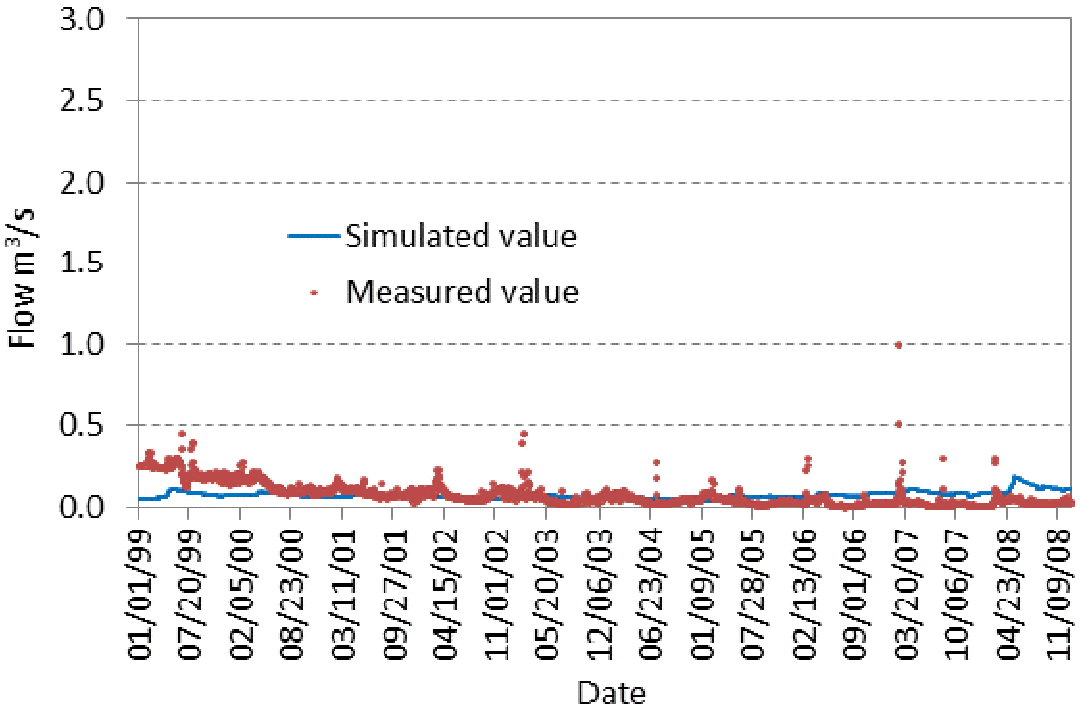

Figure 52. Calibration results for Piceance Creek at White River, CO (see Figure 44).

Ground water modeling

This task involved building a groundwater flow model (MODFLOW) that was based on data contained in the AHGW Geodatabase. The MODFLOW effort was undertaken with the understanding that existing groundwater data (e.g., hydrostratigraphic, hydraulic property, and potentiometric) were limited. The resulting model is viewed as a tool for understanding data limitations and guiding future groundwater research.

Because the AHDM was selected as a framework for managing all project data, we evaluated "MODFLOW Analyst" as a means of interfacing between MODFLOW and the AHDM. MODFLOW Analyst is a commercial extension to ArcGIS that is available for purchase from Aquaveo™ software and installed as an individual seat. During the course of the project, the geodatabase structure became increasingly specific to the Piceance Basin and deviated from the original AHDM. Though some of the tools are attractive, it is unclear how or if the MODFLOW Analyst extension will be adapted to new versions of ArcGIS or new versions of MODFLOW, and if MODFLOW Analyst tools will function on an ArcServer platform. For these reasons, we elected to build a MODFLOW model that was loosely coupled to the project geodatabase. The

desired goal was a functional MODFLOW model, but a pre- and post-processor was used to construct the model.

Groundwater model data compilation:

Hydrogeologic and potentiometric surface data were compiled from previous studies of the Piceance Basin [*Glover et al.*, 1998; *Taylor*, 1982]. Feature classes representing the model grid and boundary conditions used in the Taylor (1982) mathematical model were digitized and added to the AHGW Geodatabase. This was used as a historic record of the previous modeling effort, and to conceptualize flow patterns and boundary conditions of the groundwater system. Based on the previous studies, groundwater generally flows from south to north in the basin and crosses the major surface water divide that separates the northern Piceance Basin from the southern Piceance Basin.

Preliminary groundwater flow model:

The framework for a preliminary numerical groundwater flow model (MODFLOW2000) was built using the MFI2K program [*Harbaugh*, 2002]. The model consisted of 7 layers that were patterned after the Taylor (1982) hydrogeologic units, with an additional layer above (Layer 1) and an underlying aquitard (Layer 7). Elevations of the tops and bottoms of the layers were derived from a combination of structure contours [*USGS*, 2006], Fisher Assay well data [*Mercier et al.*, 2009], and geologic map data [*Hail and Smith*, 1994; 1997]. Layer 1 (~50 ft thick) comprised of alluvial deposits, Layer 2 (~360 ft thick) comprised of the Uinta Formation, Layer 3 (~350 ft thick) comprised of the Parachute Creek member of the Green River Formation down to the base of the A groove, Layer 4 (~141 ft thick) comprised of the Mahogany, Layer 5 (~174 ft thick) comprised of the B groove and R-6, Layer 6 (~435 ft thick) comprised of L-5 to the base of R-2, and Layer 7 comprised of the Garden Gulch member of the Green River Formation (comprised of L-1, R-1, L-0, and R-0) that forms the lower confining unit. Land-surface elevations for each cell were calculated from a 90 ft by 90 ft resolution USGS NED raster. Elevations ranged from 5,725 ft along the White River to about 9,280 ft in the drainage divide between Roan Creek and Parachute Creek. Streams (Yellow Creek and Piceance Creek) and springs were represented using constant-head nodes, similarly to the Taylor (1982) model.

The preliminary MODFLOW model setup and conditions were:

- Grid orientation: x-axis N75E, y-axis N15W
- Rows: 100 cells that are 3,000 ft wide
- Columns: 80 cells that are 3,000 ft wide

- Layers: 7
- Nodes: 8000 cells per layer for a total of 56,000 nodes

The preliminary groundwater flow model was designed in conjunction with the 3D hydrogeologic framework described in Subtask 2.3. As was seen in Subtask 2.3, the hydrogeologic framework was inconsistent with the conceptual model. Primarily, layers that were lower in the stratigraphic column (i.e., lower aquifer) were computed to be higher elevation than overlying layers (i.e., Mahogany). In addition, it was cumbersome to transfer data from ArcGIS to MODFLOW using the MFI2K processing tool. A simplified hydrogeologic framework was planned for the next phase of modeling, and a processing tool that allowed for more efficient transfer of data from ArcGIS to MODFLOW was needed.

Final groundwater flow model (MODFLOW):

The final phase of modeling focused on building a functional groundwater flow model of the Piceance Basin. In the preliminary versions of the groundwater flow model, seven hydrogeologic units were defined; however, in this phase of model development the conceptual framework was simplified to three hydrogeologic units (i.e., model layers). Layers 1, 2, and 3 corresponded with the Upper Aquifer (UA), Mahogany, and Lower Aquifer (LA), respectively similar to the conceptual framework (Figure 53) used by Glover et al. (1998).

A pre-processor and post-processor, Processing MODFLOW for Windows (PMWIN) version 8.0.28, was purchased and adopted to setup the MODFLOW model. The final MODFLOW model setup and conditions were:

- Grid orientation: x-axis N75E, y-axis N15W
- Rows: 100 cells that are 3,000 ft wide
- Columns: 80 cells that are 3,000 ft wide
- Layers: 3
- Nodes: 8000 cells per layer for a total of 24,000 nodes

This model configuration allowed for hydrogeologic characteristics from Taylor (1982) and hydraulic heads from Glover et al. (1998) to be used as model inputs. The model grid, shown in Figure 4, contains 4201 active cells (white) and 3799 inactive cells (gray) in the model domain. Within the active domain, 195 cells were designated as river (blue) cells and 294 cells were designated as springs or drain (yellow) cells. Layer 1 was modeled as unconfined, Layer 2 confined and Layer 3 confined. Each layer had the same horizontal extent in the model domain,

so Layer 1 was always present above Layer 2, and Layer 3 was always present above Layer 3. Top elevation and bottom elevation of the model layers was based on USGS (2006), while horizontal hydraulic conductivity, vertical hydraulic conductivity, and initial head were based on Glover et al. (1998). These model input values were computed at the nodes of each active cell and stored as ArcGIS point feature classes for model Layers 1 – 3.

Input parameters for each model layer were exported from ArcGIS feature classes, passed through Microsoft Access, and then imported to PMWIN to populate the corresponding matrix. The simulation was run as a steady-state solution with one time-step of 91250 days (i.e., 250 years). Wetting capability was set to -1, which allowed for dry cells to rewet from the bottom in successive iterations. PCG2 solver was used for numerical approximation with convergence criteria of 0.1 ft.

Hydraulic head measurements from seventeen observation wells (OWs) were available in the CDSS database to serve as potential calibration targets. Twelve of these OWs were screened within the Lower Aquifer (Layer 3), two were screened in the Mahogany and Lower Aquifer (Layers 2 and 3), two were screened in the Upper Aquifer and the Mahogany (Layers 1 and 2), and one OW was screened in the Upper Aquifer (Layer 1). Simulated heads were compared to observed (i.e., steady state) heads at these 17 OWs, while river and drain cell hydraulic conductances ONLY were manually adjusted to achieve a reasonable water balance and the lowest RMS Error. A water balance of -0.33% and RMS Error of 333 ft was achieved after the hydraulic conductances were set to 2 for each river cell, and 18 for each drain cell. A comparison of simulated head versus observed head for the adjusted model is shown in Figure 54.

Using the input parameters summarized above, approximately 300 active cells in the northern part of Layer 1 were dry at the end of the simulation period. Simulated heads are shown for Layer 1 (Figure 55), Layer 2 (Figure 56), and Layer 3 (Figure 57) along with representations of the simulated heads from the AHGW Geodatabase as Figures 58, 59 and 60, respectively. Simulated heads that are shown in Figures 58, 59 and 60 were stored in the MODFLOW_output feature dataset of the AHGW Geodatabase.

Formation	Member	Oil Shale Zones and Marker Units	Taylor (1982) Zones	Glover et al. (1998) Zones	Current MODFLOW Layer	Mean horizontal K (ft/day)	Mean vertical K (ft/day)
Uinta			Layer5	Upper Aquifers	Layer 1	0.4223	0.2813
Green River	Parachute Creek		Layer4				
		A groove					
		Mahogany	Layer3	Aquitard	Layer 2	0.0053	0.0016
		B groove	Layer2	Lower Aquifers	Layer 3	0.2508	0.1671
		R-6					
		L-5	Layer1				
		R-5					
		L-4					
		R-4					
		L-3					
		R-3					
		L-2					
		R-2					
	Garden Gulch	L-1	Lower Confining Unit	Aquitard			
		R-1					
		L-0					
		R-0					

Figure 53. Correlation Chart of Hydrostratigraphic Units, Conceptual Layers, and MODFLOW Model Layers

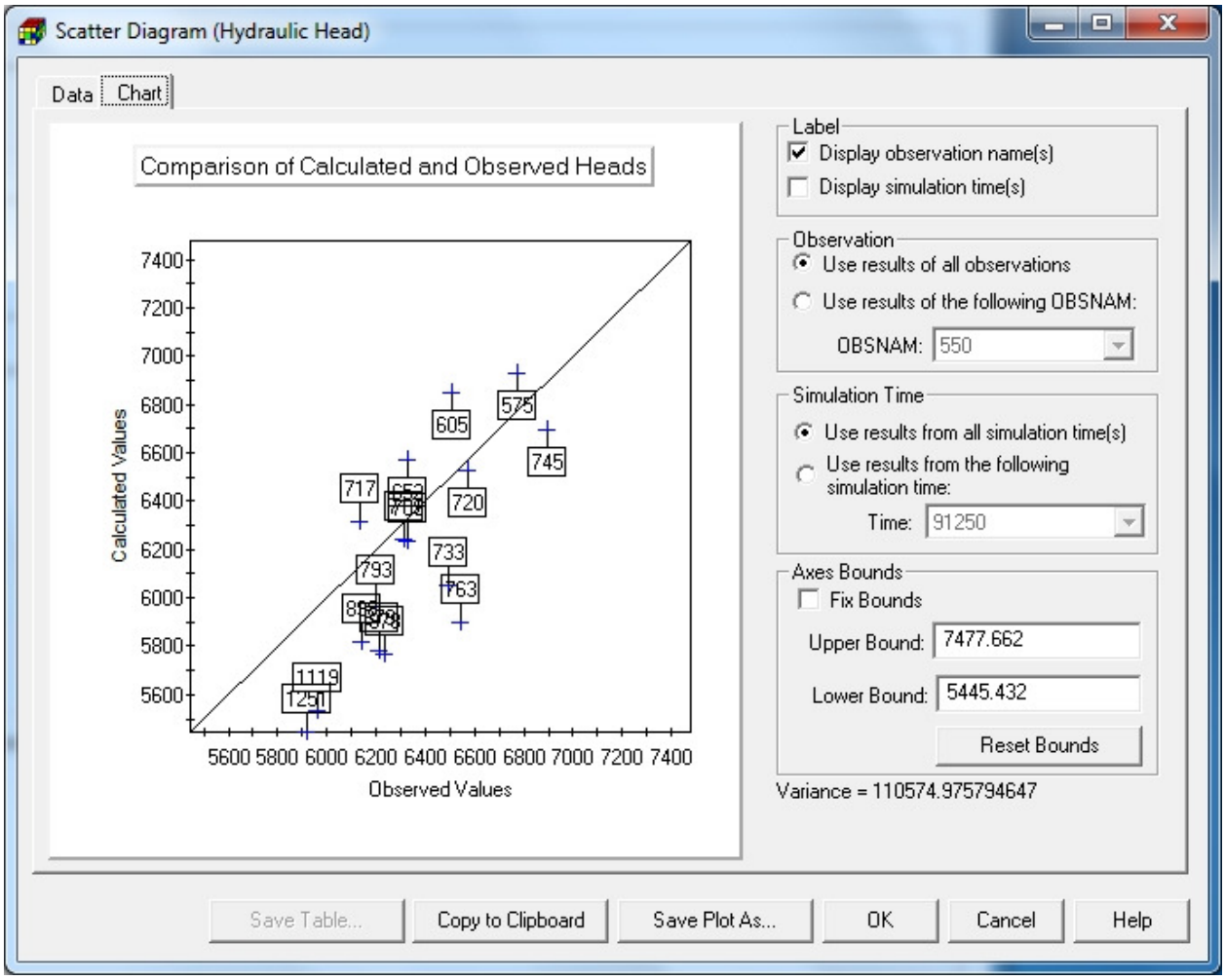

Figure 54: Simulated versus Observed Heads in 17 OWs in the Piceance Basin Final Groundwater Flow Model

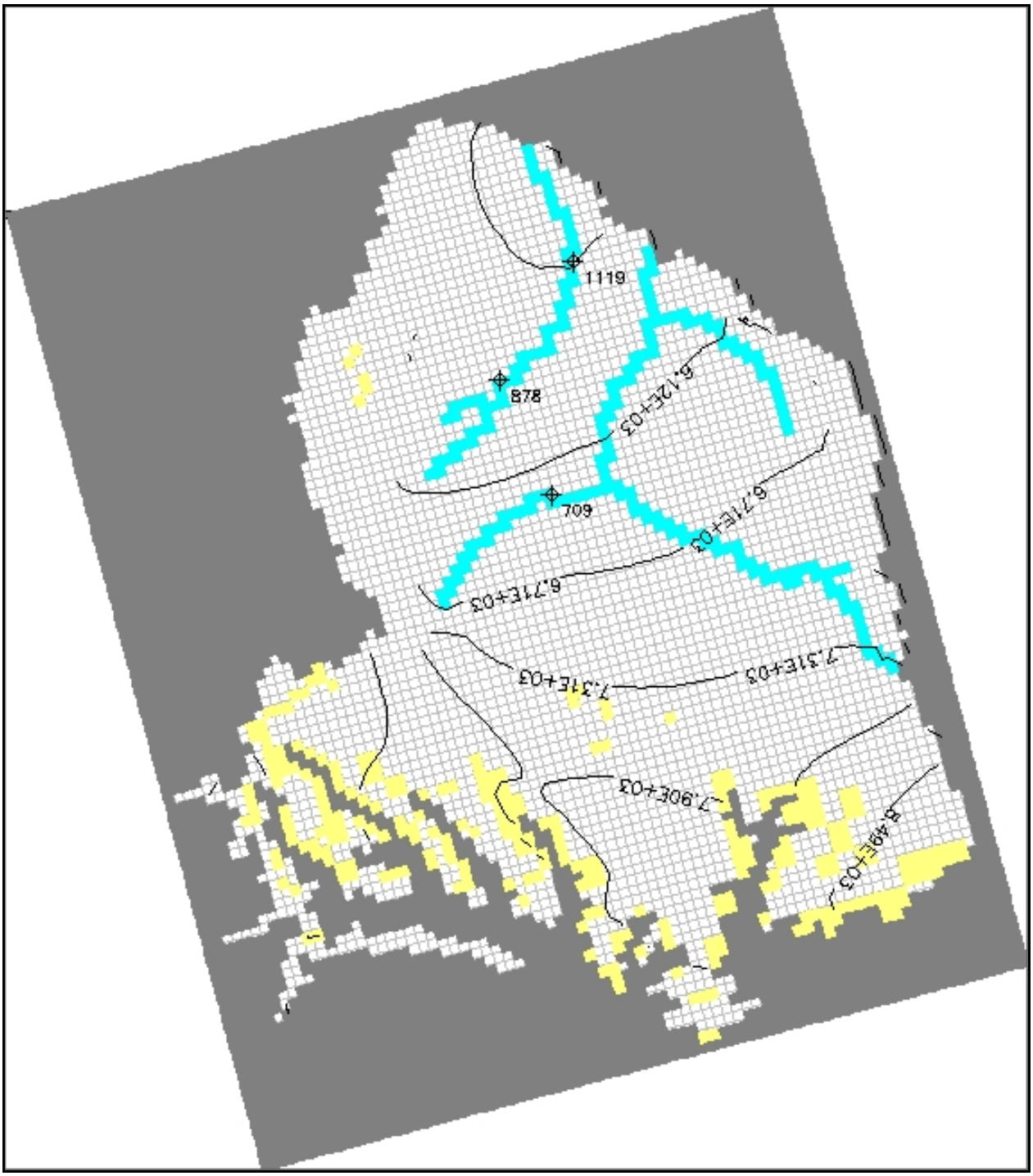

Figure 55: Simulated Head Contours for Layer 1 of Model with Cells - Active as white, Inactive as gray, River as blue, and Drain as yellow

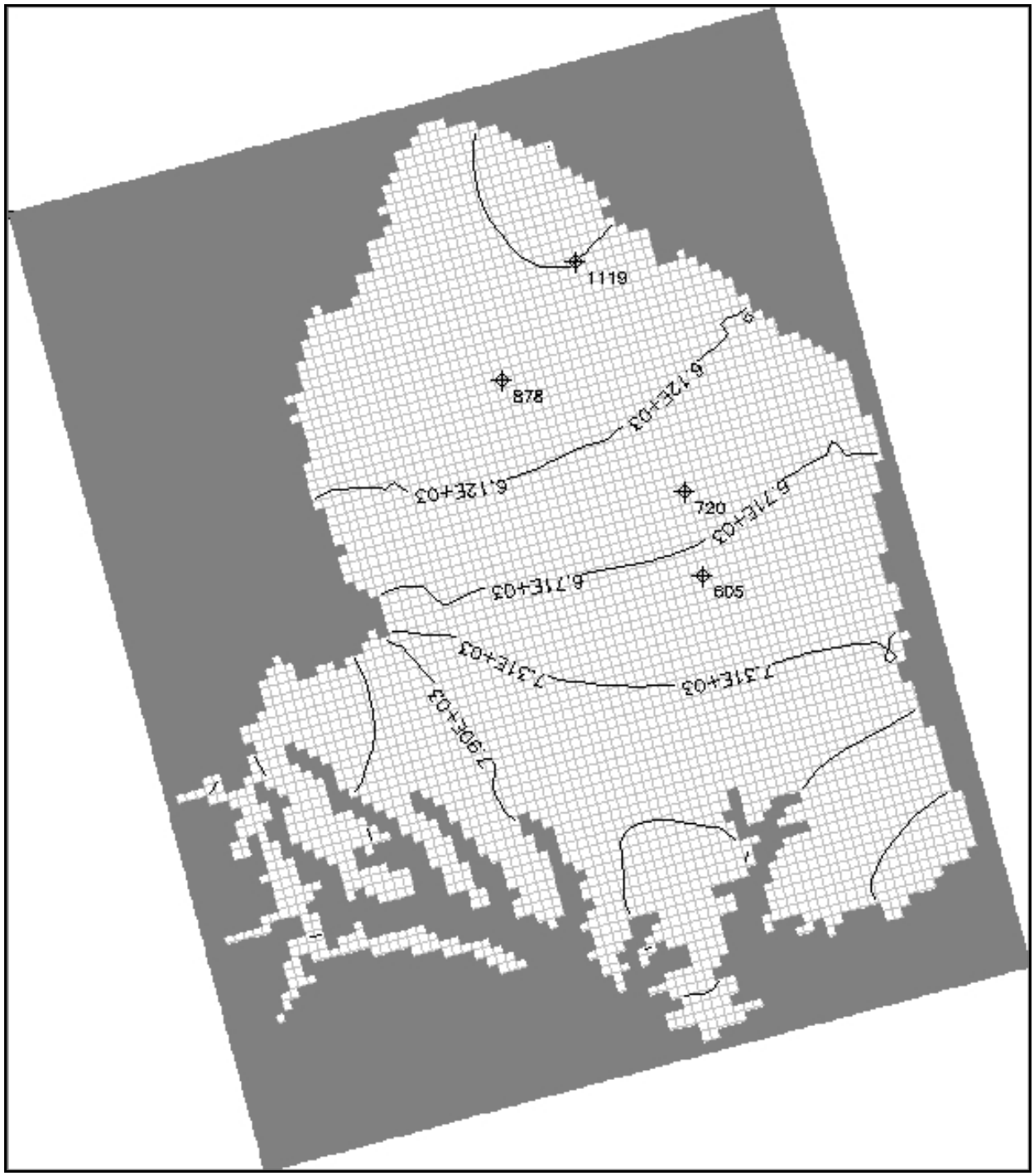

Figure 56: Simulated Head Contours for Layer 2 of Model with Cells - Active as white, Inactive as gray

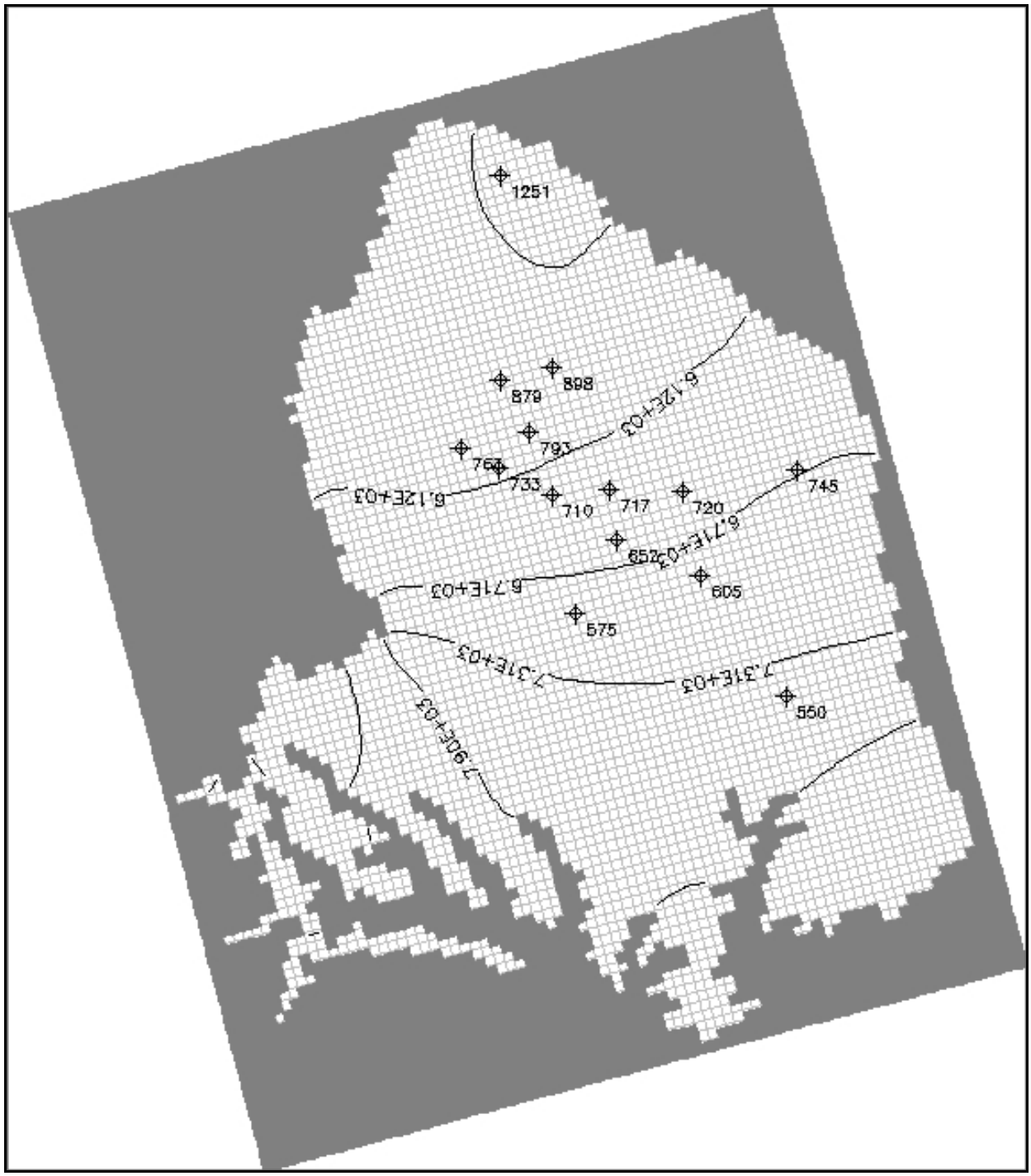

Figure 57: Simulated Head Contours for Layer 3 of Model with Cells - Active as white, Inactive as gray

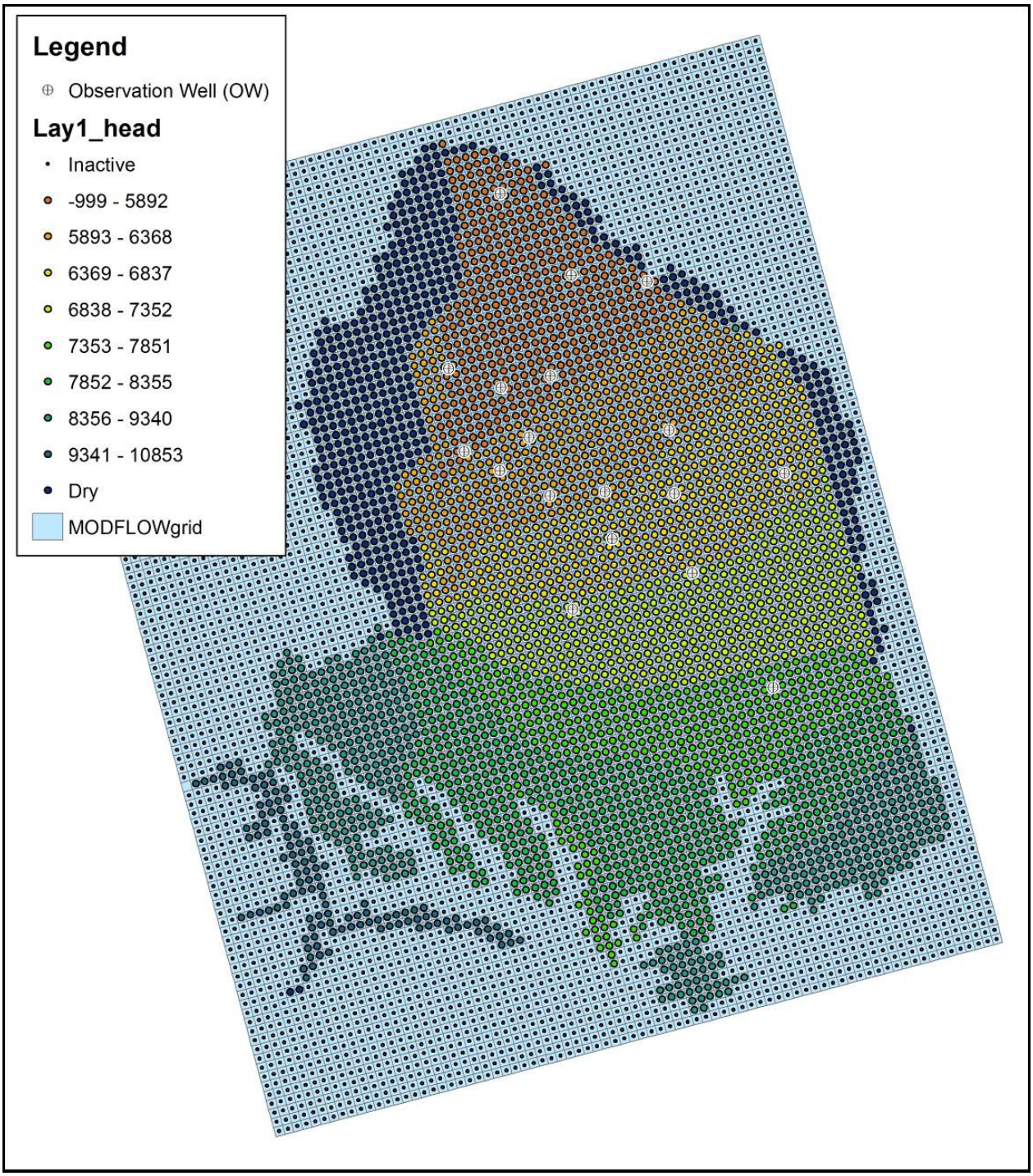

Figure 58: Simulated Head (Lay1_head feature class) Stored in MODFLOW_results Feature Dataset

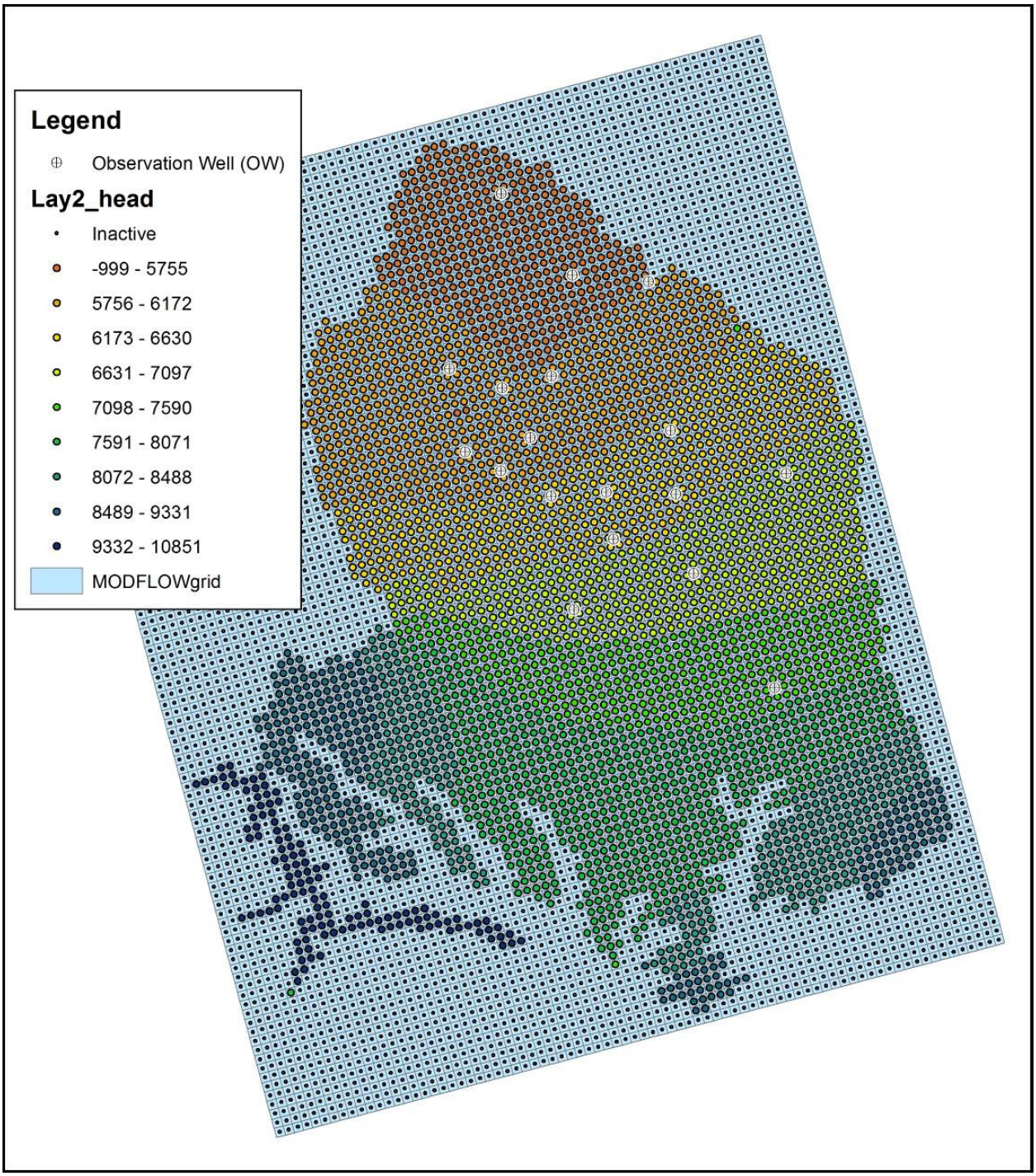

Figure 59: Simulated Head (Lay2_head feature class) Stored in MODFLOW_results Feature Dataset

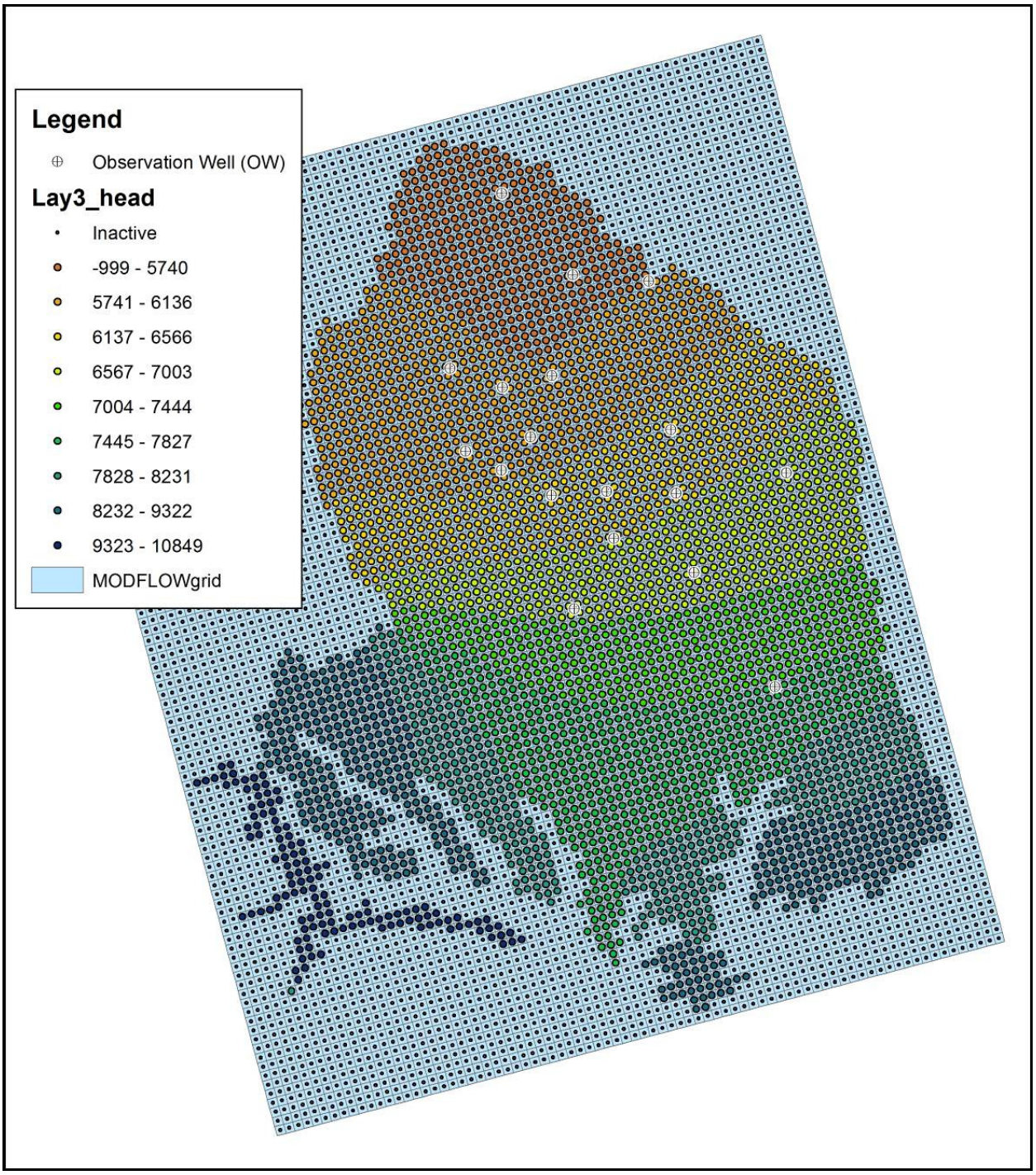

Figure 60: Simulated Head (Lay3_head feature class) Stored in MODFLOW_results Feature Dataset

Concluding Remarks

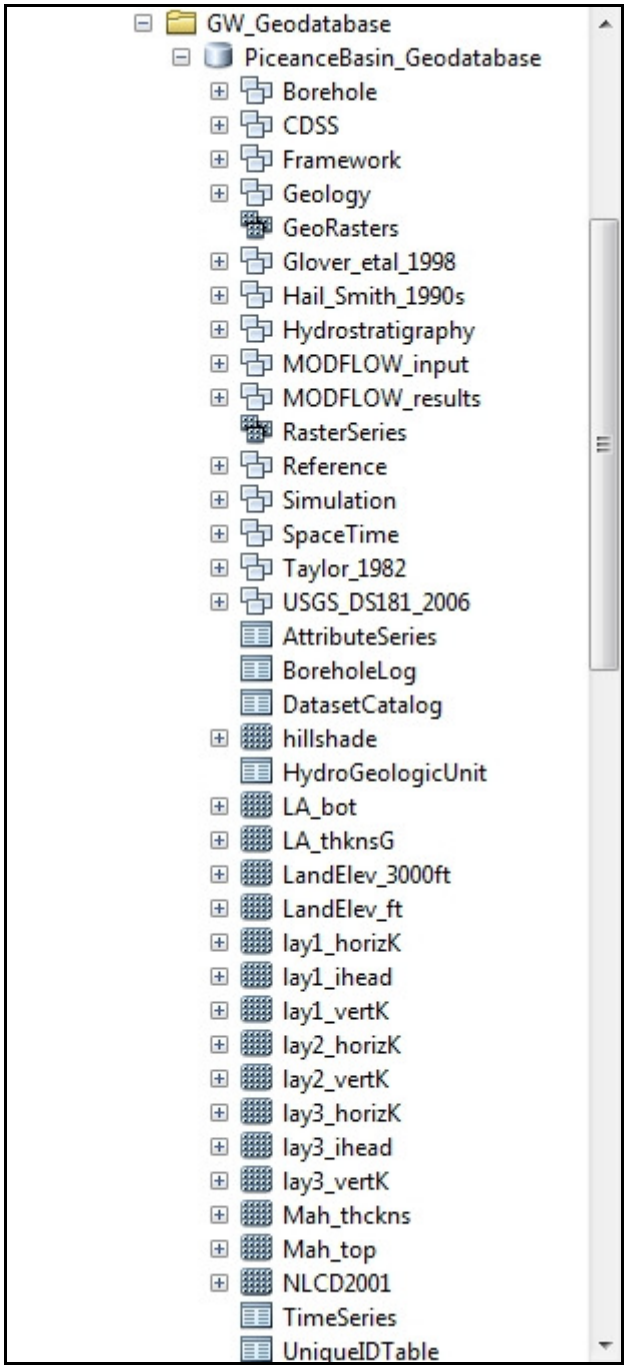

Figure 61. AHGW Geodatabase Framework showing Feature Datasets, Tables, and Rasters

Groundwater data for the GIS-based water resource geospatial infrastructure were compiled, stored, and managed into a groundwater geodatabase (Figure 61), which was a modified version of the Arc Hydro Data Model framework. Baseline data were organized into feature datasets (e.g., Framework or Taylor_1982) while groundwater flow model related inputs and results were organized into customized feature datasets (i.e., MODFLOW_input and MODFLOW_results). A simplified hydrogeologic framework consisting of Upper Aquifer (Layer 1), Mahogany (Layer 2), and Lower Aquifer (Layer 3) was used to represent the Piceance Basin groundwater system. The final groundwater flow model was manually adjusted to achieve a reasonable RMS error. Rigorous calibration was not possible due to sparse hydraulic head and hydraulic parameter data. The groundwater flow model could be enhanced and further refined by:

- Collecting additional hydrostratigraphic contact and hydraulic parameter data around the perimeter of the Piceance Basin
- Improving basin-wide water budget parameters for estimating groundwater recharge and evapotranspiration.
- Adding additional observation well locations that contain water level measurements from recent years (such as 2005 through 2012).
- Using parameter estimation procedures to improve predictive ability of model.
- Conducting sensitivity analyses and defining ranges of uncertainties for simulation of hydraulic heads.

Task 6.0: Technology Transfer

The project closeout meeting was conducted on November 19, 2012. An hour long presentation was given by the project team to the NETL participants during the meeting. The Presentation was followed by geodatabase and model demonstration and a brief Q&A section.

CONCLUSION

A water resource geospatial infrastructure has been developed in this project which creates a repository for large volumes of geological, hydro-geological, topological, water resource and oil shale data. The geodatabase in the geospatial infrastructure will allow for collaborative regional/basin assessments for future oil shale development based on the same “baseline”. This type of collaboration provides an ideal atmosphere for the development of new, generically useful approaches to the use of new technology, and procedures that promote the best and most

widespread use of our enormous data holdings despite their disparate locations and heterogeneous formats.

The components of this geospatial infrastructure including data frame, databases customized tools and models, are designed to be interlinked. These interlinks allow for "synchronized" updating. The final results of this project shall support decision makers to answer such questions as, the amount of oil shale resource, water availability, and potential environmental impacts under various development scenarios. The procedures/tools/models developed in this research are designed to be general. These procedures/tools/models are readily adapted to other study areas.

MILESTONES

Table 4. Milestones

MILESTONE NO.	DESCRIPTION	RELATED TASK/SUB TASK	COMPLETION DATE	UPDATE/COMMENTS
1	the initial prototypes of the integrated geodatabase	2.1 2.2	09/30 /2009	The initial prototypes have completed. A beta version geodatabase prototype was delivered to NETL on June 30th, 2011. New geothermal data has been integrated into the gamma version of geodatabase.
2	the initial products of customized macros, tools, or models	2.3	09/30 /2009	Completed, the tools and models are for data I/O automation and data processing. New tools were developed on a need basis.
3	prototype of the 3D geodatabase	2.2	09/30 /2010	The 3D geologic model has completed. Interfaces between the 3D geologic model and other models are developed on need basis.
4	prototype of the web-based GIS	2.4	09/30 /2010	The initial prototype of the integrated geodatabase, which is the deliverable from Milestone No. 1, has been migrated to a GIS server. Adobe Flex API development environment for ArcGIS Server has been established. The mapping web site is running.
5	the web-based geo-portal	3.0	09/30 /2011	Task 3.0 and subtask 2.4 are closely related. With the development of the project, the project team has decided that subtask 2.4 is a better way to disseminate data. The initial prototype of the web-

				mapping site has finished.
6	the results of the Energy Resource Development Systems	4.0	09/30 /2012	Model has completed.
7	the GUI and results of the Surface water and Groundwater Modeling	5.0	09/30 /2012	Watershed surface water WARMF model has completed. A three-layer MODFLOW ground water model has completed.

REFERENCES

Bar, H., R. Ikan and Z. Aizenshtat, 1986, "Kinetic Study of Isothermal Oil Shale Pyrolysis: 1. Mathematical Model of the Evolution of Organic Pyroproducts," *Journal of Analytical and Applied Pyrolysis*, 10, 153-166.

Blackett, R. E., 2004, *Geothermal Gradient Data for Utah*, Utah Geological Survey, Salt Lake City, UT.

Braun, R. L. and A. K. Burnham, 1986, "Kinetics of Colorado Oil Shale Pyrolysis in a Fluidized-Bed Reactor," *Fuel*, 65, 218-222.

Burnham, A. K. and M. F. Singleton, 1983, "High-Pressure Pyrolysis of Green River Oil-Shale," *ACS Symposium Series*, 230, 335-351.

Burnham, A. K. and R. L. Braun, 1999, "Global Kinetic Analysis of Complex Materials," *Energy & Fuels*, 13, 1-22.

Campbell, J. H., G. H. Koskinas and N. D. Stout, 1978, "Kinetics of Oil Shale Generation from Colorado Oil Shale," *Fuel*, 57, 372-376.

Campbell, J. H. and A. K. Burnham, 1980, "Reaction-Kinetics for Modeling Oil-Shale Retorting," *In Situ*, 4, 1-37.

Chen, C.W., Herr, J., Weintraub, L.H.Z., 2001. Watershed analysis risk management framework: update one: a decision support system for watershed analysis and total maximum daily load calculation, allocation and implementation, EPRI, Palo Alto, CA.

Clayton, J. L., A. Warden, T. A. Daws, P. G. Lillis, G. E. Michael and M. Dawson, 1992, Organic Geochemistry of Black Shales, Marlstones, and Oils of Middle Pennsylvanian Rocks from the Northern Denver and Southeastern Powder River Basins, Wyoming, Nebraska, and Colorado, Bulletin 1917-K, U. S. Geological Survey, Denver, CO.

Colburn, T.T., M.S. Oh, R.W Crawford, and K.G. Foster. 1989, “Water Generation during Pyrolysis of Oil Shales. 1. Sources”, *Energy & Fuels*, 3, 216-223

Earnest, C. M., 1982, "Thermogravimetry of Selected American and Australian Oil Shales in Inert Dynamic Atmospheres," *Thermochimica Acta*, 58, 271-288.

Geza M., Poeter E.P. and McCray J.E. 2009. Hydrologic-Model Parameter Selection and Estimation for a Small Mountain Watershed. Journal of Hydrology 376 (2009) 170–181

Glover, K. C., D. L. Naftz, and L. J. Martin (1998), Geohydrology of Tertiary rocks in the Upper Colorado River basin in Colorado, Utah, and Wyoming, excluding the San Juan Basin, regional aquifer-system analysis, in *U.S. Geological Survey Water-Resources Investigations Report 96-4105*, edited, p. 103.

Haar, L., J. S. Gallagher and G. S. Kell, 1984, *NBS/NRC Steam Tables, Thermodynamic and Transport Properties and Computer Programs for Vapor and Liquid States of Water in SI Units*, Hemisphere Publishing Corporation, Washington, DC.

Hail, W. J., and M. C. Smith (1994), Geologic map of the northern part of the Piceance Creek Basin, northwestern Colorado, U.S. Geological Survey Miscellaneous Investigations Series Map I-2400.

Hail, W. J., and M. C. Smith (1997), Geologic map of the southern part of the Piceance Creek Basin, northwestern Colorado, U.S. Geological Survey Miscellaneous Geologic Investigations Map I-2529.

Harbaugh, A. W. (2002), A data-input program (MFI2K) for the U.S. Geological Survey modular ground-water model (MODFLOW-2000), edited, p. 55, U.S. Geological Survey Open-File Report, OFR02-41, Reston, VA.

Huss, E. B. and A. K. Burnham, 1982, "Gas Evolution During Pyrolysis of Various Colorado Oil Shales," *Fuel*, 61, 1188-1196.

Johnson, H. R., P. M. Crawford and J. W. Bunger, 2004, *Strategic Significance of America's Oil Shale Resource*, Office of Strategic Petroleum Reserves, U. S. Department of Energy, Washington, DC.

Lee, S., 1991, Oil Shale Technology, CRC Press, Boca Raton, FL.

Mercier, T. J., M. E. Brownfield, R. C. Johnson, and J. G. Self (2009), Fischer assays of oil shale drill cores and rotary cuttings from the Piceance Basin, Colorado - 2009 update, edited, p. 16, U.S. Geological Survey Open-File Report 98-483 Version 2.

Nerurkar, N., 2012. U.S. Oil Imports and Exports. Congressional Research Service Report R4246536 p. www.crs.gov

NCDC, 2007. The National Oceanic and Atmospheric Administration (NOAA). National Climatic Data Center. US Department of Commerce. <http://www.ncdc.noaa.gov/oa/climate/stationlocator.html>.

Poeter, E.P., Hill M.C., Banta, E.R., Mehl S., Christensen S., 2005. UCODE_2005 and six other computer codes for universal sensitivity analysis, calibration, and uncertainty evaluation. US Geological Survey Techniques and Methods 6-A11. p. 283.

Rajeshwar, K., R. Nottenburg and J. Dubow, 1979, "Review Thermophysical Properties of Oil Shales," *Journal of Materials Science*, 14, 2025-2052.

Roehler, H. W., 1993, *Eocene Climates, Depositional Environments, and Geography, Greater Green River Basin, Wyoming, Utah, and Colorado*, Professional Paper, 1506-F, U. S. Geological Survey, Washington, DC.

Shell, 2006, Chemical Constituents, Source Term, and Concentration Changes with Rinsing: Basis for Design of Reclamation Plan for Post-Pyrolysis Zone, Appendix 22, Shell Frontier Oil and Gas, Denver CO, October 31, 2006

Skala, D., H. Kopsch, M. Sokic, H. J. Neumann and J. A. Jovanovic, 1990, "Kinetics and Modelling of Oil Shale Pyrolysis," *Fuel*, 69, 490-496.

Taylor, O. J. (1982), Three-dimensional mathematical model for simulating the hydrologic system in the Piceance basin, Colorado, in *U.S. Geological Survey Open-File Report 82-637*, edited, p. 91, Denver, CO.

Torrente, M. C. and M. A. Galan, 2001, "Kinetics of the Thermal Decomposition of Oil Shale from Puertollano (Spain)," *Fuel*, 80, 327-334.

U.S. Energy Information Administration (EIA), 2012. Annual Energy Outlook 2012 with Projections to 2025. DOE/EIA-0383(2012) 252 p. http://www.eia.gov/forecasts/aeo/pdf/0383(2012).pdf

USGS (2006), Piceance Creek Basin, Colorado, Oil Shale Geodatabase, edited, U.S. Geological Survey Data Series, DS-181.

Vinegar, H.J., E. Pierre de Rouffignac, K.A. Mahar, L.G. Schoeling, and S.L. Wellington, *In situ* thermal processing of an oil shale formation containing carbonate minerals, US Patent 7,735,935 B2, June 15, 2010.

Waples, D. W. and M. Ramly, 2001, "A Simple Way to Model Nonsynchronous Generation of Oil and Gas from Kerogen," *Natural Resources Research*, 10, 59-72.

Waples, D. W. and J. S. Waples, 2004, "A Review and Evaluation of Specific Heat Capacities of Rocks, Minerals, and Subsurface Fluids. Part 1: Minerals and Nonporous Rocks," *Natural Resources Research*, 13, 97-122.

APPENDIX A

Water System Dynamic Model Report by INL
(INL/EXT-12-27365 Revision 1)

INL/EXT- 12-27365
Revision 1

Water Usage for *In-Situ* Oil Shale Retorting – A Systems Dynamics Model

Earl D. Mattson
Larry Hull
Kara Cafferty

December 2012

The INL is a U.S. Department of Energy National Laboratory
operated by Battelle Energy Alliance

DISCLAIMER

This information was prepared as an account of work sponsored by an agency of the U.S. Government. Neither the U.S. Government nor any agency thereof, nor any of their employees, makes any warranty, expressed or implied, or assumes any legal liability or responsibility for the accuracy, completeness, or usefulness, of any information, apparatus, product, or process disclosed, or represents that its use would not infringe privately owned rights. References herein to any specific commercial product, process, or service by trade name, trade mark, manufacturer, or otherwise, does not necessarily constitute or imply its endorsement, recommendation, or favoring by the U.S. Government or any agency thereof. The views and opinions of authors expressed herein do not necessarily state or reflect those of the U.S. Government or any agency thereof.

INL/ EXT- 12-27365
Revision 1

Water Usage for In-situ Oil Shale Retorting -- A Systems Dynamics Model

December 2012

Idaho National Laboratory
Idaho Falls, Idaho 83415

http://www.inl.gov

Prepared for the
Battelle Memorial Institute, Inc.
Under DOE Idaho Operations Office
Contract DE-AC07-05ID14517

Water Usage for *In-Situ* Oil Shale Retorting -- A Systems Dynamics Model

INL/ EXT- 12-27365
Revision 1

December 2012

Approved by:

Name Title [optional]	Date
Name Title [optional]	Date
Name Title [optional]	Date
Name Title [optional]	Date

EXECUTIVE SUMMARY

A system dynamic model was construction to evaluate the water balance for *in-situ* oil shale conversion. The model is based on a systems dynamics approach and uses the Powersim Studio 9™ software package. Three phases of an insitu retort were consider; a construction phase primarily accounts for water needed for drilling and water produced during dewatering, an operation phase includes the production of water from the retorting process, and a remediation phase water to remove heat and solutes from the subsurface as well as return the ground surface to its natural state. Throughout these three phases, the water is consumed and produced. Consumption is account for through the drill process, dust control, returning the ground water to its initial level and make up water losses during the remedial flushing of the retort zone. Production of water is through the dewatering of the retort zone, and during chemical pyrolysis reaction of the kerogen conversion. The major water consumption was during the remediation of the insitu retorting zone.

v

CONTENTS

FIGURES

TABLES

ACRONYMS

INL	Idaho National Laboratory

Water Usage for *In-Situ* Oil Shale Retorting – A Systems Dynamics Model

1. Introduction and Background

The United States has been a net importer of oil for more most of the 20th century and the first few years of the 21st century. Recent rise in domestic production has resulted in a decrease net oil imports from a high of 60% of domestic consumption in 2005 to 45% in 2011 (Nerurkar, 2012). Nonetheless, the U.S. still imported 11.4 Mb/d of oil in 2011. This dependence on foreign oil continues to have significant strategic and economic implications.

U.S. consumption of petroleum and other liquids is expected to increase by 0.7 million barrels per day between 2010 and 2035. (EIA, 2012). while other countries, such as China, are expected to significantly increase their demand. Conventional sources of petroleum hydrocarbons have been extensively developed, so significant new developments are not expected. There are unconventional domestic supplies of solid hydrocarbons such as coal, oil sand, and oil shale that could be converted to liquids. There are an estimated 2.0 trillion barrels of oil contained in oil shale in the United States (Johnson et al. 2004). However, achieving the benefits of these oil shale resources will require significant investment by the private sector. With oil prices climbing above \$90 barrel^{-1}, there has been renewed interest in oil shale. Three companies have leased parcels from the U. S. Bureau of Land Management in the Piceance Creek Basin in Colorado to develop new technologies for oil shale development (http://www.co.blm.gov/wrra/WRFO_Oil_shale.htm). ExxonMobil has been developing its methodologies on private land.

Oil shale has long been employed as a source of energy in Estonia and Australia has recently begun development of oil shale resources. There have been several oil shale development booms in the United States including 1920, 1944, 1972, and 1981. In each case, technology demonstrations were run, but a collapse in oil prices caused the developers to lose interest. Previous attempts to develop oil shale focused on mining the shale deposits, and extracting the oil from the shale on the surface. This approach allows close control of process parameters, but results in large scale land disturbance, generates large quantities of carbon dioxide, and requires large volumes of water. Recent proposals to develop oil shale involve converting the oil shale to hydrocarbons in the subsurface, then extracting the hydrocarbons in the form of gases and liquids through production wells. The water requirements for such *in-situ* development are of concern in the semi-arid regions where oil shale occurs which is near the head waters of the Colorado River.

The purpose of this report is to evaluate the water balance for *in-situ* oil shale conversion. A model that accounts the construction, operation and remediation phases of *in-situ* oil shale development has been constructed. The model is based on an systems dynamics approach and uses the Powersim Studio 9™ software package. The construction phase primarily accounts for water needed for drilling and water produced during dewatering. The operation phase includes the production of water from the retorting process. During the remediation phase water will be required to remove heat and solutes from the subsurface as well as return the ground surface to its natural state. In this report, we provide background information on oil shale, explain the conceptual basis for the *in-situ* retorting model, describe the key components of the systems dynamics model, compare results from the model with a pilot field test, and provide preliminary results from application of the model to a hypothetical full-scale *in-situ* retorting operation.

2. Description of Oil Shale and Retorting

During the Eocene epoch (34-56 My BP), the area around the junction of Wyoming, Colorado, and Utah was covered by shallow lakes. Seasonal algae deposition in these lakes built up thick beds of organic-rich siltstones and carbonate rocks (Roehler 1993). Subsidence in the basin resulted in accumulation of lakebed deposits up to 300 m thick and transformation of the organic matter into a Type-I kerogen.

Oil is formed when the organic matter in source rocks is buried to great depth, raising the temperature, causing the kerogen to breakdown into hydrocarbons gradually over millions of years. Because the oil shale in Wyoming, Utah, and Colorado has not been subjected to these elevated temperatures, the kerogen remains in the rock. However, if the rock is artificially heated it can result in the conversion of kerogen to gaseous and liquid hydrocarbons that can be extracted from the subsurface. As the oil is distilled from the rock by heat, it can be extracted in a gaseous form and converted to liquid petroleum products by condensation. The process of thermochemical decomposition of organic matter in the absence of oxygen is called pyrolysis. The organic matter is broken down by driving off less complex (shorter chain) organic molecules. Light, hydrogen-rich products are driven off, leaving behind a carbon-rich char. Pyrolysis of oil shale is often performed at temperatures between about 350 and 500 °C. These temperatures are high enough for the conversion to occur on time scales of interest, yet low enough to avoid unnecessary cracking of the hydrocarbon molecules (which would reduce oil yields) and calcining of the carbonates in the rocks. Pyrolysis is an endothermic reaction, i.e., it consumes heat to drive the reaction.

Earlier oil shale extraction technology focused on mining oil shale, and retorting the shale in surface facilities. These facilities allowed good control of the retorting parameters, but generated large quantities of waste products. Much of the Green River formation lies at depths too deep to economically mine. Recent developments in oil shale extraction are focusing on in situ retorting. The costs of mining are avoided, large surface waste piles are not created, and much more of the resource is available for extraction, because in situ retorting can be carried out in much deeper deposits.

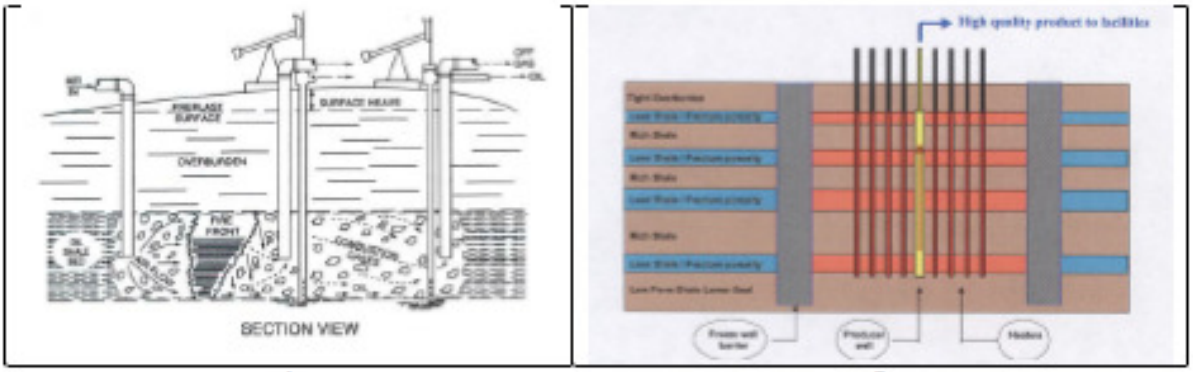

Figure 1. Two concepts of in situ oil shale retorting. A. Traditional in situ oil shale retort where the retort is first fractured, then oxygen is introduced into the formation to induce burning. Heat from the fire pyrolyses the oil shale driving off gaseous and liquid hydrocarbons. B. Shell process where heat is applied to the unfractured retort but combustion is not induced.

Harvesting the zones of carbon-rich kerogen from between the heterogeneous assemblage of rock layers, matrix porosity and larger vugs making up the oil shale is the target of *in-situ* retort processes that have been proposed by Chevron, Shell, EGL, and ExxonMobil. As originally proposed, Chevron process involves adding air to the retort and igniting the oil shale. Heat from burning the oil shale spreads through the retort, pyrolyzing the surrounding shale and generating hydrocarbons. The Shell, EGL and

ExxonMobil processes provide an external source of heat to the retort over a period of several years, and do not induce combustion. The gradual heating will allow chemical pyrolysis to take place, converting the organic matter into petroleum-like liquids and gasses that can be brought to land surface and subsequently refined.

-

3. Conceptual Model for *In-Situ* Oil Shale Retorting

Information gathered from the environmental impact statements submitted by Shell, Chevron, and EGL (http://www.co.blm.gov/wnra/WRFO_Oil_shale.htm) was used to develop a model of an *in-situ* shale oil retort. As designed by the production companies, the rock masses will be heated to temperatures approaching 400 °C (Figure 1). To date, the target depth range is 300 to 1000 m below land surface. Raising the temperature to 400 °C will result in relatively low viscosity liquids and high pressure gasses that will be extracted using production wells.

Shell and EGL provide information on the size of their proposed in situ retorts. The Shell retort is planned to be 46 m by 46 m in area and to extract oil from the entire thickness of the Green River formation, which is about 330 m thick. The EGL retort is planned to cover an area of 8000 m^2 and to extract from a thickness of 100 m. Both retorts will have a volume of about $7x10^5$ m^3

4. Systems Dynamics Model

The water usage model is based on three phases of in the overall development of the resource: construction, operation, and remediation. In each of these development stages, water usage is very different. During the construction phase water is primarily used for drilling and for dewatering the reservoir prior to heating. During the operation phase, water will be produced from the reservoir as a result of the heating and subsequent conversion of organic matter and dehydration of minerals. During the remediation phase, water will largely be used to flush the reservoir to remove heat and potential contaminants. In addition, water will likely be used to re-establish native plant growth at the surface. These interacting processes are simulated using a systems dynamics model that solves first-order differential equations in time to simulate the evolution of a system.

The model is constructed using the Powersim Studio™ (version 9.01), however, the energy and mass balance modules in the Operations phase were first simulated in the Stella computer code then transferred to PowerSim. Both system dynamic software packages consist of four key objects: levels (stocks), flows, auxiliaries (converters), and links (connectors) where the object names in parentheses used in Stella. Complex systems can be described by assembling these objects with proper descriptions of system characteristics.

- Levels (Stocks) –a reservoir that holds mass or heat.
- Flows –describe mass transfer between levels (stocks), or between the system and the surrounding environment.
- Auxiliary (Converters) –provide the parameters and equations used to calculate the flows or to summarize information.
- Links (Connectors) –show the flow of information through the system. What converters control what flows and how flows depend on the values of levels (stocks).

Using these four objects, a model of an *in-situ* retort was built.

4.1 Construction Phase

The three key uses/production of water during the construction phase are for drilling, reservoir dewatering and dust control. The modules used to describe water consumption/production during these activities are provided in the following sections.

4.1.1 Well Drilling

There are four types of wells that must be drilled to implement the oil shale development: 1) freeze wells, 2) heater wells 3) production/dewatering wells, and 4) and monitoring wells. To determine water usage we first calculate the number of required wells, then the time to complete the drilling, and finally the amount of water required for the activity.

4.1.1.1 Number of wells calculations

The number of wells is calculated from the input desired retort dimensions, and well spacing. Freeze wells are a fairly simple calculation of the calculated perimeter divided by the sum of the desired freezer well spacing and the freeze well diameter. Figure 2**Error! Reference source not found.** illustrates the linking of the necessary variables to the calculation. This figure also uses the buffer zone distance to calculate the heater area, width and length. These values are used to calculate the number of heater wells (Figure 3) which is the products of the truncated value of 4*(heated area length)*(heated area width)/(heater well diameter + $(2)^{0.5}$*heater well spacing). The number of monitoring wells is set to a

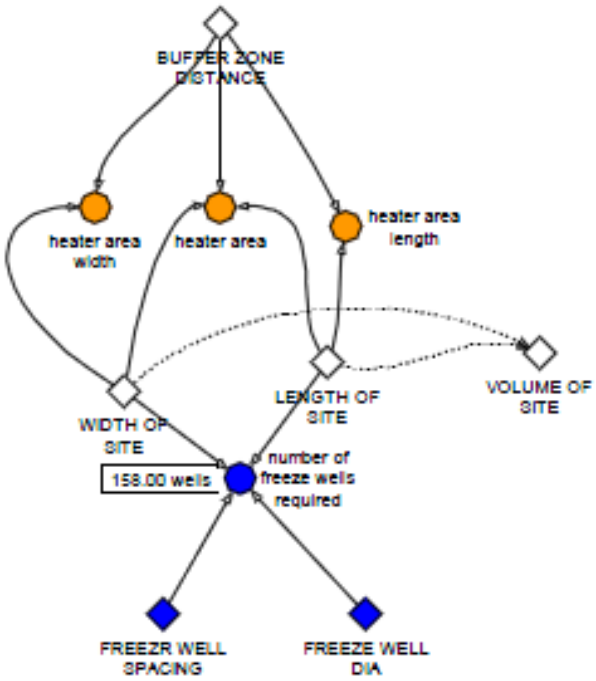

Figure 2. Calculation of the number of freeze wells, heated area width, length and area based on the inputted width and length of the site.

fixed value (currently 3).

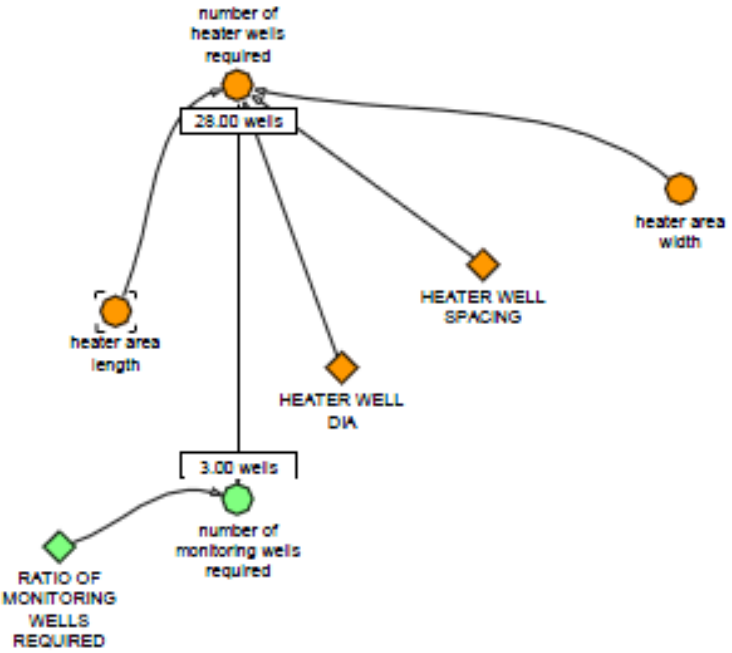

Figure 3. Calculation of the number of heater wells that are needed based on heated area calculations.

4.1.1.2 *Time to complete well drilling calculations*

Individual well drilling time is determined from the total depth of the retort below land surface divided by the estimated well drilling speed (Figure 4). In this case, the well drilling speed of 8 feet per hour calculated from the Shell's plan of operation statement that it required 2 months to complete 157 wells with two rigs. At this time, all wells are considered equal to the depth of the site, but the program was designed to easily change that assumption. It is also assumed that all wells have the same drilling speed regardless of use or the specific drilling rig used.

The sequence and timing of the drilling is calculated in a sequential fashion with the assumed order of that the freeze walls are first followed by the production/dewatering wells, heater wells, and finally the ground water monitoring wells. Variables used to calculate the total drilling time (Figure 5) are the number of drilling rigs and the time it takes to drill each well. All rigs are assumed to be working on the same set of wells at any time.

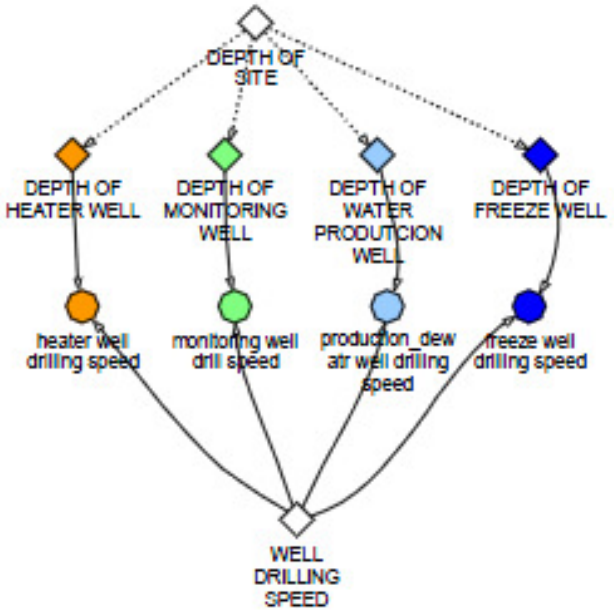

Figure 4. Calculation of the time it takes to complete each of the required wells.

7

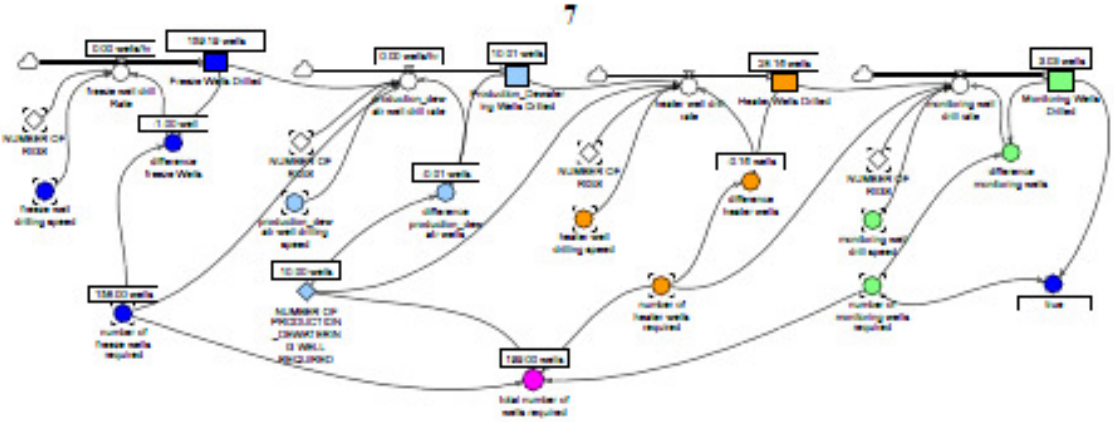

Figure 5. Calculation of the time it takes to complete all of the required wells.

4.1.1.3 *Water usage calculation*

Now that the number of wells needed and the time spent on each well is calculated, the amount of water required to construct these wells and the rate of water use can be determined. Drilling water use rate is calculated from the "drill lube and removal water requirement" (which can be thought as the volume of drilling fluids needed to fill the hole as the bit advances) multiplied by the drilling speed, plus the mud and seepage loss all multiplied by the recycle efficiency (Figure 6). In our case, the "drill lube and removal water requirement" is assumed to be 10 gallons per foot of drill advancement, mud loss and seepage loss. In our case, the mud loss makes up the greatest portion of the water use (about 5 times the amount of the seepage and drill bit advance combined).

6

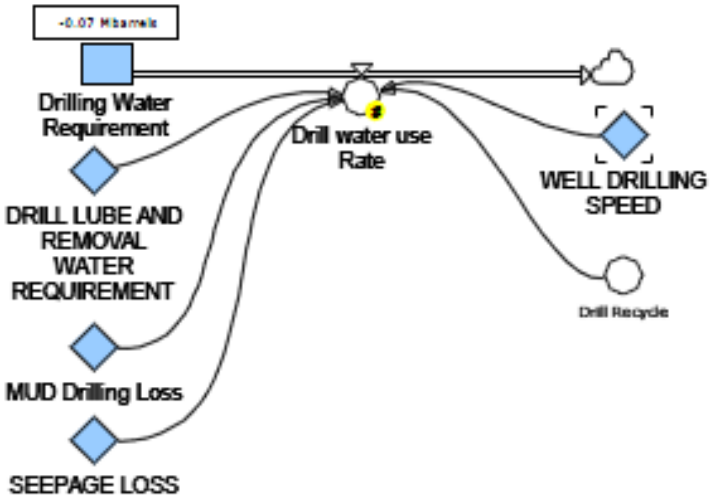

Figure 6. Calculation of drilling water rate.

4.1.2 Reservoir Dewatering

Prior to heating of the oil shale, water contained in the pore space of the oil shale retort volume will be removed by pumping. The volume of water to be removed is calculated from the volume of oil shale within the freeze wall and the effective porosity of the oil shale. A logic variable "dewater start" is used to initiate the dewatering of the retort volume once the freeze wells are in place. The rate of water extraction is a function of the user defined pumping rate for each well multiplied by the number of water production wells. At this time, the pumping rate is set as a constant but could be modified at a later date to be a more realistic function. The amount of water to be pumped from the retort is determined from the effective porosity multiplied by the retort volume.

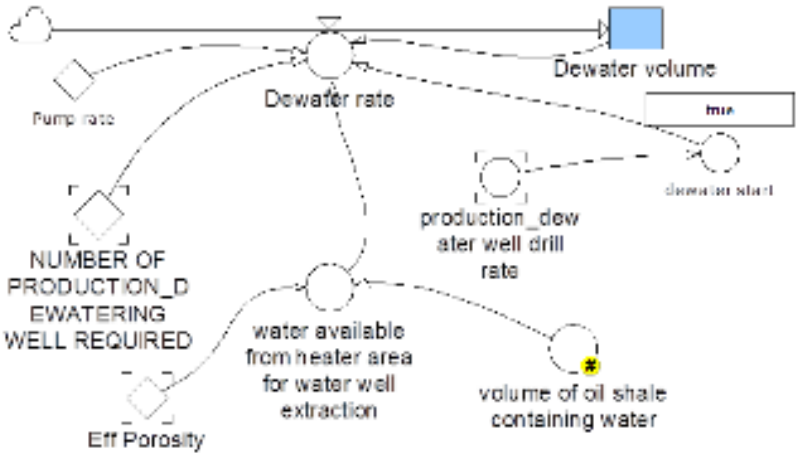

Figure 7. Calculation of water extraction rate.

4.1.3 Dust Mitigation

Dust mitigation is assumed to be a constant rate of water use based on delivery of one 10,000 gallon truck delivered to the site each day (equivalent to 3 gpm). To determine the total amount of water during drilling, the dust mitigation rate is added to the drill water use rate for the time required to drill the wells. Total water usage during construction was 0.16 Mbarrels for this example. Main water uses were for dust mitigation and drill. Dust mitigation resulted in 0.09 Mbarrels of water required. Drilling water requirements were slight less at 0.07 Mbarrels.

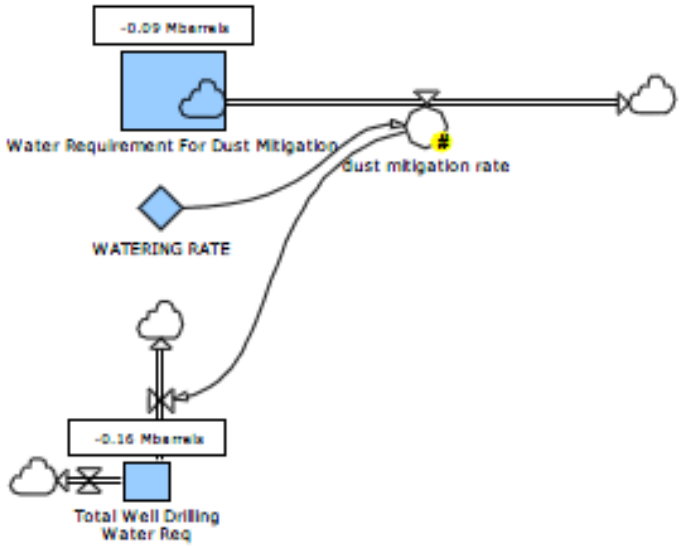

Figure 8. Calculation of dust mitigation rate.

4.2 Operation Phase

The second phase of oil shale development is the operation of the retort. A simple model is used to calculate the temperature increase in the retort. *In-situ* retort heaters are often designed in terms of their power output in kilowatts (kW). Therefore we will input heat into the retort and calculate the temperature of the retort. The temperature will be used to update the heat capacity, phase change and reaction kinetics. The operation model will be composed of 5 components; a temperature/pressure model to update properties, a heat model, a rock model, a water model and an oil/kerogen model. The energy and mass balance modules in the were first simulated in the Stella computer code then transferred to PowerSim.

4.2.1 Temperature / Pressure model

The retort is assumed to start off in equilibrium with the natural geothermal gradient and the natural hydrostatic pressure head. Using the geothermal gradient of 34 °C km^{-1} (Blackett 2004) and an overburden thickness of 330 m, and a retort zone thickness of 330 m gives a median retort initial temperature of about 25 °C. Hydrostatic head calculated for the same depth is 3000 kPa.

The relation between temperature and heat is important for the retorting operation. There is a causal loop relation between temperature and heat through the specific heat of the components of the retort. The

specific heat is a function of temperature, and the relation between temperature and heat depends on the specific heat. The relation between heat and temperature for a system is given by:

$$Q_s = \sum_i m_i \left(s_i T + v_i \right) \quad (1)$$

where:

Q_s = total heat in the system (J)

m_i = mass of component i (kg)

s_i = specific heat of component i ($J\,kg^{-1}\,K^{-1}$)

T = temperature of system (K)

v_i = heat associated with any phase changes ($J\,kg^{-1}$)

Equation 1 can be solved for T, and used to calculate temperature from the total heat and the masses of components in the retort. Thus, heat is the independent variable, and temperature is the dependent variable.

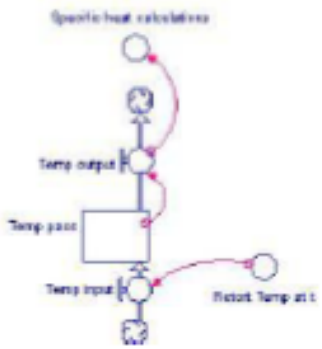

Figure 9. Stella routine to pass temperature between time steps.

The properties of water and steam as a function of temperature and pressure have been extensively studied and very comprehensive, and complicated, equations defining the properties of water as a function of these two state variables have been developed (Haar, Gallagher, and Kell 1984). For our purposes, simple relations were determined by fitting equations to data using a non-linear, least squares fitting program. The equations are given in the text, and plots are shown that illustrate the fit of the equations to the data.

The component's specific heat in the model are functions of temperature. Therefore, a feedback loop is included in the model (see Figure 9) that saves the current retort temperature, and allows it to be used in the next time step to calculate the specific heats for the next time step. Temperature variable specific heat is included in the model for water, steam, rock, and kerogen. Temperature-dependent specific heat of vaporization of water is also included. Pyrolysis is endothermic, and some heat will be consumed in the reaction. This consumption of heat for pyrolysis is not included in the model.

4.2.1.1 *Specific heat of water and steam*

The specific heat of water is relatively constant from 0 to about 300 °C (Figure 10). Above that temperature, it rises sharply reaching a peak at the critical point. In this model, the equation for specific heat is extrapolated to as high in temperature as needed. This is not an important issue for water as water has all boiled off to steam long before the critical point is reached. The equation used for the specific heat of water is:

$$s_w = \frac{4163.773 - 0.02363 \cdot T^2}{1 - 7.1383 \times 10^{-6} \cdot T^2} \quad (2)$$

where temperature is in °C.

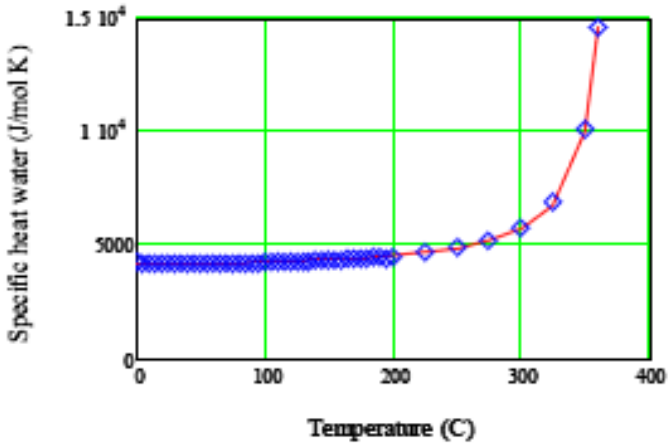

Figure 10. Specific heat of water as a function of temperature below the critical point.

The specific heat of steam increases gradually as a function of temperature. Data from the NIST chemistry web book were fit to a polynomial:

$$s_{st} = 1831.27 + 0.476158 \cdot T + 3.3172 \times 10^{-4} \cdot T^2 - 1.6206 \times 10^{-7} \cdot T^3 \quad (3)$$

This equation is continuous through the critical point of water, and so is used for all temperatures.

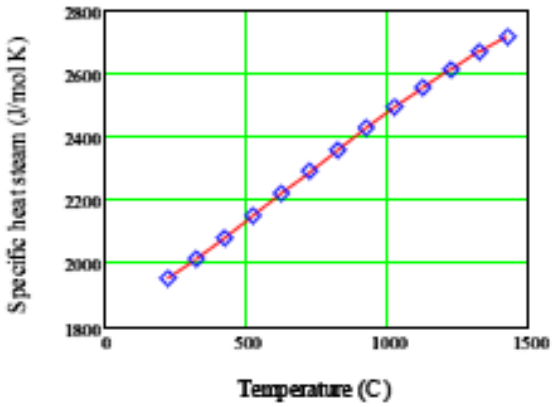

Figure 11. Specific heat of steam as a function of temperature.

The heat of vaporization of water is also a function of temperature (Figure 12). The heat of vaporization is not continuous through the critical point, as the heat of vaporization looses meaning above the critical point. As almost all phase changes between water and steam take place well below the critical point, this should not be a problem. A linear equation (dashed brown line) was fit to the heat of vaporization data below a temperature of 200 °C to prevent negative values of heat of vaporization. The polynomial used is given by:

$$v_w = 2.5 \times 10^6 - 2649.8 \cdot T \quad (4)$$

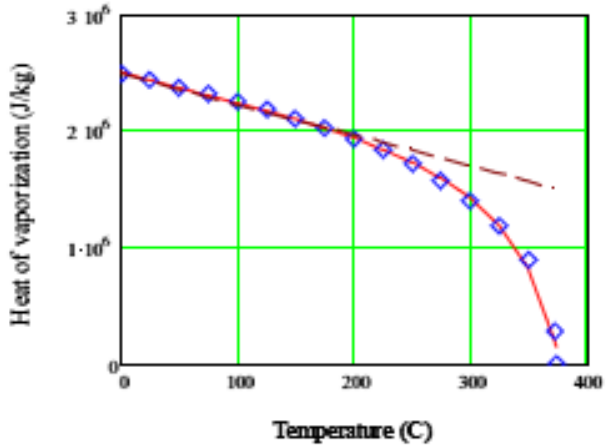

Figure 12. Heat of vaporization of water as a function of temperature.

4.2.1.2 *Specific heat of rocks and kerogen*

Data on the specific heat for a wide range of rocks and minerals was analyzed by Waples and Waples (2004). These authors found that the specific heat data as a function of temperature (°C) were fit well by normalizing the data to the specific heat at 200 °C. The polynomial used to fit the reduced data is plotted in Figure 13 and is given by:

$$s_r \quad 0.716 + 1.720 \times 10^{-3} \cdot T \quad 2.13 \times 10^{-6} \cdot T^2 + 8.95 \times 10^{-10} \cdot T^3 \qquad (5)$$

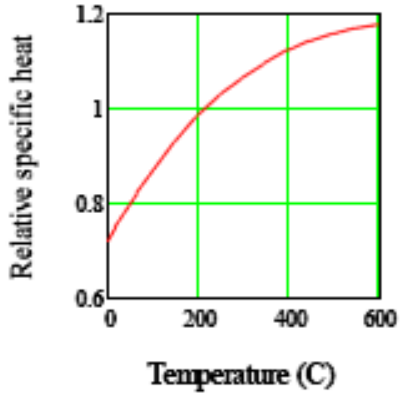

Figure 13. Reduced specific heat referenced to 200 ºC as a function of temperature.

This equation fits both the mineral matter in the Green River formation, and the kerogen content. The specific heat at 200 °C for the kerogen is 1965 J kg^{-1} K^{-1} and for the shale is 1113 J kg^{-1} K^{-1} (Waples and Waples 2004).

4.2.2 Heat model

The primary objective of this exercise is to quantify the energy balance for an oil shale retort. We therefore need a model for the flow of energy into the retort, between the different components within the

retort, losses of energy to the surrounding environment, and finally, the amount of energy extracted from the retort. This balance will drive the economics of the retorting process. Heat or energy is the proper variable to use in the retorting model, not temperature. Temperature is an intensive state variable that will depend on the heat in the system, but is not a conserved component. The relation between temperature and heat is given by equation 1.

The primary object of the heat model is a stock identified as retort heat (Figure 14). This stock contains all the heat that is present in the reservoir. This heat is distributed among a number of different phases within the reservoir, but the sum total of heat is recorded in this one stock. The units for the stock retort heat are joules (J).

The initial condition for the amount of heat in this stock depends on the ambient temperature in the reservoir, the mass of other components in the reservoir, and the heat capacity of those components. For initial conditions, an ambient temperature was determined using the geothermal gradient of 34 °C km^{-1} (Blackett 2004). From the Shell EIS, the overburden is about 330 m thick, and the retort zone is about 330 m thick. The median depth of the retort is then about 500 m. Surface temperature is set at 8 °C. This gives a retort initial temperature of about 25 °C. Using Equation 1, an initial temperature of 25 °C, the masses of other components in the retort, and the specific heat of those components at 25 °C, the initial retort heat is calculated by the model.

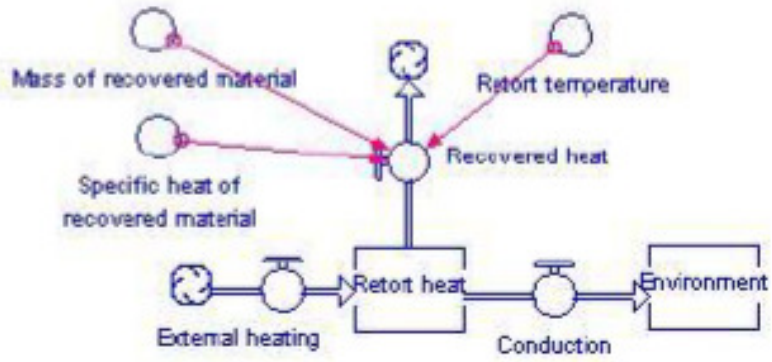

Figure 14. Heat model.

Two other stocks are included in the heat model, a stock for heat lost to the environment (i.e., the formation outside the retort), and a stock for heat recovered at the surface in produced products (steam, oil, and gas). These stocks sum the heat removed from the retort, and are initially 0 J.

There are three flows associated with retort heat: external heating, conduction to the environment, and heat extracted to the surface. As energy flows, the units are J day^{-1}. External heating represents the energy added to the retort to raise the temperature to induce pyrolysis of the kerogen. This is assumed to be a constant flux boundary condition. Two parameters are used to describe this heating; a heating rate in J day^{-1}, and a duration in days of total heating. The duration is used in a STEP function to turn off heating after the heating duration has elapsed. From the EGL EIS and the Shell EIS, heating durations on the order of several years are indicated. EGL provides a heating rate in their EIS of 2.1×10^{11} Btu yr^{-1} (6.1×10^{11} J day^{-1}). Heats of retorting are also given by EGL and by Rajeshwar et al. (1979) that give the amount of heat required to retort 1 kg of oil shale. These numbers range from 4.4×10^{5} J kg^{-1} to 1.7×10^{6} J kg^{-1} depending on the grade of the oil shale involved. Given some estimates of the mass of kerogen in the retort (~2×10^{9} kg, discussed below), and the heat of retorting, the total amount of heat needed to complete the retort can be estimated to be between 4×10^{14} and 1.6×10^{15} J. For heating rates on the order of 6×10^{11} J

day^{-1}, the heating duration ranges from 1.8 to about 7 years. These calculations give us a range of heating rates and durations to serve as a starting point for defining the energy input to the retort, and are generally consistent with estimates provided by the energy companies.

Heat added to the retort will be lost by thermal conduction to the surrounding country rock. Thermal conduction is described by Fourier's law of heat conduction:

$$Q = -A \cdot k \cdot \frac{\Delta T}{\Delta x} \tag{6}$$

where

Q = heat transfer (J day^{-1})

A = area across which heat is conducted (m^2)

k = thermal conductivity (J m^{-1} day^{-1} K^{-1})

ΔT = temperature difference (K)

Δx = distance between retort and environment (m)

The thermal conductivity of Green River oil shale ranges from 6x10^4 to 1.6x10^5 J m^{-1} day^{-1} °K^{-1} (Rajeshwar et al. 1979). From geometry of the retorts given by Shell and EGL, the surface area of the retort is calculated to be 60,000 m^2. From the Shell EIS, which gives a distance of 75 m from the retort edge to the freeze wall, a distance to the environment is set at 75 m. The temperature difference is calculated from the difference between the retort temperature, and the temperature of the environment, 25 °C. This is therefore a constant temperature boundary condition. Once the retort is up to temperature, the conductive heat loss will be on the order of 1x10^{10} J day^{-1}. We will assume that heat conduction is in steady state at all times. This is a large simplification as there will be a significant temperature transient during heating. For this model, we assume a linear temperature drop between the retort and the environment is maintained at all times and that the distance to the constant temperature boundary conditions does not change.

Once retort operations start, steam, oil, and gas will be produced from the retort. As these components are removed from the reservoir, they will carry a certain amount of heat with them. The amount of heat extracted from the reservoir will depend on the mass extracted, the temperature of the extracted component, the specific heat of the component, and any heat consumed by phase changes. Equation 1 is used to calculate the heat extracted from the retort by removing steam, oil, and gas. For steam, an extra term is added that accounts for the heat of vaporization of the steam. No heat of reaction or vaporization is included for oil or gas. For calculation of the heat extraction, the mass of extracted components is obtained from other calculations in the model. How these masses are calculated is discussed later. The equation used to calculate the flow of heat to the surface is:

$$Q = M_{st}\left(c_{st}T - v_{st}\right) + M_{oil}s_{oil}T - M_{gas}s_{gas}T \tag{7}$$

where:

Q = heat flow to the surface (J day^{-1})

M_{st} = mass of steam extracted (kg day^{-1})

M_{oil} = mass of oil extracted (kg day^{-1})

M_{gas} = mass of gas extracted (kg day^{-1})

s_{st} = specific heat of steam (J kg^{-1} K^{-1})

s_{oil} = specific heat of oil (J kg^{-1} K^{-1})

s_{gas} = specific heat of gas (J kg^{-1} K^{-1})

v_{st} = heat of vaporization of steam (J kg^{-1})

T = temperature of retort (K)

The heat extracted from the retort can be used on the surface in plant operations. However, no credit in the model is taken for this recovery of energy. Operations that do recover some of the heat from the retort would increase the overall efficiency of the operation.

4.2.3 Rock model

The rock model consists of two objects. There is a single stock that represents the mineral grains of the Green River shale formation. The second object is used to calculate the kerogen mass associated with the retort rock mass. We assume no geochemical reactions with regard to the mineral grains at the temperatures achieved by in situ retorting, so there are no changes in the rock model. The purpose of the rock model is to include the mass of inorganic solids into the calculation of the amount of heat needed to bring the reservoir to the desired temperature for pyrolysis. The mass of rock is calculated from the volume of the retort and the bulk density of Green River shale. The retort volume is calculated to be 6.37×10^5 m^3. At a bulk density of 2500 kg m^{-3}, there is a total rock mass of 1.59×10^9 kg. There are no flows to or from this stock.

A second component of the rock model is to calculate the mass of kerogen in the retort. This mass is then passed as an initial condition to the oil model. The kerogen model takes as input the grade of the oil shale in gal ton^{-1}, because this is the number most often used to describe how rich the formation is. The grade is determined from a Fischer assay of the oil shale. For this model, we assume the Fischer assay extracts all of the kerogen from a sample. The laboratory yield in gal ton^{-1} is converted to m^3 kg^{-1}, then multiplied by the oil density. This gives kg of oil generated. Not all kerogen is converted to oil, some remains as char and some is lost to gases. From the stoichiometry of the pyrolysis reaction (Campbell et al. 1980), we estimate that 69.5% of the kerogen is converted. Therefore, the kg of oil is divided by 0.695 to convert the oil to total kerogen. For an oil shale with a grade of 25 gal ton^{-1}, the grade is 1.04×10^{-4} m^3 kg^{-1}. Assuming an oil specific gravity of 35 °API (850 kg m^{-3}), the kerogen content of the rock is 0.127 kg kerogen per kg of oil shale. This is a typical number from the published literature. For the total rock mass in the retort, the total kerogen is calculated to be 2.0×10^8 kg. The expected oil yield from pyrolysis is calculated to be 1.4×10^8 kg or 1×10^6 barrels. The kerogen model takes as input the grade in gal ton^{-1}, and calculates the kg of kerogen associated with the kg of oil shale in the retort. This is passed to the oil model as an initial condition.

4.2.4 Water model

The water model in the oil shale retort model is very important for the energy balance calculations. Water has very high specific heat, and the heat of vaporization of water to steam is also very high. Therefore, the heating and vaporization of water in the retort will play a very important role in heating of the retort. The water model consists of three stocks, one for water, a second for steam, and third for steam produced to the surface (Figure 15). These water and steam stocks are connected by a two directional flow representing boiling and condensation. Mass transfer through this flow will depend on the temperature and pressure of the reservoir. Connected to the steam stock is a flow from the retort to the surface that represents steam extraction. We assume no pumping of water from the retort to draw-down water in the system prior to heating. Because this activity would precede heating, it could be incorporated by changing the initial conditions in the water stock.

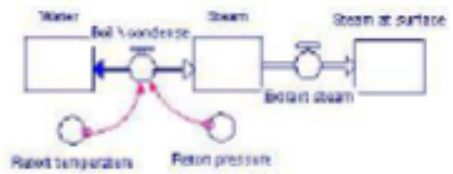

Figure 15. Water model used in Stella.

The steam stock is initially set to 0 kg. The water stock is initialized assuming the oil shale is water saturated. The initial mass of water in the stock is calculated form the volume of the retort ($6.37x1^{-5}$ m^3), the porosity of the retort (0.057), and the density of water (1000 kg m^{-3}). The initial water mass calculated in this way is $3.61x10^7$ kg. The flow that represents boiling and condensation of water is based on the pressure and temperature at which water boils or steam condenses in the retort. These calculations depend on the temperature and pressure of the retort. A very simplified model of the thermal properties of water and steam is included in the model. We assume that the system is constrained to the water - steam equilibrium curve. Retort pressure is equal to the saturated steam - water curve plus hydrostatic pressure. When, during heating, the vapor pressure of steam exceeds the hydrostatic pressure, water begins to boil. When cooling, when the pressure drops below hydrostatic pressure, water begins to condense.

Hydrostatic pressure is calculated from the mass of water above the retort, and is given by

$$\rho gh = 1000 \text{ kg m}^{-3} * 9.8 \text{ m sec}^{-2} * 300 \text{ m} = 3000 \text{ kPa} \quad (8)$$

where

ρ = density of water (kg m^3)

g = acceleration of gravity (m sec^{-2})

h = depth of retort (m)

The equation for steam pressure (P_v) in the retort in kPa as a function of temperature (°C) is given by:

$$P_v \quad \exp\left(\frac{-0.534487 + 0.72 \cdot T}{1 + 0.00443\ T}\right) \quad (9)$$

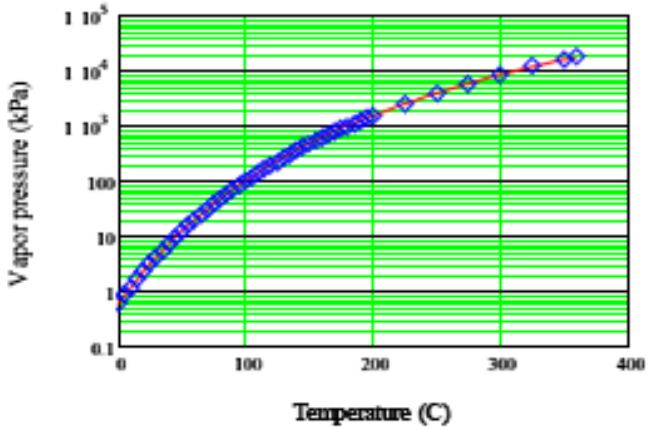

Figure 16. Vapor pressure of steam as a function of temperature used in retort model.

We can also solve this equation to calculate the boiling temperature (T_b °C) of the reservoir from the hydrostatic confining pressure (P_c kPa):

$$T_b = \frac{7.00766 - 14.00823 \cdot \ln(P_c)}{1 - 0.06127 \cdot \ln(P_c)} \tag{10}$$

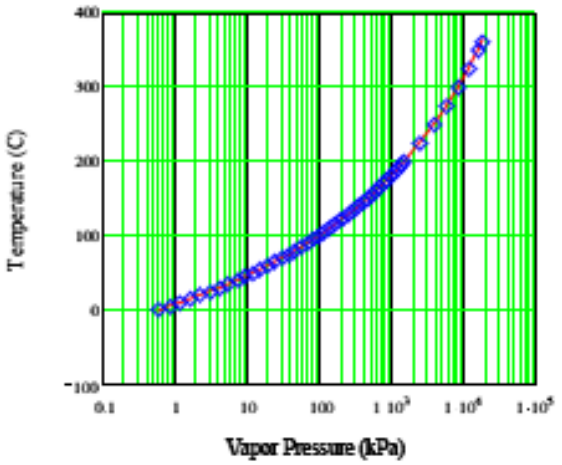

Figure 17. Function and curve to calculate boiling temperature from the hydrostatic confining pressure on the reservoir.

In the model, heat is added to the water raising the temperature. When the temperature of the retort exceeds the boiling temperature based on the hydrostatic pressure, then water begins to turn into steam. The logic of the calculation must allow for flow in both directions, that is both boiling and condensation. The equation used for the flow is:
If (confine_temp > retort_temp) then

$$M_{s\_w} = \frac{(T_r - T_c) M_s \cdot s_s}{v_s} \tag{11a}$$

else

$$M_{w\_s} = \frac{(T_r - T_c) M_w \cdot s_w}{v_s} \tag{11b}$$

When the retort temperature either exceeds the boiling temperature or drops below the boiling temperature, there is a temperature difference that has to be corrected. Multiplying this temperature difference by the specific heat of the phase and the mass of phase defines the number of joules needed to bring the temperature back into equilibrium. Dividing by the number of joules kg^{-1} consumed or liberated by the phase transformation reaction, gives the mass of phase transfer needed to bring the temperature back into equilibrium. Note that T_r–T_c changes sign giving positive and negative flows through this flow object.

The final component of the water model is a flow from the steam stock to the surface that represents extraction of steam from the retort. Flow to the surface is assumed to be a function of the amount of steam with a constant fraction of the remaining steam removed per unit time. This gives the mass of steam extracted to the surface (M_s) used in equation 7.

4.2.5 Kerogen / Oil model

Pyrolysis occurs in the absence of oxygen, so that the organic matter is broken down into less complex (shorter chain) organic molecules. Light, hydrogen-rich products are driven off, leaving behind a carbon-rich char. Formation of oil occurs at temperatures between about 400 and 500 °C. Kerogen, with an initial C/H mole ratio of about 0.67 undergoes three pyrolysis reactions (Campbell et al. 1980; Huss and Burnham 1982):

1) Primary pyrolysis occurs between 350 and 500 °C, oil is driven off generating a residual char with a C/H ratio in the range of 1 to 1.6;
2) Secondary char pyrolysis occurs between 500 and 650 °C, hydrogen gas and methane gas are driven off, the residual char has a C/H ratio between 1.6 and 4.3.
3) above 650 °C, hydrogen gas, ammonia, and hydrogen sulfide are driven off, leaving the char with little hydrogen.

Writing out the stoichiometry of the primary pyrolysis reaction, we get the following generalized (and much simplified) reaction for pyrolysis (Huss and Burnham 1982):

$$C_1H_{1.5}O_{0.05} \rightarrow 0.014\ CO_2(g) + 0.015\ H_2(g) + 0.012\ C_3H_8\ (g) + 0.018\ H_2O + 0.72\ C_1H_{1.7}\ (oil) + 0.228\ C_1H_{0.63}\ (char) \quad (12)$$

Temperatures during *in-situ* retorting will be constrained to less than 500 °C, unless combustion is induced in the retort by introducing air. In writing this simplified reaction, we assume all O in carboxyl groups forms carbon dioxide, and that hydrogen is combined in hydrocarbon products with a C/H ratio of about 0.5 representing paraffins, olefins, and naphthenes. This indicates that about 20% of the initial carbon will end up in char. Converting the reactants and products in Equation 12 back to weights, we get that for each kg of kerogen pyrolyzed, the yield will be 0.043 kg of CO_2(g), 0.695 kg of liquid hydrocarbons, 0.037 kg of hydrocarbon gases, and 0.202 kg of char. The mass of hydrocarbons, or the lengths of the hydrocarbon chains, will range from methane to much more complex molecules. This range of molecules will result in a wide range of boiling points for the reaction products. As result, there will be a mix of volatile and liquid hydrocarbons, and the mix will vary as the retort temperature varies relative to the boiling points of the hydrocarbons.

The reaction kinetics of kerogen pyrolysis have been extensively investigated (Campbell and Burnham 1980; Braun and Burnham 1986; Bar et al. 1986; Skala et al. 1990). Experimental conditions have mainly covered the very high heating rates and atmospheric pressure conditions of surface retorts. Kerogen is a complex organic molecule, and is broken down into a wide range of product molecules during pyrolysis. The composition of the products will depend on temperature, pressure, and the heating rate. Therefore, a single, or even a series, of kinetic reactions can not readily describe the kinetics of kerogen pyrolysis. Most thermogravimetric analyses of oil shale response to heating, however, indicate that kerogen breakdown occurs in a single peak around 400 °C (Figure 18). An additional reaction occurs at a temperature of about 700 °C, but this is higher than temperatures expected for in situ retorting. Because the thermal gravimetric response shows a single peak, a number of authors have used simple one component models of kerogen pyrolysis.

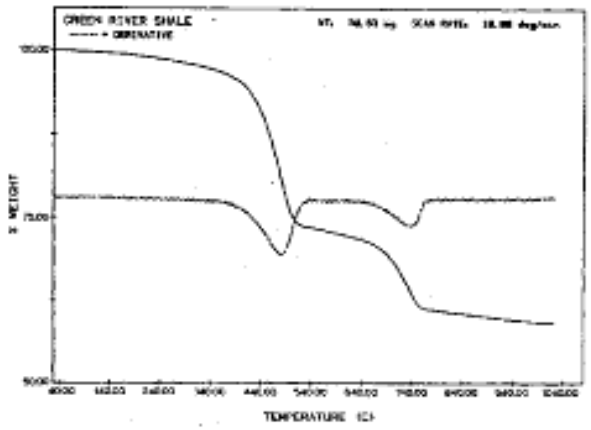

Figure 18. Thermal gravimetric and differential thermal gravimetric curves for a Green River oil shale specimen (Earnest 1982).

For systems that are too complex to be characterized in a fundamental way, it is common to describe the reaction in terms of a lumped pseudo species (Burnham and Braun 1999). A first order lumped parameter kinetic model was fit to kerogen decomposition by Campbell et al. (1978) and is adopted for this model. It is a single reaction model that describes the overall reaction of kerogen to oil. Combining this kinetic model with the stoichiometric model in equation 12, provides a means to model the retort. For a single first order pyrolysis reaction taking place under a constant heating rate ($dT/dt = C_r$), the rate of product evolution is given by (Burnham and Braun 1999):

$$\frac{dM}{dT} = \frac{-A_f}{C_r} \cdot \exp\left[-\frac{E_a}{RT} - \left(1 - \frac{2RT}{E_a}\right)\right] \cdot \left(\frac{A_f R T^2}{C_r E_a}\right) \cdot \exp\left(\frac{E_a}{RT}\right) \tag{13}$$

where

E_a = Activation energy (J mol^{-1})

A_f = Preexponential frequency factor (day^{-1})

M = Mass of kerogen (kg)

R = Gas constant (J mol^{-1} °K^{-1})

T = Temperature (°K)

C_r = Constant heating rate (°K day^{-1})

t = time (day)

Temperature and time are related by the heating rate so that the change is mass with respect to temperature can also be related to the change in mass with respect to time.

$$\frac{dM}{dt} = \frac{dM}{dT} \cdot \frac{dT}{dt} \tag{14}$$

Several studies have been conducted to measure the activation energy and frequency factor for oil shale pyrolysis. These have been conducted at both constant temperature increase and at constant temperature. Results of a few of these studies are summarized in Table 1.

Table 1. Compilation of kinetic rate parameters for oil shales.

Source Rock	Frequency Factor (day^{-1})	Activation energy ($J\ mol^{-1}$)
Spanish[a]	$1.8x10^{13}$	150
Anvil Points[a]	$7.3x10^{20}$	247
Clear Creek[a]	$2.4x10^{21}$	254
Israel[b]	$8.0x10^{10}$	118
Anvil Points[c]	$2.6x10^{18}$	220

a. Torrente and Galan (2001)
b. Bar et al. (1986)
c. Campbell et al. (1978)

The temperature of maximum pyrolysis yield for kerogen falls within a narrow range of about 420 to 440 °C (Huss and Burnham 1982; Clayton et al. 1992), but only for high heating rates; on the order of 2880 °K day^{-1} (2 °C min^{-1}). At lower heating rates, the conversion of kerogen occurs at lower temperatures (Figure 19). At the lower heating rates expected for an *in-situ* retort, the conversion should occur at lower temperatures. Figure 19 shows that kerogen conversion can be expected to happen relatively quickly once temperatures reach the vicinity of 400 °C.

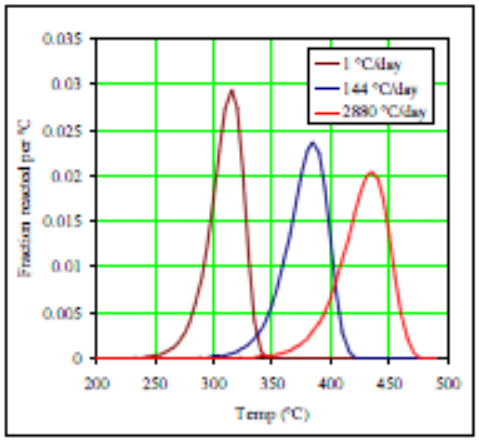

Figure 19. Mass reaction rate of kerogen as a function of retort temperature at different heating rates. Highest rates are representative of surface retorts. Lowest rate is more representative of in situ heating rates.

Surface retorting takes place at atmospheric pressures, so little work has been done on the effects of pressure on kerogen conversion. Burnham and Singleton (1983) investigated pyrolysis of Green River oil

shale at pressures to 2.74 MPa (Figure 20). The experiments were kinetic experiments carried out at constant heating rate. They found a small decrease in oil yield with increasing pressure for the same heating rate. There are insufficient data to parameterize a pressure effect on pyrolysis of oil shale, so pressure was not included in the Stella model.

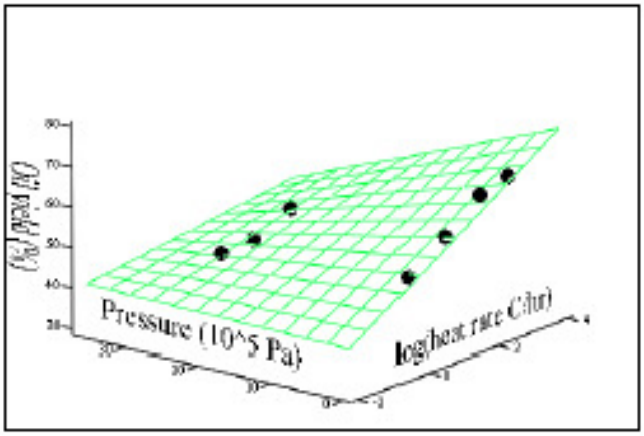

Figure 20. Effect of heating rate and pressure on oil yield (Burnham and Singleton 1983).

The kinetic model used to simulate kerogen pyrolysis is given by:

$$\Delta M = M_{t-1} A_f \cdot \exp\left(\frac{-E_a}{R \cdot T}\right) \cdot \Delta t \qquad (15)$$

The oil model calculates the mass of kerogen pyrolyzed in a time step using equation 15, then uses the mass fractions of products calculated from equation 12 to distribute mass to the product stocks (Figure 21).

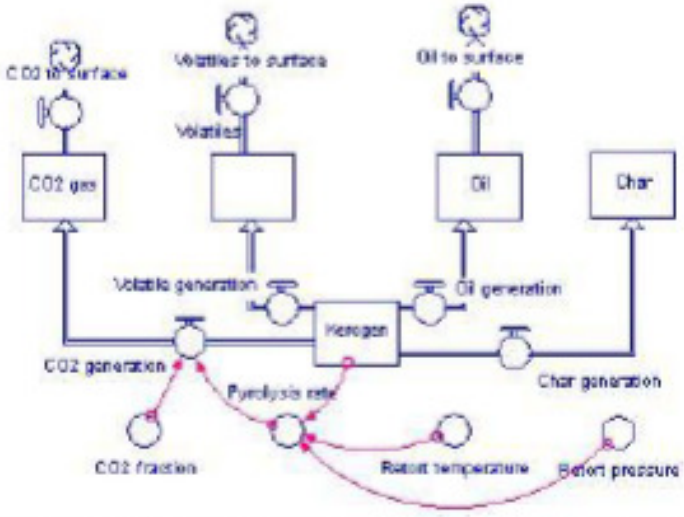

Figure 21. Model used to calculate the pyrolysis of kerogen to products in the retort. Calculation of flows is illustrated for CO_2. The other flows are calculated in the same fashion.

The initial kerogen content is calculated from the oil shale grade in the rock model. The other stocks are set to 0 as an initial condition.

4.2.6 Converters and Accumulators

There are a number of accumulators that keep track of the total masses of components extracted at the land surface. The amount of energy recovered in joules is calculated from the mass of oil and gas extracted at the surface. The Carbon Trust gives an energy content of oil of 12,751 kW hr ton^{-1}. This converts to a conversion factor of $4.6x10^7$ J kg^{-1} for liquid hydrocarbons. For hydrocarbon gas, the energy content is 11 kW hr m^{-3} according to the Carbon Trust. Because we generate kg of gas, the volumetric energy content must be converted to a mass based energy content. We assume that the gas is methane with a mass of 10 g mol^{-1} and use the ideal gas law to convert a volume of gas to kg of gas. The energy content of the gas hydrocarbons is calculated to be $9.7x10^7$ J kg^{-1}.

The model also accumulates carbon dioxide at the surface so that the generation of greenhouse gases from in situ retorting can be evaluated.

The model was run using a 1-day time step for a period of 4,000 days. The Runge-Kutta 4 integration method was used. A time step of 5 days gave results that differed by 0.2% from the 1-day time step. A time step of 0.5 days gave the same results as the 1-day time step. One day was selected for modeling runs.

4.2.7 Base Case Results

The model was simulated using the parameters discussed above. The grade of the oil shale was set at 25 gal ton^{-1}. As heat is added to the retort, the pressure and temperature increase until the vapor pressure of steam exceeds the confining hydrostatic pressure. This occurs at a temperature of 232 °C at 860 days (Figure 22). The temperature profile flattens while boiling occurs as heat added to the retort is consumed by boiling. The pressure increases during boiling, and so the boiling temperature increases slightly and is not constant as it would be for atmospheric conditions.

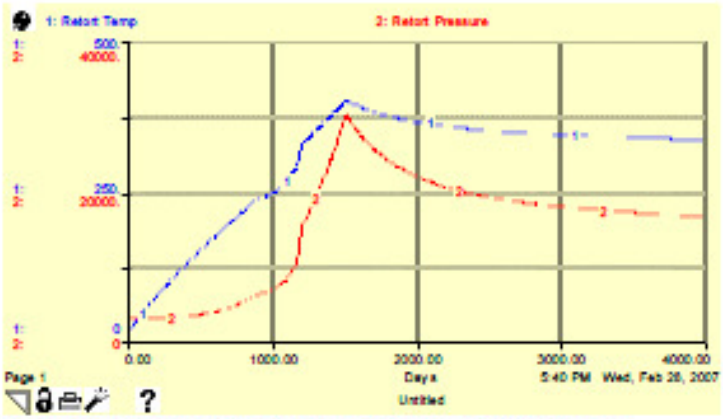

Figure 22. Increase in temperature and pressure with heating of the retort.

The rate of kerogen pyrolysis reaches a critical point at about 1100 days (Figure 23) and kerogen is rapidly converted to products. This rate of conversion is based on very small scale laboratory experiments, and may not be realistic for application to retort scale simulation. Measurements of the frequency factor and activation energy for the kerogen pyrolysis reaction show a wide range of values (Table 1), so there may be some uncertainty in this transformation rate. The laboratory rates predict complete conversion of the kerogen in about 200 days. Gas volatiles in the model are extracted rapidly and have been recovered at the surface by 1550 days.

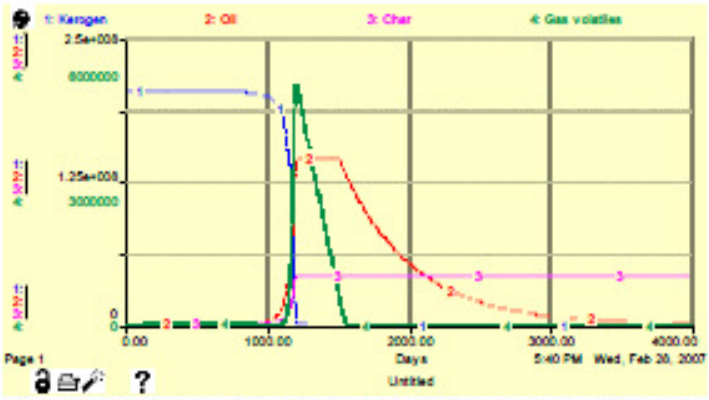

Figure 23. Distribution of kerogen and kerogen pyrolysis products as a function of time.

Most of the heat added to the retort goes to heating up the rock matrix (Figure 24). Water and kerogen also heat up. At day 860, boiling of the water releases all the energy contained in water and transfers the energy to steam. There is more energy in the steam than in the water because the steam contains the heat of vaporization. About day 1100, the heat in kerogen is released as kerogen is pyrolyzed to gas and liquid hydrocarbons. As soon as the retort temperature rises above ambient, conduction to the surrounding environment serves as a heat loss. When heating stops on day 1500, heat in the retort begins to decline by conduction to the environment.

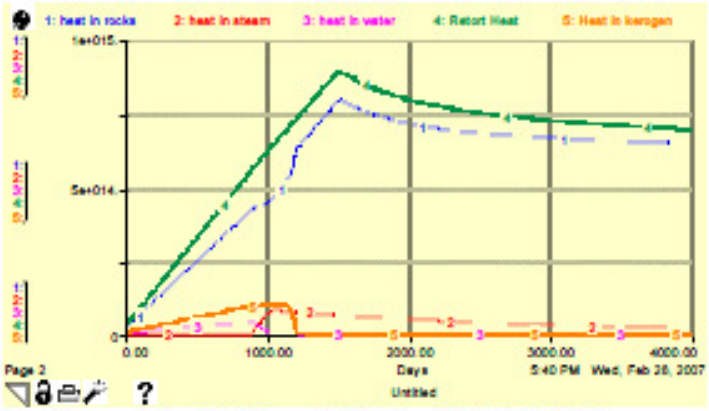

Figure 24. Distribution of energy (heat) in the retort during the first 1500 days.

The simulation indicates that the *in-situ* retorting produces much more energy than consumed to drive the pyrolysis reaction (Figure 25). A total of 9.4×10^{14} joules of energy are needed to bring the retort up to 400 °C. The energy contained in the oil and gas withdrawn from the retort amounts to 7.3×10^{15} joules, or about 8 times the energy expended. Oil recovered from the retort (Figure 26) are 1.0×10^{6} barrels. Based on the initial estimate of 25 gal ton^{-1} as the grade of oil shale, the predicted recovery is 1.05×10^{6} barrels. To recover 1 million barrels of oil, 8700 tonnes of carbon dioxide are generated. This oil recovery is probably optimistic. There are only about 7400 barrels of oil left in the retort. It is unlikely that the oil would drain from the pores so completely. The factor of 8 energy recovery factor is probably optimistic by a factor of 2. This would suggest that something like 500,000 barrels of oil could be recovered from this retort.

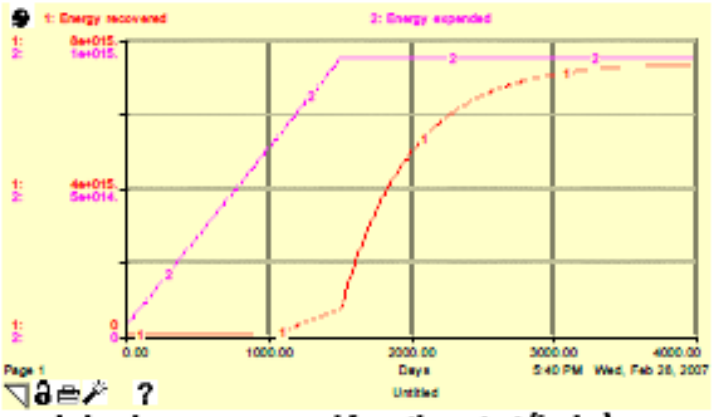

Figure 25. Energy expended and energy recovered from the retort (joules).

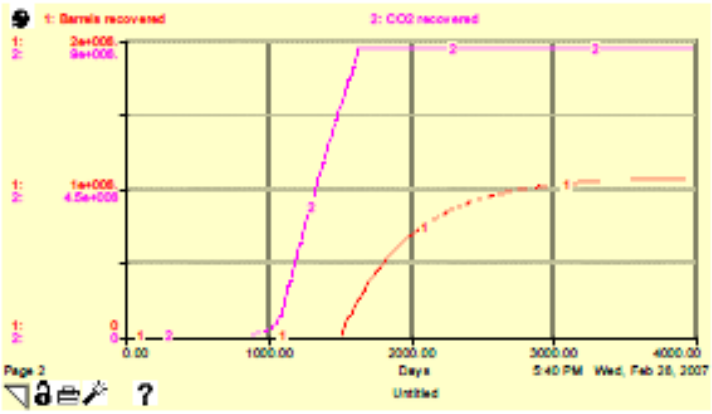

Figure 26. Barrels of oil and kg of CO2 recovered from the retort.

4.2.8 Sensitivity studies

Evaluating the parameters in the model that have the most uncertainty leads to identification of the following parameters:

- The rate of kerogen conversion
- Initial water content
- Heat conduction out of the retort

A wide range of kinetic parameters are reported in the literature. If the rate of conversion is much slower than predicted, then the heating time may not be sufficient to convert all of the kerogen to oil. The longer the heating time, the more energy needed to start the reaction. The frequency factor and activation energy cannot be varied independently. Therefore, values for the two Anvil Points samples shown in Table 1 were simulated. The base case was the Anvil Point values from Campbell et al. (1978). It turns out that the number of barrels recovered is not very sensitive to the reaction kinetics over a wide range of values. As can be seen from Figure 23, the pyrolysis reaction is very rapid. Slowing the reaction to some extent delays the conversion a little bit, but does not prevent conversion. Only when extreme values are used for

the kinetic parameters does the reaction rate slow to the point that conversion is not complete. Therefore, kinetic factors are not likely to be an important consideration for in situ retorting.

The initial water content can increase the heat capacity of the retort, diverting heat from the raising the temperature, and impacting the conversion of kerogen. The water content of the retort was doubled. This may have the effect of including water bound to minerals, which will be driven off the minerals when boiling occurs, and so does need to be included in the water model. When this simulation is run, the peak retort temperature drops, and the amount of heat bound up in steam increases. However, the temperature drops only to 367 °C from about 400 °C. The pyrolysis reaction is still fast enough to convert all the kerogen to oil, and the oil yield is relatively unaffected.

The final simulation evaluates heat conduction out of the retort. Thermal conductivity for oil shale reported by Rejeshwar et al. (1979) range from $6x10^4$ to $1.5x10^5$ J m^{-1} day^{-1} $°K^{-1}$. The base case uses the lower number; the upper number would allow more heat to be lost to the surrounding rocks. When a thermal conductivity of $1.6x10^5$ J m^{-1} day^{-1} $°K^{-1}$ is used, the retort takes longer to heat up. The retort still hits a maximum temperature of 393 °C, which is sufficient to drive pyrolysis, but it doesn't reach this temperature until day 1492. Pyrolysis occurs about day 1180 versus day 1100 under the base case. This is not significant. Oil generation does occur somewhat later, but there is generally complete conversion of the kerogen.

4.2.9 Operation summary

The above analysis is necessary to determine the approximate length of time needed to operate the retort and remove the gas and oil products. Over this time, a small amount of water is produced via the kerogen conversion during heating (Equation 12). Most of the produced water is from the conversion of water entrapped in the isolated pores (and residual water in effective pores) as steam. A small amount of water consumption would be necessary during daily operations. Water used for cooling of surface equipment is not included in these calculations. The operation time is also used to establish the beginning of the site remediation stage.

4.3 Remediation Phase

Once the operation stage is completed, the site must be remediated. As part of this remediation effort, the retort zone may be flushed with water to remove excess heat and mobile contaminants. A calculation was performed to examine the number of pore volumes of water injected into an expired retort to evaluate the cooling rate due to the heat extraction of the injected water. Input water was assumed to be 25°C and the system was assumed to be a well mixed reactor. The final porosity was assumed to be 10% and therefore a pore volume is equilvent to 10% of the total volume. During the first few injected pore volumes heat is removed from the reservoir via heating of the water to its boiling point, vaporization of the water, and heating the steam to the retort temperature. Within 3 pore volumes, the temperature drops from 350°C to 100°C. Below this temperature, the rate of cooling significantly decreases because the only heat removal mechanism is the sensible heating of the water injected water. At this time, each pore volume of injected water will decrease the retort temperature approximately 5° to 10°C (depending on the initial retort temperature) and ambient temperature is achieved in less than 10 pore volumes. Although these calculations do not take into account actual transport or pressure changes within the retort, it does provide enough information to suggest that the flushing to reduce contaminant concentrations will determine the number of pore volumes that need to be flushed through the system.

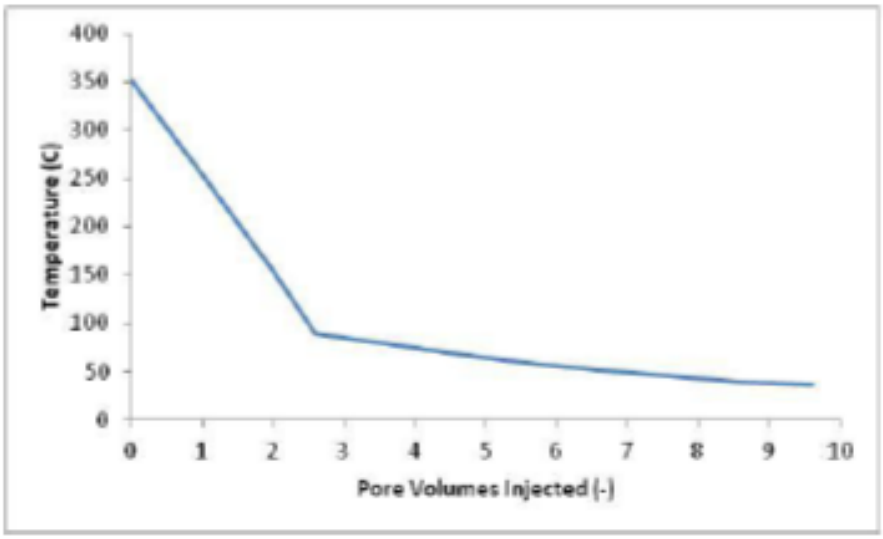

Figure 27. Retort cooling as a function of injected pore volumes.

Modeling results for Shell's Oil Shale Test Project (Shell, 2006) suggest that a 20 pore volume flush will be necessary for reduce contaminants down to an acceptable level. In their simulations they thought this would be achievable in 2 years of flushing. We used a similar approach for the remediation phase in the system dynamic model. Since flushing of contaminants takes more pore volumes than the cooling of the retort, we will assume that 20 pore volumes is the volume of water that needs to be handled. We will also assume that the water will be treated at the surface and reused during subsequent flushes.

Figure 28 illustrates the system dynamic module for the remediation system. The total remediation water required is a function of the total porosity, retort volume and the required number of pore volumes needed to be flushed through the system. The total porosity is a user defined value typically higher than the initial effective porosity, due to the removal of kerogen during the retort process. The actual water needed is less than the total remediation water required due to recycling of the water. The first pore volume is needed to refill the retort volume with water. After that initial filling, water will be recycled from the injection wells to the production wells and any water losses will be accounted for in the recycle water percentage. At this time the recycle water percent is set as a constant, and would account for water loss through the freeze wall, and makeup water needed for the water treatment on the surface.

The time necessary to complete the remediation is determined by the injection rate and the total amount of water required. We used a one dimensional form of Darcy's Law to describe the injection rate. The area was determined from retort length parameters. The hydraulic conductivity was from the initial site information that can be multiplied by a factor to account for any increases in the hydraulic conductivity due to the retorting process. The pressure gradient is currently based on the lithostatic pressure (via the overburden depth) and $1/10^{th}$ the width of the site. These values are used to calculate the time to pump 20 pore volumes of water and to develop the water requirement values as a function of time.

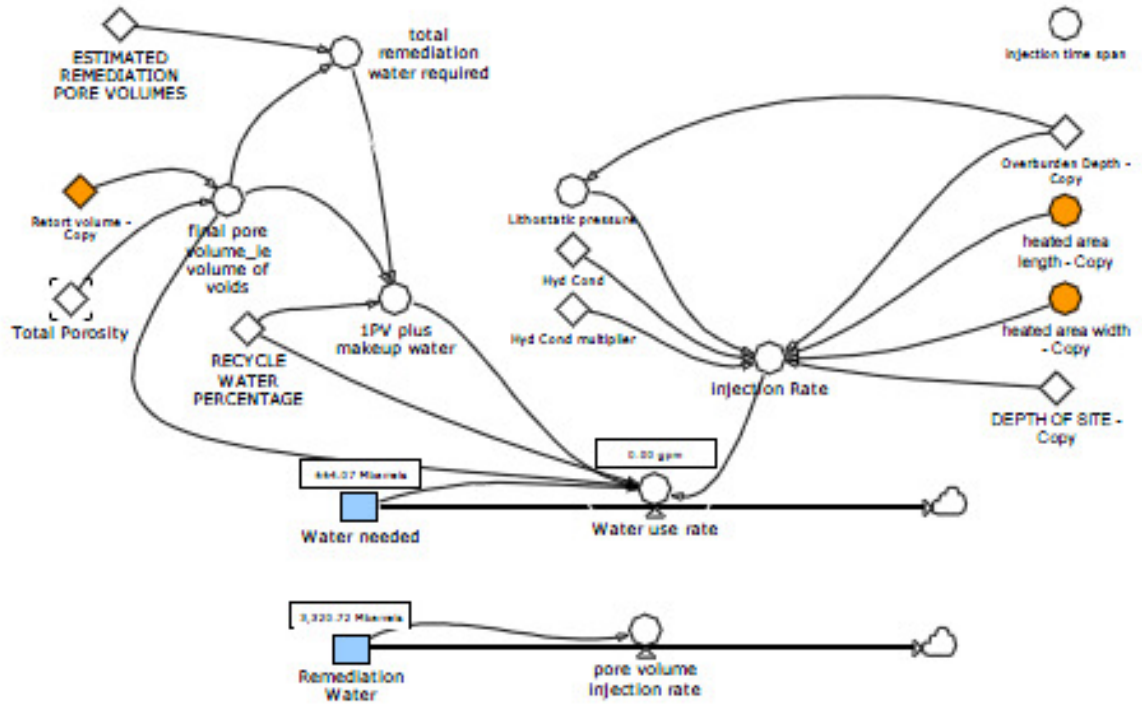

Figure 28. Remediation of the retort through subsurface flushing.

5. Comparison to Shell Patent Example

Shell conducted a small scale field experiment and presented some of the results in their patent application (Vinegar et al., 2010). The objective of their test was to substantiate laboratory experimental results, however, there is enough information to test portions the system dynamic model. The field experiment consisted of an unconfined hexagonal seven spot pattern drilled at 8 foot spacing (Figure 29). Six heater wells (triangles) were drilled to a depth of 40 meters and contained 17-meter heater elements. A single producer well (hexagon) was placed at the center to capture liquids and gases. Four monitoring wells (pentagons) were installed along with a 6 dewatering wells (squares) surrounding the heaters. There is no freeze wall system in this field test. There are 17 total wells in the configuration.

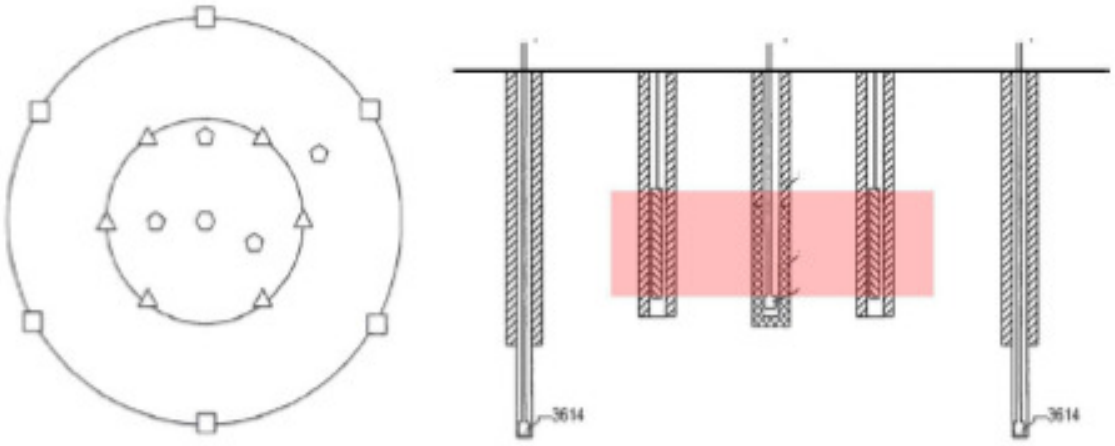

Figure 29. Shell field experiment layout. A) plan view, B) cross section [no scale] (modified from Vinegar et al. 2010)

Our current system dynamic model assumes a rectangular retort area. Therefore assuming there is some overlap in the heating well area, the effective radius of the Shell retort zone would be approximately 4 meters in radius. A square with an equivalent area would have sides of approximately 3.5 meters, with a heater well spacing of approximately 1.25 meters (assuming a 5 spot pattern) (Figure 30).

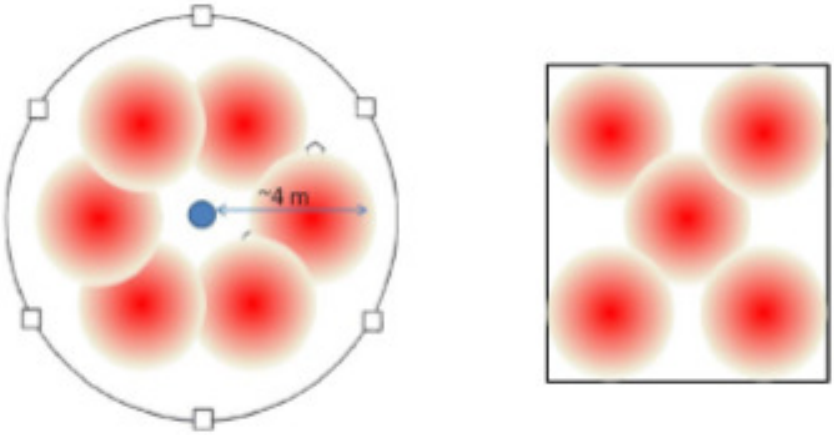

Figure 30. Equivalent layout for the system dynamic model.

The heater wells were powered for 216 days and the temperature within the retort reached approximately 480 degrees (Figure 31). The monitoring wells were spaced approximately 1 to 1.5 meters from the heater wells and assuming radial conduction from the heater well, it is likely that the heater wells were much hotter. Oil and gases were collected in the production wells with the first initiation of production at 80 to 90 days (Figure 32). At this time, the measured temperature at the monitoring well was approximately 260°C (a temperature with little kerogen conversion) suggesting that the area near the heater well was

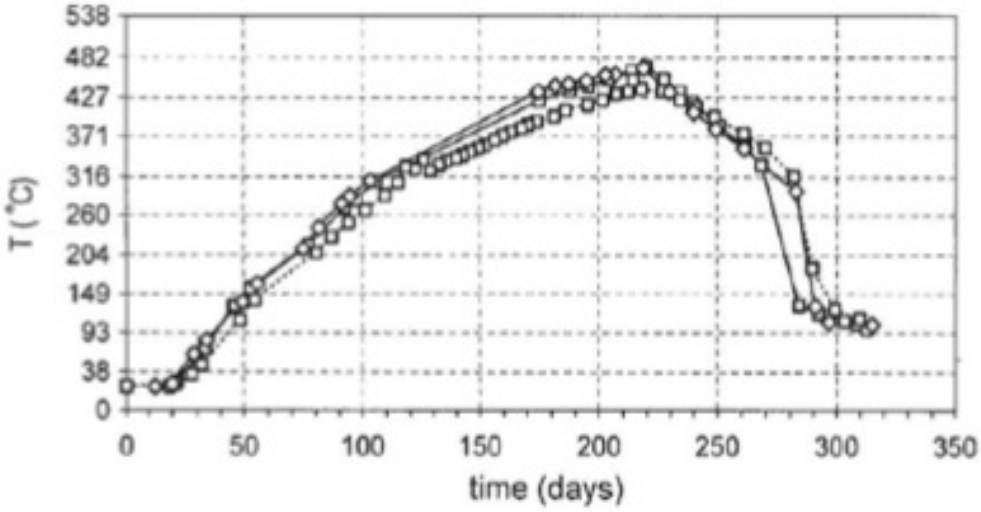

Figure 31. Temperature verses time plot of the maximum temperature in the interior monitoring wells.

responsible for the production of product. Our system dynamic model assumes uniform heating of the retort and thus we expect a delay in product production. The maximum production rate was at approximately day 150 which corresponds to a monitoring well retort temperature of approximately 360°C (Figure 33).

Water production was also monitored during the test (Figure 34). For the simulation, we assume all water production is from the production well and not from the dewatering wells. Figure 34 and Figure 35 illustrate the production of water as a function of MW-hrs and the retort temperature, respectively. Assuming that the applied power is constant during the test, we can relate water production to temperature. Water is produced prior to 100°C measured at the monitoring wells likely due to radial heat transport from the heater wells. Water reaches an initial local maximum then drops only to increase to a fairly constant recovery rate of approximately 1.5 barrels per day. After the heaters are turned off, the rate of water recovery increases possibly due to adjustments to the dewatering wells.

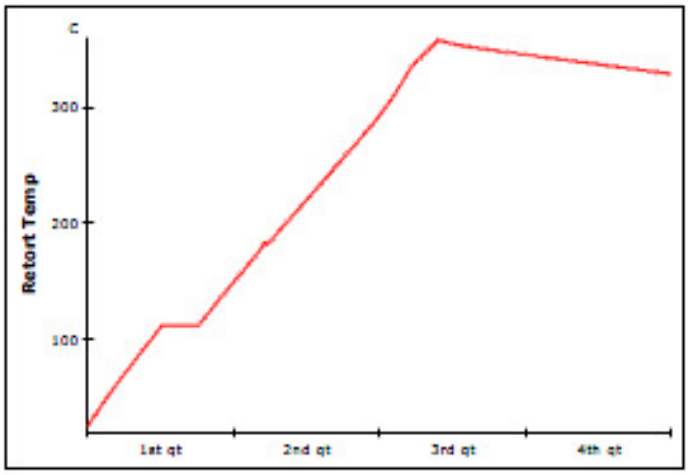

Figure 32. Temperature verses time plot for the retort simulation.

The cumulative water extracted as a function of the monitoring well temperature (Figure 35) was calculated by digitizing Figure 32 and Figure 34 to capture the dynamics of the water extraction rate vs input energy and the monitoring well temperature as a function of time. We assumed that the applied power to the heaters was constant (calculated to be 85 kW) to change energy into time. Next we calculated the cumulative water extracted from the water extraction rate and time values. Finally, we interpolated the temperature and cumulative water extract on a daily time step for plotting purposes.

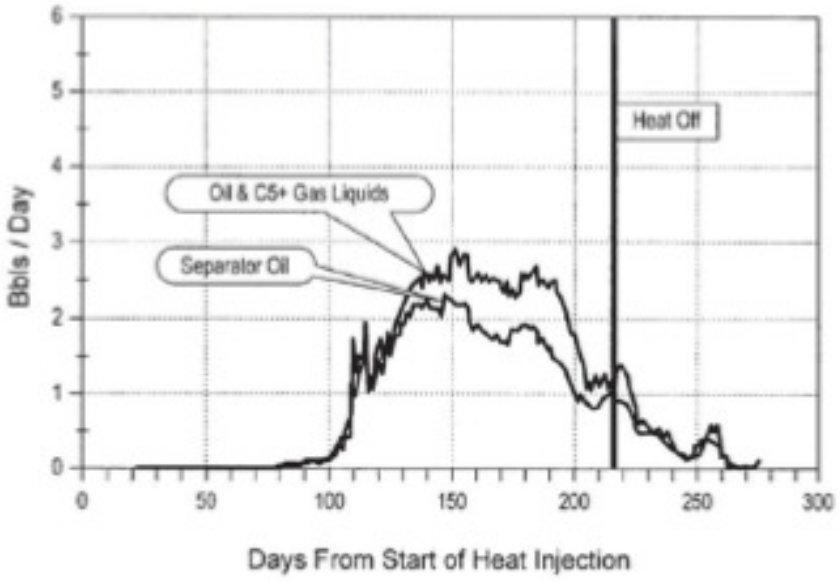

Figure 33. Barrels of oil and gas per day as a function of heating.

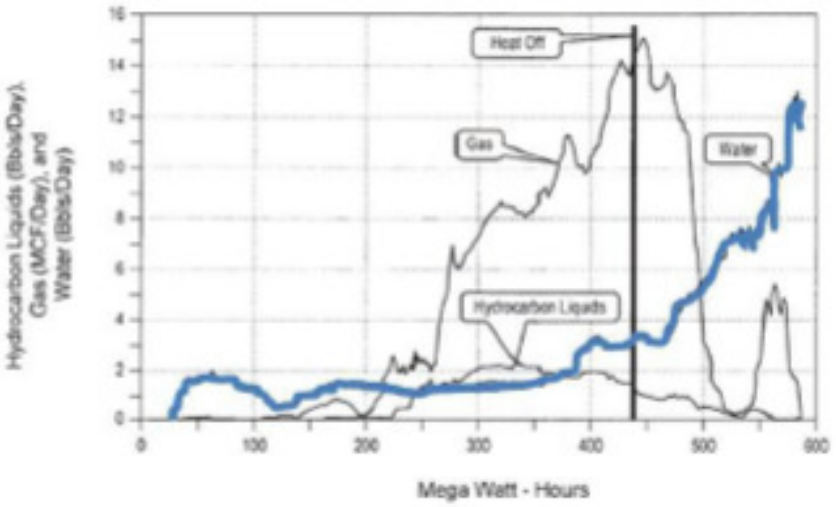

Figure 34. Temperature verses time plot of the maximum temperature in the interior monitoring wells.

Figure 35 illustrates that the water extracted is mostly a linear function of temperature up to approximately 400°C (0.43T-19, R^2 0.97) then rises sharply as the temperature reaches 500°C. The total data better matches an exponential fit (13.2e0.0065T, R^2 0.93).

During the heating stage, 300 barrels of water were extracted. Mass balance calculations suggest that all water is likely derived from the retort area and not from the surrounding oil shale. The approximate volume of the retort is approximately 362 cubic meters (2.4^2*3.14*20). Assuming 10 percent total porosity this could produce approximately 230 barrels of water. Additional water would come from inorganic hydrates (eg. nacolite), acid-base reactions of iron compounds (eg. iron carbonates), organic oxygen (likely a minor amount), and equilibrated water (water shift reaction above 550°C) (Coburn et al, 1989). Their data suggests that the bulk of the water is released between 150° and 450°C and that it is from these chemical reactions for Colorado shales.

Water is being produced at the production well prior to 100°C (the assumed boiling point of water) at the monitoring wells. Since the production well is further displaced from the heater well than the monitoring wells, it is likely that the production well is also less than 100°C. Therefore the extracted water is likely still in the liquid phase and is being transported to the production well via pressure gradients from steam generation near the heating wells.

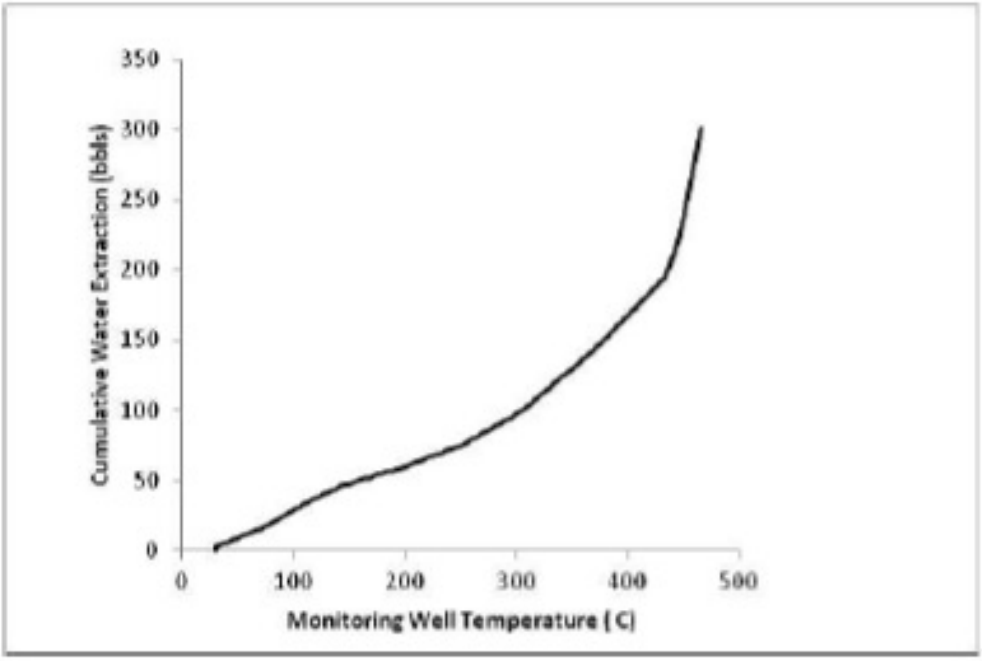

Figure 35. Cumulative water extracted verses temperature of an interior monitoring well.

In comparison, the calculated water extracted predicted by the system dynamic model (Figure 36), suggests a different shape of the cumulative production of water in an oil shale retort. In this case, no water is produced until after 100°C, then a rapid production followed by a leveling off by 300°C. The rapid production after 100°C is due boiling of the water at this hydrostatic pressure is slightly above 100°C. Since all the retort volume is assumed be heated to the same temperature, any energy input into the system will continue to turn water into steam until all the liquid water is evaporated. The temperature

will then continue to rise heating the shale and steam in the system. The curvature of the graph in Figure 36 is dependent on the rate of vapor extraction from the retort to the surface.

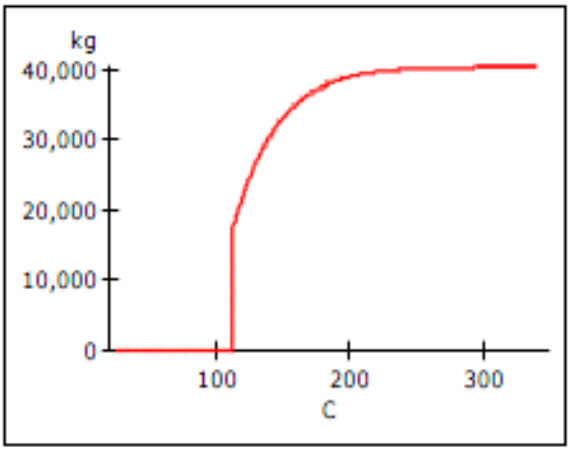

Figure 36. Cumulative water extracted verses temperature for test case.

Although the shape of the two water extraction curves (Figure 35 and Figure 36) are not the same the overall mass of water is nearly identical. The system dynamic model appears to under predict the initiation of water production and then over predict the water production between 100° and 400°C. This is believed to be due to the well mixed assumption in the system dynamic model as compared to transient radial heat conduction in field test. The total amount of water extracted appears to be similar in both the model and the field test suggesting that the processes being measured (heating the water in the shale pores to steam) is correct. The overall amount of extracted water is small as compared to the water needed for site preparation and drilling and therefore the inaccuracy of the rate of production in not a major concern.

6. Application to Large-Scale Hypothetical *In-Situ* Oil Shale Retort

A large-scale hypothetical in situ oil shale retort was simulated with the Powersim system dynamic model in the Piceance Basin. The site location was southwest of the Shell demonstration sites #1 and #3 (see Figure 37) and was assumed to have an aerial dimension of 3000 by 3000 feet. At this location was limited subsurface information from well CO213 that was assessable in the GIS data base (see Table 2). Based on this information it was assumed that oil shale from the A Groove through the L0 unit would be retorted (398 feet to 1476 feet). The total volume of the retort is 360 million cubic meters.

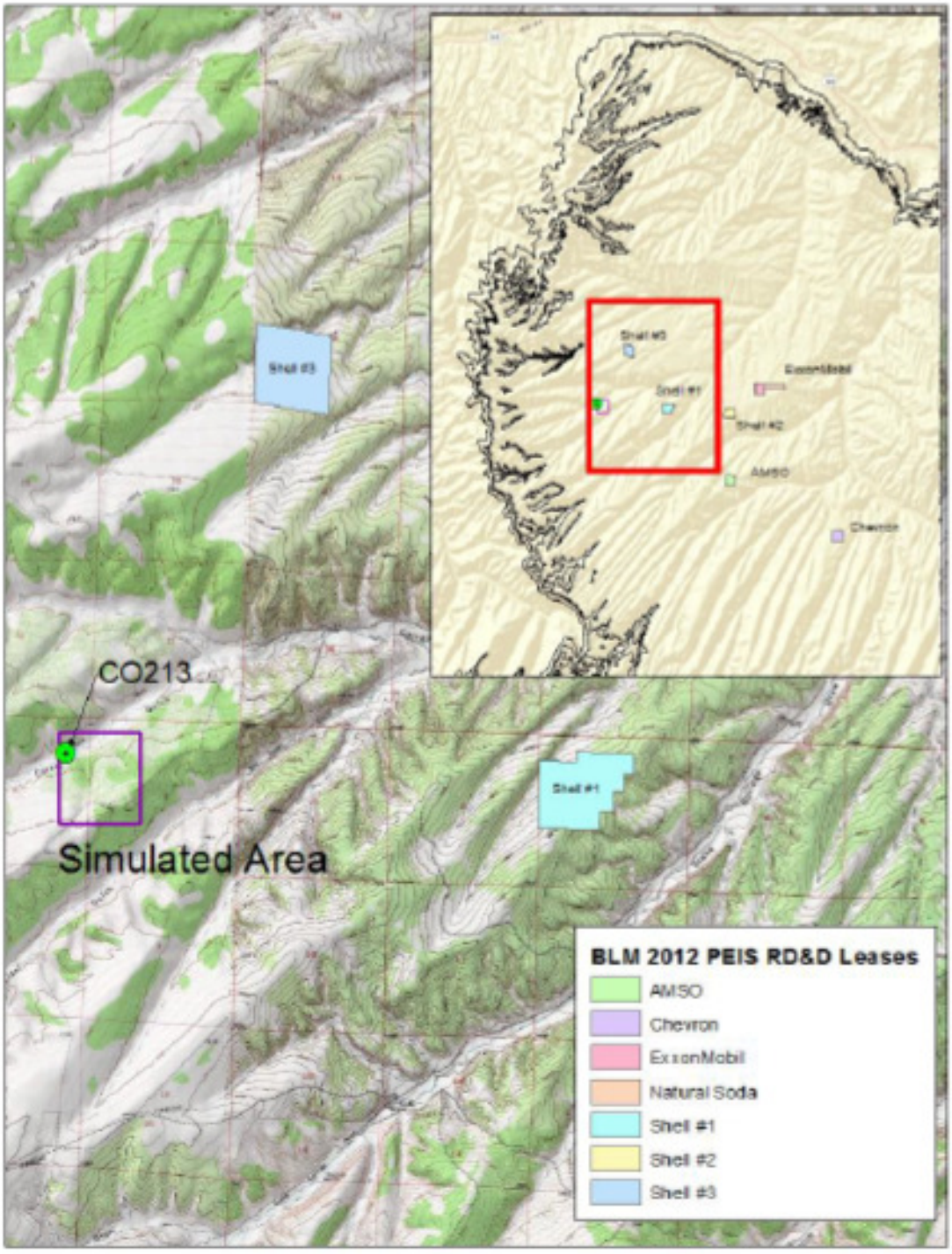

Figure 37. Location map from the GIS data base for the simulated retort.

Table 2. Subsurface information from the GIS data base.

Layer Name	Thickness Average ft	Vol (cf)	Porosity n %	Hydraulic Conductivity K (ft/day)	OilGPT (Average) Based on CO213	WaterIn MatrixGPT	Oil volume gal
UpperGre	398	3580000000	10	1.2	na	na	
A Groove	12	114000000	10	1.2	6.2	1.3	44104320
Mahogany	119	1080000000	1	0.01	25.4	3.75	1711756800
B Groove	24	216000000	10	1.2	5.7	1	76826880
R6	118	1070000000	1	0.01	19.9	3.38	1328683200
L5	81	737000000	10	0.6	11.7	5.4	538068960
R5	181	1640000000	15	0.4	28.9	9	2957510400
L4	66	593000000	20	2	21.8	7.1	806669760
R4	70	636000000	15	0.4	33.3	4.75	1321557120
L3	37	383000000	8	0.4	11.3	4.5	270060960
R3	75	680000000	1	0.01	24.5	4.23	1039584000
L2	26	249000000	5	0.2	15.3	4.8	237725280
R2	80	722000000	1	0.01	26.9	6.35	1211920320
L1	31	281000000	3	0.2	5.4	10.54	94685760
R1	111	1000000000	0.5	0.01	19.4	9.13	1210560000
L0	47	425000000	3	0.2	5.5	7.78	145860000
R0	144	1300000000	0.5	0.01	na	na	

The construction model parameters are fairly similar to that described in the previous section with the exception that the retort site is much larger. Freezer well spacing is set at 12 feet, the buffer zone is assumed to be 7.6 feet, 10 drill rigs are to be working at any one time, drilling speed is 8 feet per hour (~175 hours per well). A total of 2638 wells are needed (893 freeze wells, 5 monitoring wells, 100 production wells, and 1641 heating wells). Time to drill these wells will take approximately 5 years.

Water consumption during drilling is fairly small at a total volume of 0.16 Mbarrels (Figure 38). An additional 0.19 Mbarrels would be needed for dust control (assuming one 10,000 gallon truck per shift).

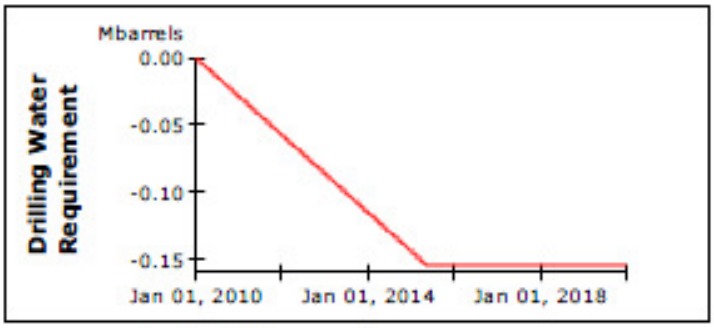

Figure 38. Water consumption for drilling operations.

The volume of dewatering of the retort volume is based on the retort volume multiplied by the effective porosity. For this scenario, we calculated the effective porosity based on the data from the GIS.

Figure 39 illustrates the porosity as a function of depth and an average effective porosity of 6.7 percent. The model calculates a dewatering volume of 106 Mbarrels (Figure 40). We assume that dewatering begins as soon as the freeze wall wells have been completed. This value may overestimate the produced water as it assumes that all water in contained in the pore space can be extracted by dewatering via pumping.

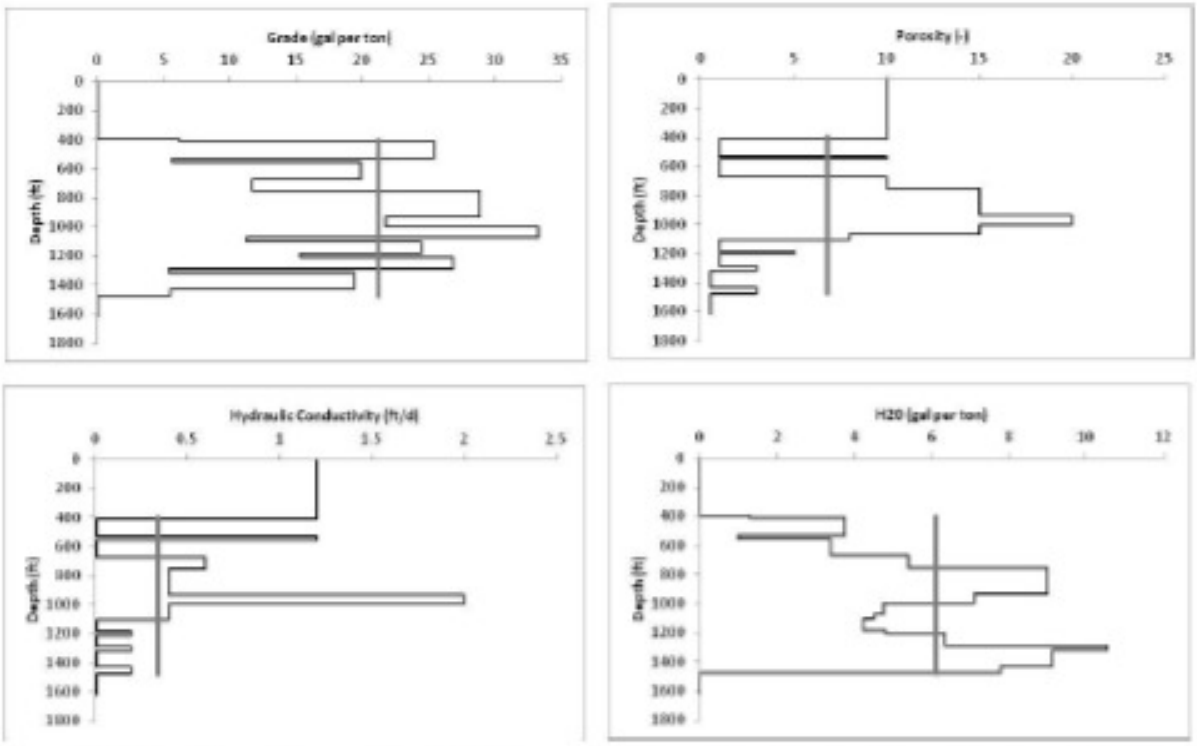

Figure 39. Oil shale grade, porosity, hydraulic conductivity and produced water as function of depth and weighted average values for the Piceance Basin hypothetical simulation.

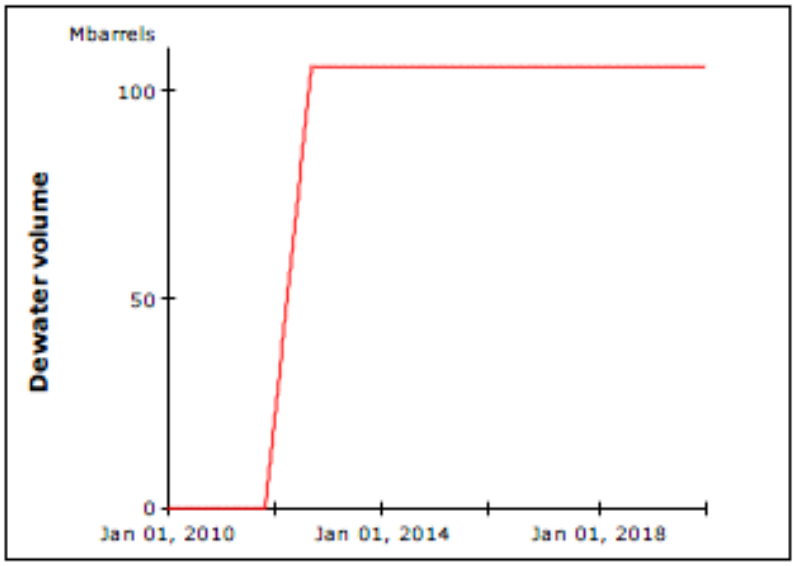

Figure 40. Water production for dewatering operations.

Additional water is produced (and consumed) during the operation phase of the retort. During the operation phase a constant input of energy of 1500 MWatts are used over a period of 4 years. This will bring the average temperature of the retort to 330 C. Although we have assume a constant energy input, the temperature ramping rate does have a small rate change at 111.4 C (Figure 42) due to the evaporation of residual water in the retort volume. The residual volume is calculated as the total porosity minus the effective porosity multiplied by the retort volume.

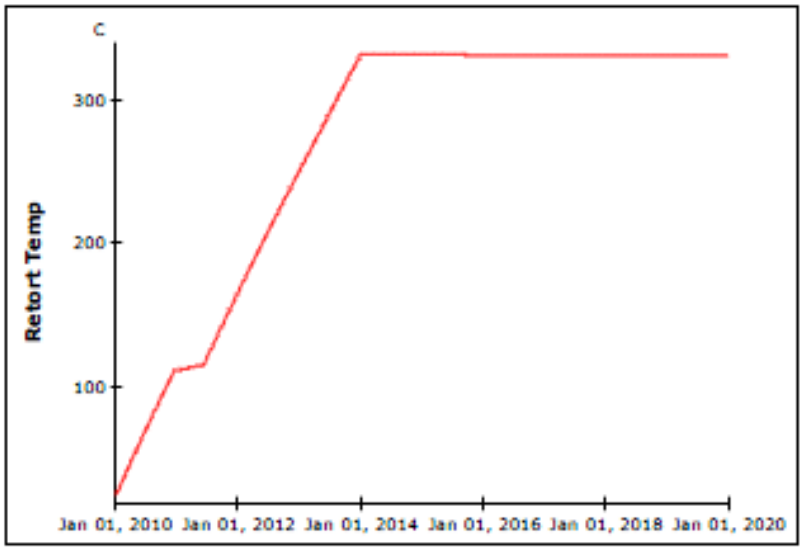

Figure 41. Retort temperature as a function of time.

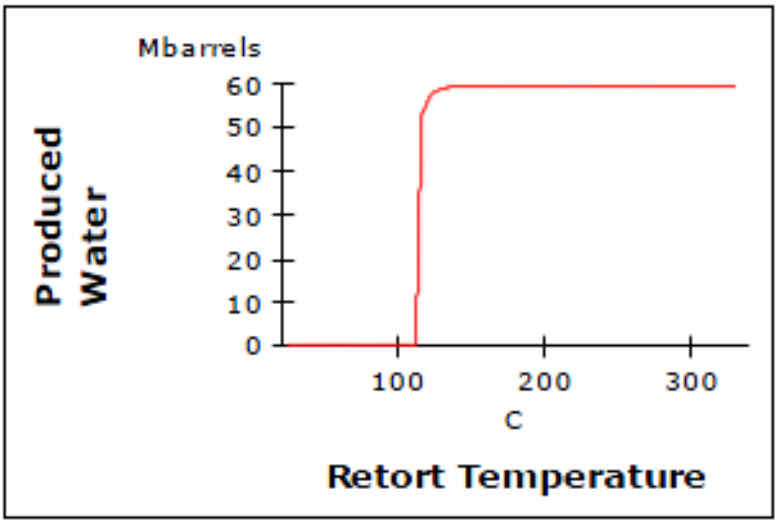

Figure 42. Steam as liquid barrels of water as a function of retort temperature.

The remediation phase has the largest water consumption of all the phases. During remediation the pore space in the retort volume will first have to refilled. We assumed that retort porosity is the total porosity (due to the removal of kerogen). For this example, the approximately 1.6 Mbarrels of water are needed to initially fill this pore space. As indicated in Figure 27 the first 3 pore volumes will produce steam and will have to be re-condensated at the surface prior to reinjection. We have also assumed a 15% loss of each injected volume and that 20 pore volumes will be needed. Total time of remediation is approximately 4 years at an overall injection rate of 72 thousand gallons per minute. Figure 43 illustrates the water consumption as a function of remediation time.

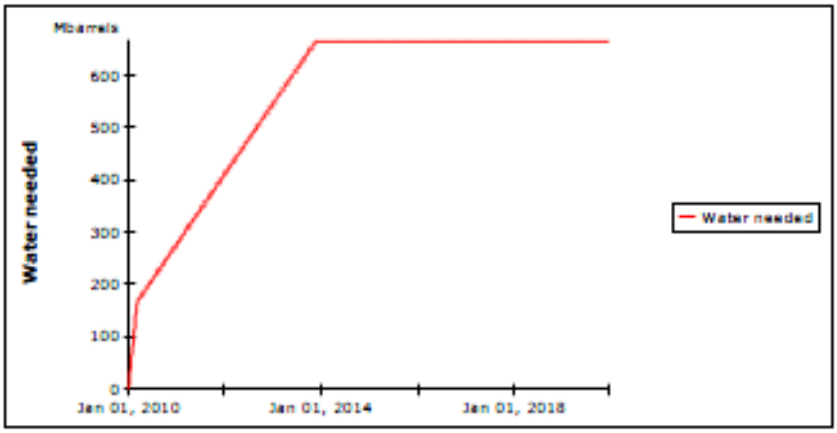

Figure 43. Remediation water required for filling and flushing the retort volume.

The three models run independently from one another and therefore water production/consumption of the three phases must be sequentially added. Figure 36 illustrates the cumulative water consumption for all phases of the hypothetical retort. Positive slopes represent water production while negative slopes represent water consumption. As seen in Figure 44, although some water is consumed during drilling and dust control, water is generally produced in the first half of a retort operation due to dewatering of the

retort volume and steam production of residual water during heating, whereas water is consumed in the final remediation phase.

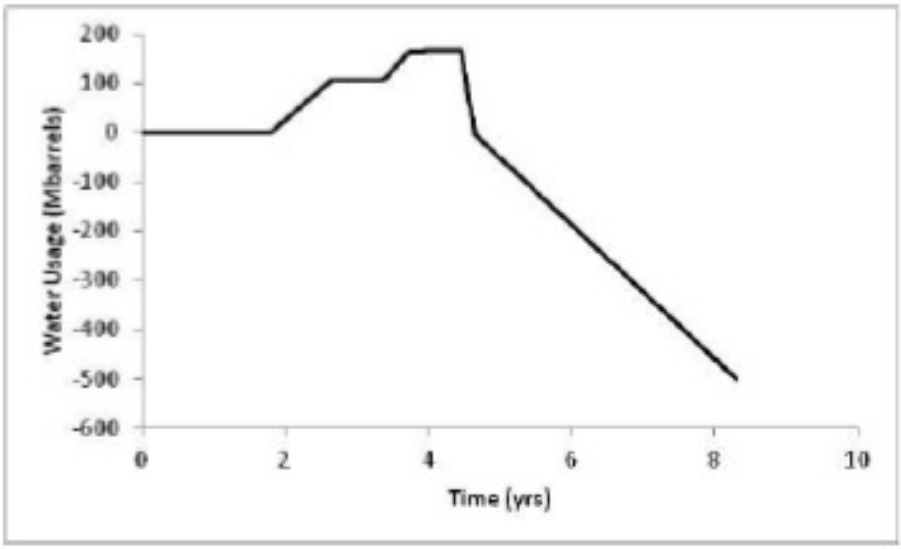

Figure 44. Cumulative water extracted verses temperature from hypothetical simulation.

Overall, approximately 500 Mbarrels of water is consumed (loss) for this hypothetical retort. However, the retort is calculated to produce 341 Mbarrels of oil. The ratio of water to oil is 1.47 and is in the range of what the industry has claimed as the expected water use rate.

Data used to create Figure 44 can be easily exported to a comma delineated text file and imported into the GIS data base for subsequent analysis of the retort on the basin water.

7. Summary

A system dynamic model was construction to evaluate the water balance for *in-situ* oil shale conversion. The model is based on a systems dynamics approach and uses the Powersim Studio 9™ software package. Three phases of an insitu retort were consider; a construction phase primarily accounts for water needed for drilling and water produced during dewatering, an operation phase includes the production of water from the retorting process, and a remediation phase water to remove heat and solutes from the subsurface as well as return the ground surface to its natural state. Throughout these three phases, the water is consumed and produced. Consumption is account for through the drill process, dust control, returning the ground water to its initial level and make up water losses during the remedial flushing of the retort zone. Production of water is through the dewatering of the retort zone, and during chemical pyrolysis reaction of the kerogen conversion. The major water consumption was during the remediation of the insitu retorting zone.

In this report, we provide background information on oil shale, explain the conceptual basis for the *in-situ* retorting model, describe the key components of the systems dynamics model, compare results from the model with a pilot field test, and provide preliminary results from application of the model to a hypothetical full-scale *in-situ* retorting operation.

8. References

Bar, H., R. Ikan and Z. Aizenshtat, 1986, "Kinetic Study of Isothermal Oil Shale Pyrolysis: 1. Mathematical Model of the Evolution of Organic Pyroproducts," *Journal of Analytical and Applied Pyrolysis*, 10, 153-166.

Blackett, R. E., 2004, *Geothermal Gradient Data for Utah*, Utah Geological Survey, Salt Lake City, UT.

Braun, R. L. and A. K. Burnham, 1986, "Kinetics of Colorado Oil Shale Pyrolysis in a Fluidized-Bed Reactor," *Fuel*, 65, 218-222.

Burnham, A. K. and M. F. Singleton, 1983, "High-Pressure Pyrolysis of Green River Oil-Shale," *ACS Symposium Series*, 230, 335-351.

Burnham, A. K. and R. L. Braun, 1999, "Global Kinetic Analysis of Complex Materials," *Energy & Fuels*, 13, 1-22.

Campbell, J. H., G. H. Koskinas and N. D. Stout, 1978, "Kinetics of Oil Shale Generation from Colorado Oil Shale," *Fuel*, 57, 372-376.

Campbell, J. H. and A. K. Burnham, 1980, "Reaction-Kinetics for Modeling Oil-Shale Retorting," *In Situ*, 4, 1-37.

Clayton, J. L., A. Warden, T. A. Daws, P. G. Lillis, G. E. Michael and M. Dawson, 1992, Organic Geochemistry of Black Shales, Marlstones, and Oils of Middle Pennsylvanian Rocks from the Northern Denver and Southeastern Powder River Basins, Wyoming, Nebraska, and Colorado, Bulletin 1917-K, U. S. Geological Survey, Denver, CO.

Colburn, T.T., M.S. Oh, R.W Crawford, and K.G. Foster. 1989, "Water Generation during Pyrolysis of Oil Shales. 1. Sources", *Energy & Fuels*, 3, 216-223

Earnest, C. M., 1982, "Thermogravimetry of Selected American and Australian Oil Shales in Inert Dynamic Atmospheres," *Thermochimica Acta*, 58, 271-288.

Haar, L., J. S. Gallagher and G. S. Kell, 1984, *NBS/NRC Steam Tables, Thermodynamic and Transport Properties and Computer Programs for Vapor and Liquid States of Water in SI Units*, Hemisphere Publishing Corporation, Washington, DC.

Huss, E. B. and A. K. Burnham, 1982, "Gas Evolution During Pyrolysis of Various Colorado Oil Shales," *Fuel*, 61, 1188-1196.

Johnson, H. R., P. M. Crawford and J. W. Bunger, 2004, *Strategic Significance of America's Oil Shale Resource*, Office of Strategic Petroleum Reserves, U. S. Department of Energy, Washington, DC.

Lee, S., 1991, Oil Shale Technology, CRC Press, Boca Raton, FL.

Nerurkar, N., 2012. U.S. Oil Imports and Exports. Congressional Research Service Report R4246536 p. www.crs.gov

Rajeshwar, K., R. Nottenburg and J. Dubow, 1979, "Review Thermophysical Properties of Oil Shales," *Journal of Materials Science*, 14, 2025-2052.

Roehler, H. W., 1993, *Eocene Climates, Depositional Environments, and Geography, Greater Green River Basin, Wyoming, Utah, and Colorado*, Professional Paper, 1506-F, U. S. Geological Survey, Washington, DC.

Shell, 2006, Chemical Constituents, Source Term, and Concentration Changes with Rinsing: Basis for Design of Reclamation Plan for Post-Pyrolysis Zone, Appendix 22, Shell Frontier Oil and Gas, Denver CO, October 31, 2006

Skala, D., H. Kopsch, M. Sokic, H. J. Neumann and J. A. Jovanovic, 1990, "Kinetics and Modelling of Oil Shale Pyrolysis," *Fuel*, 69, 490-496.

Torrente, M. C. and M. A. Galan, 2001, "Kinetics of the Thermal Decomposition of Oil Shale from Puertollano (Spain)," *Fuel*, 80, 327-334.

U.S. Energy Information Administration (EIA), 2012. Annual Energy Outlook 2012 with Projections to 2025. DOE/EIA-0383(2012) 252 p. http://www.eia.gov/forecasts/aeo/pdf/0383(2012).pdf

Vinegar, H.J., E. Pierre de Rouffignac, K.A. Mahar, L.G. Schoeling, and S.L. Wellington, *In situ* thermal processing of an oil shale formation containing carbonate minerals, US Patent 7,735,935 B2, June 15, 2010.

Waples, D. W. and M. Ramly, 2001, "A Simple Way to Model Nonsynchronous Generation of Oil and Gas from Kerogen," *Natural Resources Research*, 10, 59-72.

Waples, D. W. and J. S. Waples, 2004, "A Review and Evaluation of Specific Heat Capacities of Rocks, Minerals, and Subsurface Fluids. Part 1: Minerals and Nonporous Rocks," *Natural Resources Research*, 13, 97-122.

National Energy Technology Laboratory

626 Cochrans Mill Road
P.O. Box 10940
Pittsburgh, PA 15236-0940

3610 Collins Ferry Road
P.O. Box 880
Morgantown, WV 26507-0880

One West Third Street, Suite 1400
Tulsa, OK 74103-3519

1450 Queen Avenue SW
Albany, OR 97321-2198

2175 University Ave. South
Suite 201
Fairbanks, AK 99709

Visit the NETL website at:
www.netl.doe.gov

Customer Service:
1-800-553-7681